

High strength steel in conventional building structures

Master's Thesis in the Master's Programme Structural Engineering and Building Technology

JAKOB NORDENSTAM
GUSTAV SVANTESSON

MASTER'S THESIS BOMX02-16-98

High strength steel in conventional building structures

Master's Thesis in the Master's Programme Structural Engineering and Building Technology

JAKOB NORDENSTAM

GUSTAV SVANTESSON

Department of Civil and Environmental Engineering

Division of Structural Engineering

Steel and Timber structures

CHALMERS UNIVERSITY OF TECHNOLOGY

Göteborg, Sweden 2016

High strength steel in conventional building structures

Master's Thesis in the Master's Programme Structural Engineering and Building Technology

Jakob Nordenstam

Gustav Svantesson

© JAKOB NORDENSTAM, GUSTAV SVANTESSON 2016

Examensarbete BOMX02-16-98/ Institutionen för bygg- och miljöteknik,
Chalmers tekniska högskola 2016

Department of Civil and Environmental Engineering

Division of Structural Engineering

Steel and Timber structures

Chalmers University of Technology

SE-412 96 Göteborg

Sweden

Telephone: + 46 (0)31-772 1000

Cover:

Steel structure of Prioritet Serneke Arena

Chalmers Reproservice, Göteborg, Sweden, 2016

High strength steel in conventional building structures

Master's thesis in the Master's Programme Structural Engineering and Building Technology

Jakob Nordenstam

Gustav Svantesson

Department of Civil and Environmental Engineering

Division of Structural Engineering

Steel and Timber structures

Chalmers University of Technology

ABSTRACT

The steel grade S355 is very often used in building structures today. Methods to produce high strength steel have been around since the 1960's and today there are products available with yield strengths above 1300 MPa. Especially in the automotive industry it has been advantageous to use steels of higher grades, since a direct weight reduction is possible which results in lighter vehicles and thereby reduced fuel consumption.

The purpose of this thesis was to investigate and evaluate if steels with yield strengths between 420-700 MPa could be a beneficial alternative to S355 steel in conventional building structures.

The investigation was carried out by first studying literature available regarding how different steel grades have been used until today. Then, a parametric study was performed which showed that quadratic columns could be reduced in weight and area if they were made of high strength steel. Therefore, columns was the objective in a case study which evaluated the quadratic columns in the existing structure of Prioritet Serneke Arena.

The case study showed that if the existing S355 columns in the structure were to be replaced by columns with higher yield strengths, both weight and area reductions are possible. Depending on what design that was desired, the range of reductions varied. It was concluded that the non-dimensional slenderness of columns matter, where a decreasing non-dimensional slenderness results in larger benefits when implementing high strength steel. With a known price of different HSS it can be concluded what non-dimensional slenderness that is critical in order to lower the cost of steel columns.

Keywords: High Strength Steel, Conventional Building, Hot Rolled Quadratic Columns

Contents

ABSTRACT	I
CONTENTS	III
PREFACE	VI
NOTATIONS	VII
1 INTRODUCTION	1
1.1 Background	1
1.2 Aim and objectives	1
1.3 Methodology	2
1.4 Limitations	2
1.5 Outline	2
2 LITERATURE STUDY	4
2.1 Structural steel	4
2.2 Manufacturing of steel	5
2.3 Mechanical properties	7
2.3.1 HSS types	8
2.3.2 Toughness	9
2.4 Chemical properties	10
2.5 Steel design according to Eurocode 3	11
2.5.1 Classification of cross sections	11
2.5.2 Flexural buckling	13
2.5.3 Lateral torsional buckling	14
2.5.4 Deflection	16
2.6 Effects of an increased steel grade	17
2.6.1 Weldability	17
2.6.2 Properties of HSS on elevated temperatures	19
2.7 High strength steel in existing structures	22
2.7.1 Truss structures	22
2.7.2 Bridges	24
2.7.3 Tension rods	25
2.8 Example of experimental studies	25
2.8.1 Columns	26
2.8.2 Beams	33
3 CONCLUSIONS FROM LITERATURE STUDY	38
3.1 Columns	38
3.2 Beams	38

3.3	Standard profiles	39
3.4	Fire resistance	39
3.5	Weldability	39
3.6	Continuation of thesis	39
4	MEMBERS SUBJECTED TO TRANSVERSAL LOADS	40
4.1	Moment resistance	40
4.2	Lateral torsional buckling resistance ratio	40
4.3	Deflection	41
5	MEMBERS SUBJECTED TO AXIAL LOADING	43
5.1	MATLAB script	43
5.1.1	Cross section approximation	45
5.1.2	Script verification	46
5.1.3	Analysis 1, 2 and 3	48
5.1.4	Analysis 1	48
5.1.5	Analysis 2	49
5.1.6	Analysis 3	49
5.2	Results	50
5.2.1	Analysis 1	50
5.2.2	Analysis 2	57
5.2.3	Analysis 1 and 2 – influence of cross section class	63
5.2.4	Analysis 3	64
5.2.5	Summary of analysis	66
5.2.6	Column analysis - Final conclusions	69
6	CASE STUDY	71
6.1	Columns in structure	73
6.2	Steel area optimization	75
6.3	Thickness optimization	80
6.4	Column area optimization	82
6.5	Recommendation	85
7	DISCUSSION	87
7.1	Member subjected to transversal load	87
7.2	Member subjected to axial loading	87
7.3	Case study	88
8	CONCLUSIONS	90
8.1	Further studies	90

APPENDIX A – IPE330 beam subjected to transversal loads

APPENDIX B – Script verification

APPENDIX C – Corrugated cross section

APPENDIX D – Length break point of steel area optimization according to analysis 2

APPENDIX E – MATLAB script

Preface

In this Master's thesis, an investigation was carried out regarding possible benefits high strength steel could have in conventional building structures.

The project was carried out in collaboration with the structural consulting firm Integra Engineering AB and the Department of Civil and Environmental Engineering at Chalmers University of Technology.

We would like to thank our examiner Mohammad Al-Emrani for the support that he has given us during the project. We would also like to show our appreciation to our supervisor Mattias Larsson who has been a big help and given us invaluable guidance and feedback.

Gratitude is also given to SSAB in Borlänge, and particularly Jan Kuoppa who gave us the opportunity to participate at a steel course regarding high strength steel. But also thanks to Hans Björke for his highly committed guided tour inside the steel mill in Borlänge.

Finally, we would like to thank the entire department at Integra Engineering AB who has given us a very warm welcome and given us the opportunity to carry out our work at their offices, and thanks to our opponents Stefan Olander and Andreas Jonsson.

Gothenburg June 2016

Jakob Nordenstam

Gustav Svantesson

Notations

Abbreviations

<i>AHSS</i>	Advanced high strength steel
<i>HSS</i>	High strength steel
<i>NSS</i>	Normal strength steel
<i>DP</i>	Dual phase
<i>CP</i>	Complex phase
<i>LT</i>	Lateral torsional
<i>TRIP</i>	Transformation induced plasticity
<i>MS</i>	Martensitic
<i>HF</i>	Hot formed
<i>TWIP</i>	Twinning induced plasticity
<i>CEV</i>	Carbon equivalent value
<i>Q</i>	Quenched
<i>QT</i>	Quenched and tempered
<i>M</i>	Thermomechanically rolled
<i>HAZ</i>	Heat affected zone
<i>RF</i>	Reduction factor
<i>FEA</i>	Finite element analysis
<i>FEM</i>	Finite element method
<i>MC</i>	Thermomechanically rolled cold formable
<i>TM</i>	Thermo-mechanical rolling process

Roman upper case letters

<i>A</i>	Cross sectional area
<i>A_{eff}</i>	Effective cross sectional area
<i>B</i>	Borium
<i>C</i>	Carbon
<i>C_e</i>	Carbon equivalent
<i>Cr</i>	Chromium
<i>Cu</i>	Copper
<i>E</i>	Young's modulus ($E=210000 \text{ N/mm}^2$)
<i>G</i>	Shear modulus ($G=80770 \text{ N/mm}^2$)

H	Hollow section
J	Minimum toughness of 27 Joule
K	Minimum toughness of 40J
L	Length
L_{cr}	Buckling length
I_y	Moment of inertia about the strong axis
I_z	Moment of inertia about the weak axis
I_t	Torsion constant
I_w	Warping constant
M_{Rd}	Design resistance moment
M_{cr}	Elastic critical moment
Mn	Manganese
Mo	Molybdenum
N	Normalized
Nb	Niob
N_{cr}	Elastic force for the relevant buckling mode
$N_{b,Rd}$	Design buckling resistance of the compression member
N_{Ed}	Design value of compression force
Ni	Nickel
P	Phosphorus
P_{cm}	Critical metal parameter
S	Sulfur
Si	Silicon
Ti	Titanium
V	Vanadium
$W_{el,y}$	Elastic section modulus
$W_{eff,y}$	Effective section modulus
$W_{pl,y}$	Plastic section modulus
W_y	Section modulus

Roman lower case letters

b	Width of cross section
d	Thickness of web
f_{eu}	Ultimate strength of filler material
f_u	Ultimate tensile strength

f_y	Yield strength
h	Height of cross section
h_w	Height of web
i	Radius of gyration
t	Thickness
z_g	Distance between the point of load application and shear center

Greek lower case letters

α	Imperfection factor corresponding to the relevant buckling curve
α_{LT}	Imperfection factor corresponding to the relevant buckling curve regarding lateral torsional buckling
ε	Strain
$\bar{\lambda}$	Non-dimensional slenderness
λ_1	Slenderness
λ_{LT}	Non-dimensional slenderness regarding lateral torsional buckling
χ	Reduction factor for the relevant buckling mode
χ_{LT}	Reduction factor for the relevant buckling mode regarding lateral torsional buckling
γ_{M1}	Partial factor ($\gamma_{M1}=1$)

1 Introduction

1.1 Background

A few decades ago, the steel grade S275 was the norm and S355, the expectation. Today, S355 is the norm but there is steel with higher strengths available. The trend is heading towards a new norm of steel, high strength steel.

High strength steel (HSS) is today found in bridges, offshore and truss structures as well as in different types of vehicles such as aircrafts and ships. A large part is found in the automotive industry where substantial weight reductions are possible by using HSS. This directly reduces fuel consumption and greenhouse emissions.

Implementation of HSS in the design of structures could result in more slender structures. Less material consumption results in reduced weights and transport costs, which means a smaller environmental impact. Also from an architectural view, more appealing structures could be accomplished. Structural problems such as local and global buckling, deflection, fatigue and fracture and weldability need to be investigated in order to establish differences between conventional steel and HSS. Potential problems regarding for example initial imperfections may have a larger impact on the capacity of HSS compared to normal steel.

The use of HSS in conventional building structures has not been evaluated to any great extent. There are examples where HSS has been applied and benefits have been made. In Sweden, one good example is Friends arena. This project used steel with quality up to S900 (Hållbart byggande, 2012). By this implementation, the weight of the roof was reduced from 4585 tons to 4000 tons, which resulted in cost savings and less CO₂ emissions.

Some experimental testing have also been carried out. For example columns with different slenderness and yield strengths have been tested in order to investigate the influence of these parameters regarding the load bearing capacity, but further research needs to be done that will illustrate what parts of a structure are best suited to be made of HSS. The general impression regarding HSS in structures is that there are few or no benefits when increasing the yield strength of steels. This general impression often comes from the fact that the *E-modulus* is the same for all steel grades. However research of any larger extent have not been made to really show when this general impression is true, and when it is not.

1.2 Aim and objectives

This Master's thesis aims to investigate and evaluate if high strength steel could be a beneficial alternative to S355 steel in conventional building structures. The investigation includes a literature study which aims to give broader knowledge about the different steel grades and how they have been used.

A parametric study and a case study is also included in the thesis. The purpose of the parametric study is to evaluate the behaviour of structural members made by different steel grades subjected to transversal and axial loads. The case study aims to present differences in weights and areas between columns subjected to pure compression with

varying lengths and steel grades and how an increasing steel grade would influence an existing steel structure.

1.3 Methodology

In order to gain knowledge in the subject, a literature study was carried out. At this point, few limitations was set in order to obtain a basis of knowledge and for the authors to have an open mind in order to get an overall impression of the material and its potential benefits and limitations. Experiences from other industries, tests and experiments will show which structural members in structures that is most suitable to consist of HSS.

Based on the knowledge accumulated during the literature study, a general parametric study and a case study was outlined. With the programming software MATLAB, a script was written which evaluates the behaviour of columns and beams made by different steel grades. The script was also used to present differences in weights and areas for hot rolled quadratic columns made by different steel grades and how an existing structure with regard to this could be optimized.

1.4 Limitations

In the evaluation of high strength steels focus was given to structural steel grades varying between S355 and S700. The span of steel grades was chosen in collaboration with Integra Engineering AB and also due to limitations in SS-EN 1993-1-12 which only includes steel up to 700 MPa.

This master's thesis investigates the design possibilities and limitations that varying steel grades could have in building structures, no extensive environmental or economic analysis was performed.

1.5 Outline

The report is divided into 8 chapters. The introduction is followed by chapter 2, which is a literature study presenting the material steel. The literature study gives a general impression on how the material have been developed over the years and how steels of different capacities are used today. This is done with examples of existing structure and experimental studies where both advantages and disadvantages have been seen with HSS.

Chapter 3 presents conclusions from the literature study and arguments for how the parametric study and case study should be outlined.

Chapter 4 presents an analysis of IPE beams subjected to transversal loading where moment resistances, lateral torsional buckling resistances and deflection limits were evaluated for different steel grades.

Chapter 5 consists of two sub chapters. The first part describes the MATLAB script that was used along with the different analysis. The second part presents results from the analysis performed on hot rolled quadratic columns made by different steel grades. In the end, conclusions from the analysis are presented.

Chapter 6 presents the case study that was performed. A general introduction of the building is given followed by a declaration of the method used to for the evaluation of the structure. In the end, conclusions from the case study are presented.

Chapter 7 presents a discussion regarding the report and what is most important.

Chapter 8 present the main conclusions that can be drawn from the thesis. Also some recommended further studies will be presented in this chapter.

2 Literature study

2.1 Structural steel

At low strain levels, the relationship between the stress and strain is elastic and the stress-strain relationship is described by the modulus of elasticity, E . The E -modulus for steel is constant regardless of the yield limit and has the value of approximately 210 GPa. Figure 2.1 illustrates the typical stress-strain relationship of steel with a yield strength of 235, 355, 460 and 690 MPa. The figure shows that the initial state of the tension tests gives the same gradient of the curve which means that the E -modulus is the same. When the steel starts to yield, a plateau in the stress-strain relationship is formed, followed by a non-linear behaviour until the ultimate stress in the steel is reached and failure occurs. Figure 2.1 shows steel with yield strength up to 690 MPa, but there are steels available with yield limits well above 1000 MPa.

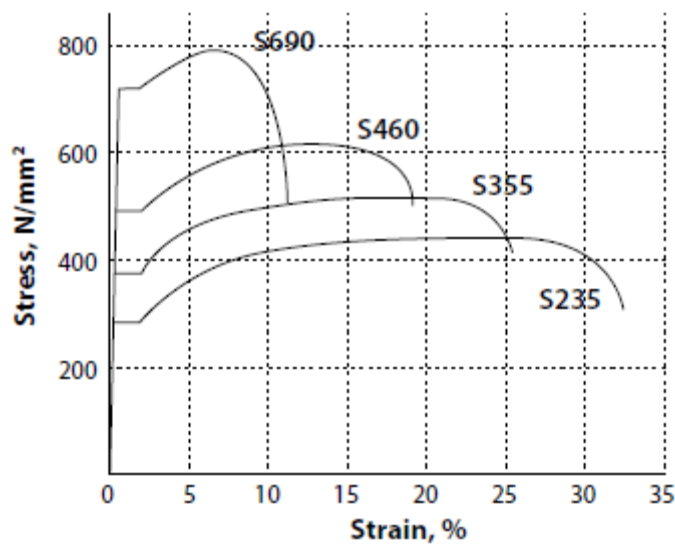


Figure 2.1 Stress-strain behaviour of steels (Baddoo & Brown, 2015).

In this report, *High Strength Steels* (HSS) are defined as steel with a yield limit of 420 MPa and greater. Steel grades below 420 MPa are considered as *Normal Strength Steel* (NSS), see Table 2.1. The quality and steel grades covered in the European standards generally used in the steel industry are summarized in Table 2.2.

Table 2.1 Yield limits for NSS steel and HSS.

Steel type	Yield limit
NSS	$f_y < 420$ MPa
HSS	$f_y \geq 420$ MPa

Table 2.2 *Steel grades and steel quality in European standards (Baddoo & Brown, 2015).*

Standard		Steel Grade	Steel Quality
EN 10025 -2	Non-alloy structural steel	S275, S355	JR, J0, J2, K2
EN 10025 -3	Normalized/normalized rolled weldable fine grain structural steels	S275, S355, S420, S460	N, NL
EN 10025 -4	Thermomechanical rolled weldable fine grain structural steels	S275, S355, S420, S460	N, ML
EN 10025 -6	Flat products of high yield strength structural steels in the quenched and tempered condition	S460, S500, S550, S620, S690, S890, S960	Q, QL, QL1
EN 10210 -1*	Hot finished structural hollow sections of non-alloy and fine grain steel	Non alloy S275, S355	JRH, JOH, J2H, K2H
		Fine grain S275, S355, S420, S460	NH, NLH
EN 10219	Cold formed welded structural hollow sections of non-alloy and fine grain steels	Non alloy S275, S355	JRH, JOH, J2H, K2H
		Fine grain S275, S355, S420, S460	NH, NLH

* The next revision of EN 10210 will include up to S960.

In Table 2.2 the steel grades are denoted SXXX, where the S stands for structural steel and XXX represents the minimum yield strength. The column to the right indicates the steel quality. The notations H, J, K, L, M, N and Q are described as:

H	Hollow section
J	Minimum toughness of 27J
K	Minimum toughness of 40J
N	Normalized
M	Thermomechanically rolled
L	Low notch test temperature
Q	Quenched

The notations R, 0, 1 and 2 indicates the test temperature for the Charpy V-notch test which is described in more detail in chapter [2.3.2].

2.2 Manufacturing of steel

Steel manufacturing principally involves five different production processes which are listed and described below.

- As-rolled steel
- Normalized steel
- Normalized-rolled steel

- Thermomechanically rolled steel
- Quenched and tempered steel

A typical hot rolling with a finish temperature of approximately 750 °C followed by a slow natural cooling gives a steel called ‘as-rolled’. If the as-rolled steel is heated back up to approximately 900 °C, and held at that temperature for a specific time before again cooling off naturally, a ‘normalized’ steel is made. Normalized steel has a finer and more homogenous grain structure compared to as-rolled steel (Samuelsson & Schröter, 2005).

‘Normalized-rolled’ steel have similar properties as the normalized steel. The difference in production process is that the rolling finish temperature is 900 °C, from where the steel is cooled down naturally. The reheating is thereby not necessary for normalized-rolled steel.

There are essentially two predominant methods to increase the yield strength of normalized and normalized-rolled steels (Samuelsson & Schröter, 2005).

- Alloying: Alloying elements such as carbon and manganese increases the yield strength of steel. There are however some negative effects with this method, in particular the weldability.
- Heat treatment: By heat treatment the microstructure and grain size of a steel is influenced. A fine grained micro structure results in both a higher strength as well as better toughness compared to a course grained micro structure.

Regarding production methods, there are essentially two methods used to achieve steels of higher grades, the Quench and Tempering (QT) and the Thermo-Mechanical (TM) rolling process (Samuelsson & Schröter, 2005). Figure 2.2 shows historical development of steel grades and the influence that the QT-method and TM-rolling has had regarding the yield stress of steels.

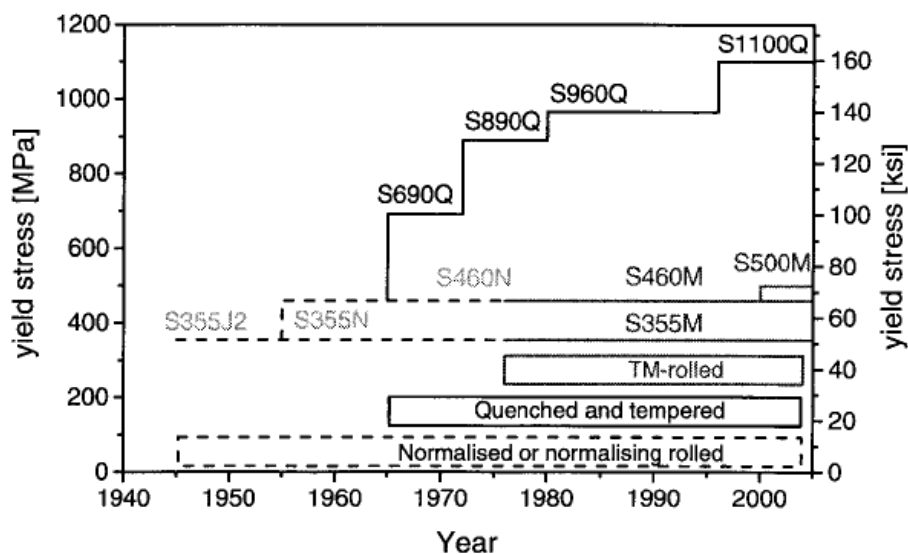


Figure 2.2 Historical development of production processes for steel (Samuelsson & Schröter, 2005).

In TM-rolling, final deformation is carried out in a certain temperature range which results in a steel with material properties not possible by heat treatment alone (Samuelsson & Schröter, 2005). Aside from increased strength and toughness, the weldability of a TM-rolled steel is very good because a minimum alloying content is possible. Some micro-alloying elements such as niobium, vanadium and titanium are usually added to achieve some additional strengthening.

The QT method originates from a normalized steel at around 900 °C. The material is rapidly cooled or ‘quenched’ which gives the steel high strength and hardness, but low toughness (Samuelsson & Schröter, 2005). It is then reheated to 600°C where it is kept for a specific time before another natural cooling (tempering) takes place. This last process restores the toughness of the steel. The QT steel has several micro-alloying elements such as niobium, vanadium and titanium. These elements are added to achieve an improved strength and toughness.

Both TM-rolled and QT steels are standardized in EN 10149-2 and EN 10025-6 respectively. Eurocode provides guidelines for qualities up to S690 for QT and S700 for TM, see Table 2.3 Table 2.4 respectively.

Table 2.3 Nominal values of yield strength f_y and ultimate tensile strength f_u for hot rolled structural steel.

EN10025-6 Steel grade and qualities	Nominal thickness of the element t mm					
	$t \leq 50$ mm		$50\text{mm} \leq t \leq 100$ mm		$100\text{mm} \leq t \leq 150$ mm	
	f_y [N/mm ²]	f_u [N/mm ²]	f_y [N/mm ²]	f_u [N/mm ²]	f_y [N/mm ²]	f_u [N/mm ²]
S 500Q/QL/QL1	500	590	480	590	440	540
S 550Q/QL/QL1	550	640	530	640	490	590
S 620Q/QL/QL1	620	700	580	700	560	650
S 690Q/QL/QL1	690	770	650	760	630	710

Table 2.4 Nominal values of yield strength f_y and ultimate tensile strength f_u for hot rolled flat products.

EN 10149-2 ^{a)}	$1.5\text{mm} \leq t \leq 8$ mm		$8\text{mm} \leq t \leq 16$ mm	
	f_y [N/mm ²]	f_u [N/mm ²]	f_y [N/mm ²]	f_u [N/mm ²]
S 500MC	500	550	500	550
S 550MC	550	600	550	600
S 600MC	600	650	600	650
S 650MC	650	700	630	700
S 700MC	700	750	680	750

a) Verification of the impact energy in accordance with EN 10149-1 Clause 11, Option 5 should be specified

2.3 Mechanical properties

What mechanical properties a steel develop is determined by their chemical composition and microstructure (Demeri, 2013). The microstructure of a steel depends on the cooling rate from the austenite or austenite plus ferrite (for hot rolled products) phase or regulation of the cooling section of the continuous annealing furnace for continuously annealed or hot dipped coated products.

2.3.1 HSS types

WorldAutoSteel have written a guide regarding application of HSS and divides new high strength steels in two different categories, high strength steels (HSS) and advanced high strength steels (AHSS). In addition, AHSS is divided into three generations.

- 1st generation: dual phase (DP), complex phase (CP), transformation induced plasticity (TRIP), martensitic (MS)
- 2nd generation: hot formed (HF), twinning induced plasticity (TWIP)

The microstructures of the first generation of AHSS are shown in Table 2.5.

Table 2.5 *Microstructure and strength ranges for steel grades of the first generation of AHSS (Demeri, 2013).*

First generation AHSS	Microstructure	Strength [MPa]
DP	Ferrite + Martensite	400-1000
CP	(Ferrite + bainite) matrix + small amounts of pearlite, martensite and retained austenite	400-1000
TRIP	Ferrite + martensite/bainite + austenite	500-1000
MS	Martensite	700-1600

The third generation of AHSS is still under development. This generation will have an improved strength-ductility compared to the 1st and 2nd generation, and potentially a more efficient joining capability (Keeler & Kimchi, 2014). The Global Formability Diagram illustrates the relation between tensile strength and elongation for different steel types, see Figure 2.3.

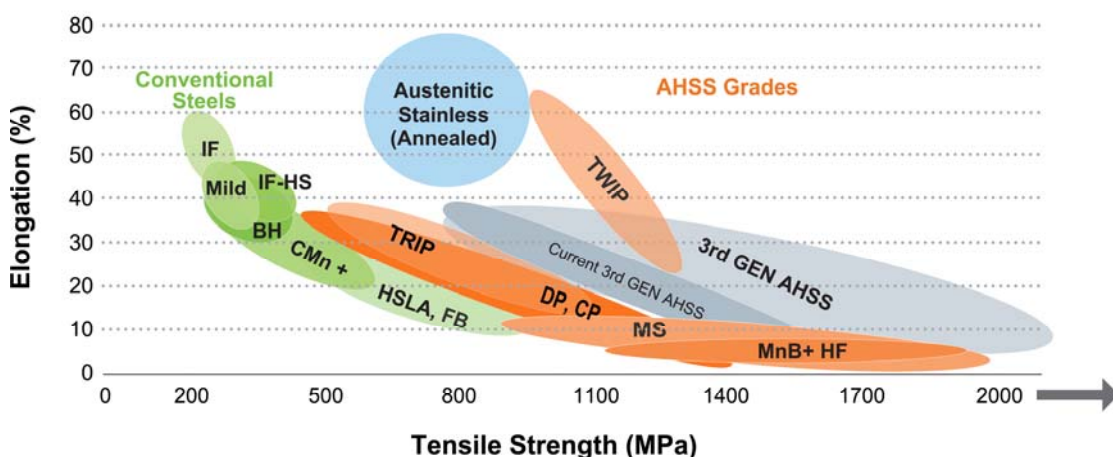


Figure 2.3 *Formability diagram of various types of steel (Keeler & Kimchi, 2014).*

The principle difference between HSS and AHSS is their microstructures (Keeler & Kimchi, 2014). Conventional HSS usually consist of a single phase ferritic steel. AHSS have a microstructure containing not just a ferrite phase, but also other phases.

The processing schemes for DP, TRIP, CP and MS steels can briefly be described as (Demeri, 2013):

- DP steels are produced by controlling the cooling rate from the austenite phase in hot rolled products, or from the two phase ferritic austenite region in hot rolled products or continuously annealed and hot dip products. This controlled cooling rate transforms some of the austenite to ferrite before a rapid cooling takes place which transforms the remaining austenite to martensite.
- TRIP steels get their microstructure via the use of an isothermal hold at an intermediate temperature, which produces some bainite. The high silicon and carbon content results in significant volume fractions of retained austenite.
- CP steels have a similar cooling configuration as TRIP steels with the difference that the chemistry is adjusted to produce less retained austenite and also to include fine precipitates in order to strengthen the martensite and bainite phases.
- MS steels are produced by a rapid quenching which transforms most of the austenite to martensite.

2.3.2 Toughness

Toughness defines the ability to absorb energy in a material. To avoid brittle failure, i.e. failure that occurs without prior notice and negligible plastic deformations, steel with high toughness are necessary. Toughness is measured by a standardized test, called Charpy-V notch test, which should be carried out according to EN 10045. To consider steel as ductile, the test specimen should have a toughness of 27J or higher at the test temperature. The type of fracture depends on the magnitude of the load, the user temperature and thickness (Kuoppa, et al., 2010). Extracts from SS EN 1993-1-10 which illustrates the impact strength for different HSS compared to NSS are summarized in Table 2.6. The table show that HSS have higher toughness than NSS at tested temperatures, which results in more advantageous welding properties (Samuelsson & Schröter, 2005).

Table 2.6 *Impact strength of NSS and HSS with different delivery conditions.*

Steel grade	Subgrade	Test temperature [°C]	Impact energy [J _{min}]
S355	JR	20	27
	J0	0	27
	J2	-20	27
S460	Q	-20	30
	M, N	-20	40
	QL	-40	30
	ML, NL	-50	27
	QL 1	-60	30
S690	Q	-20	30
	QL	-40	30
	QL1	-40	40

2.4 Chemical properties

Different mixtures of chemical compositions in steel will influence the various properties that a steel can achieve. Table 2.7 refers to the HSS grades S460ML and S690QL, which are examples of two available steel grades manufactured by the Swedish steel producer SSAB. The chemical properties of the S355J2 steel (Samuelsson & Schröter, 2005) is given for comparison.

Table 2.7 Chemical composition of S355J2, S460ML and S690QL with extracts from the EN 10025 requirements.

	S355J2		S460ML		S690QL	
	EN 10025 Part 2	typical analysis t = 50 [mm]	EN 10025 Part 4	Analysis values 8 ≤ t ≤ 70 [mm]	EN 10025 Part 6	Analysis values 3.1 ≤ t ≤ 30 [mm]
C	≤0.22	0.17	≤0.16	0.14 (max%)	≤0.20	0.20 (max%)
Si	≤0.55	0.45	≤0.60	0.50 (max%)	≤0.80	0.60 (max%)
Mn	≤1.60	1.50	≤1.70	1.70 (max%)	≤1.70	1.60 (max%)
P	≤0.025	0.018	≤0.025	0.020 (max%)	≤0.020	0.020 (max%)
S	≤0.025	0.015	≤0.020	0.015 (max%)	≤0.010	0.010 (max%)
Al	-	-	-	0.02 (min%)	-	-
Nb	-	-	≤0.05	0.05 (max%)	≤0.06	-
V	-	-	≤0.12	0.10 (max%)	≤0.12	-
Ti	-	-	≤0.05	0.05 (max%)	≤0.05	-
Mo	-	-	≤0.20	-	≤0.70	0.70 (max%)
Ni	-	-	≤0.80	-	≤2.0	2.0 (max%)
Cu	≤0.55	-	≤0.55	-	≤0.50	0.30 (max%)
Cr	-	-	≤0.30	-	≤1.50	0.80 (max%)
B	-	-	-	-	≤0.0050	0.005 (max%)
CEV	0.47	0.42	0.47	0.43 (max%)	0.47	0.49
Pcm	-	0.26	-	-	-	-
CET	-	0.32	-	0.24 (max%)	-	0.32

Table 2.7 show that HSS consist of more micro-alloying elements than conventional steel. This influences the weldability. The carbon equivalent value (CEV) can be used to indicate the weldability of different steel grades which contains several different micro-alloying elements, as steel containing only carbon (Keeler & Kimchi, 2014). Different formulas exist to describe the carbon equivalent, see (2.1)-(2.3). The CEV-formula is often used as a measurement of the weldability for a specific steel, and is based on a publication from the International Institute of Welding (IIW - International Institute of Welding , 1968). The CEV is also incorporated in SS-EN 1011-2.

$$CEV = C + \frac{Mn}{6} + \frac{Cr + Mo + V}{5} + \frac{Cu + Ni}{15} \quad (2.1)$$

$$Pcm = C + \frac{Si}{30} + \frac{Mn + Cu + Cr}{20} + \frac{Ni}{60} + \frac{Mo}{15} + \frac{V}{10} + 5B \quad (2.2)$$

$$CET = C + \frac{Mn + Mo}{10} + \frac{Cr + Cu}{20} + \frac{Ni}{40} \quad (2.3)$$

Table 2.8 summarizes the range of CEV.

Table 2.8 Benchmark values of CE according to equation (2.3).

CEV	Weldability
Up to 0.35	Excellent
0.36-0.40	Very good
0.41-0.45	Good
0.46-0.50	Fair
Over 0.50	Poor

The CEV depends mainly on chemical composition of the steel, which can differ between steel manufacturers. The CEV depends also on the plate thickness, increasing thickness results in higher CEV. Regarding the weldability between the M-steel and Q-steel, it is obvious that M-steel has better properties for welding than Q-steel. However the weldability of Q-steel are though good enough to satisfy the quality of the weld, this is more closely described in section [2.6]

2.5 Steel design according to Eurocode 3

Three parts of the 1993 Eurocode are of interest in this Master's thesis:

- EN 1993-1-1: General rules and rules for buildings
- EN 1993-1-5: Plated structural elements
- EN 1993-1-12: Additional rules for the extension of EN 1993 up to steel grades S700

EN 1993-1-1 and EN 1993-1-5 only considers steel grades with yield strengths up to 460MPa. There area however a complimenting part, EN 1993-1-12, which gives additional rules for steel grades up to S700. This chapter describes the rules that needs to be followed in the design of steel members according to the Eurocodes listed above.

2.5.1 Classification of cross sections

EN 1993-1-1 defines four (1-4) cross section classes used in the design of steel members. The role of cross section classification is to identify the extent to which the resistance and rotation capacity of cross sections is limited by its local buckling resistance.

- 1) The cross section can form a plastic hinge with the rotation capacity required from plastic analysis without reduction of the resistance.
- 2) The cross section can develop their plastic moment resistance, but have limited rotation capacity because of local buckling.
- 3) The cross sections are those in which the stress in the extreme compression fiber of the steel member assuming an elastic distribution of stresses can reach the yield strength, but local buckling is liable to prevent development of the plastic moment resistance.
- 4) The cross sections are those in which local buckling will occur before the attainment of yield stress in one or more parts of the cross section.

Table 2.9 show how to determine what cross section class for an internal part subjected to bending, compression or a combination of bending and compression.

Table 2.9 Maximum width to thickness ratio for internal compression parts according to Eurocode 3.

Internal compression parts						
				Axis of bending		
Class	Part subject to bending	Part subject to compression	Part subject to bending and compression			
1						
	$c/t \leq 72\epsilon$	$c/t \leq 33\epsilon$	when $\alpha > 0,5$: $c/t \leq \frac{396\epsilon}{13\alpha - 1}$ when $\alpha \leq 0,5$: $c/t \leq \frac{36\epsilon}{\alpha}$			
2						
	$c/t \leq 83\epsilon$	$c/t \leq 38\epsilon$	when $\alpha > 0,5$: $c/t \leq \frac{456\epsilon}{13\alpha - 1}$ when $\alpha \leq 0,5$: $c/t \leq \frac{41,5\epsilon}{\alpha}$			
3						
	$c/t \leq 124\epsilon$	$c/t \leq 42\epsilon$	when $\psi > -1$: $c/t \leq \frac{42\epsilon}{0,67 + 0,33\psi}$ when $\psi \leq -1^*)$: $c/t \leq 62\epsilon(1 - \psi)\sqrt{(-\psi)}$			
$\epsilon = \sqrt{235/f_y}$	f_y	235	275	355	420	460
	ϵ	1,00	0,92	0,81	0,75	0,71

*) $\psi \leq -1$ applies where either the compression stress $\sigma \leq f_y$ or the tensile strain $\epsilon_y > f_y/E$

As

Table 2.9 shows, the cross section class of a member is dependent on the $\frac{c}{t}$ ratio which has a limit depending on ϵ . The value of ϵ is calculated according to (2.4).

$$\epsilon = \sqrt{\frac{235}{f_y}} \quad \text{Where } f_y \text{ is the yield strength in MPa} \quad (2.4)$$

Equation (2.4) shows that an increasing yield strength results in a lower value of ε , see Table 2.10.

Table 2.10 Value of ε for different steel grades.

	S355	S420	S460	S500	S550	S620	S690
ε	0.81	0.75	0.71	0.69	0.65	0.62	0.58

2.5.2 Flexural buckling

According to EN 1993-1-1 the buckling resistance of a member in compression should be verified against buckling as:

$$\frac{N_{Ed}}{N_{b,Rd}} \leq 1.0 \quad (2.5)$$

Where

N_{Ed} is the design value of the compression force

$N_{b,Rd}$ is the design buckling resistance of the compression member

The design buckling resistance of the compression member should be taken as:

$$N_{b,Rd} = \frac{\chi A f_y}{\gamma_{M1}} \quad \text{For class 1,2 and 3 cross-section} \quad (2.6)$$

$$N_{b,Rd} = \frac{\chi A_{eff} f_y}{\gamma_{M1}} \quad \text{For class 4 cross-sections} \quad (2.7)$$

Where χ is the reduction factor for the relevant buckling mode which is determined from the relevant buckling curve according to:

$$\chi = \frac{1}{\Phi + \sqrt{\Phi^2 - \bar{\lambda}^2}} \quad \chi \leq 1.0 \quad (2.8)$$

$$\text{Where} \quad \Phi = 0.5[1 + \alpha(\bar{\lambda} - 0.2) + \bar{\lambda}^2] \quad (2.9)$$

$$\bar{\lambda} = \sqrt{\frac{A f_y}{N_{cr}}} = \frac{L_{cr}}{i} \frac{1}{\lambda_1} \quad \text{For class 1,2 and 3 cross-sections} \quad (2.10)$$

$$\bar{\lambda} = \sqrt{\frac{A_{eff} f_y}{N_{cr}}} = \frac{L_{cr}}{i} \sqrt{\frac{A_{eff}}{A}} \frac{1}{\lambda_1} \quad \text{For class 4 cross-sections} \quad (2.11)$$

Where $\bar{\lambda}$ is the non-dimensional slenderness and where:

$$N_{cr} = \frac{\pi^2 EI_y}{L_{cr}^2} \quad \text{Elastic force for the relevant buckling mode} \quad (2.12)$$

$$\lambda_1 = \pi \sqrt{\frac{E}{f_y}} \quad \text{Slenderness} \quad (2.13)$$

$$i = \sqrt{\frac{I}{A}} \quad \text{Radius of gyration} \quad (2.14)$$

The imperfection factor α corresponds to the buckling curve obtained from EN 1993-1-1, the buckling curves are shown in Figure 2.4. According to SS-EN 1993-1-12 the rules of S460 in Figure 2.4 also applies for steel grades between S460 and S700.

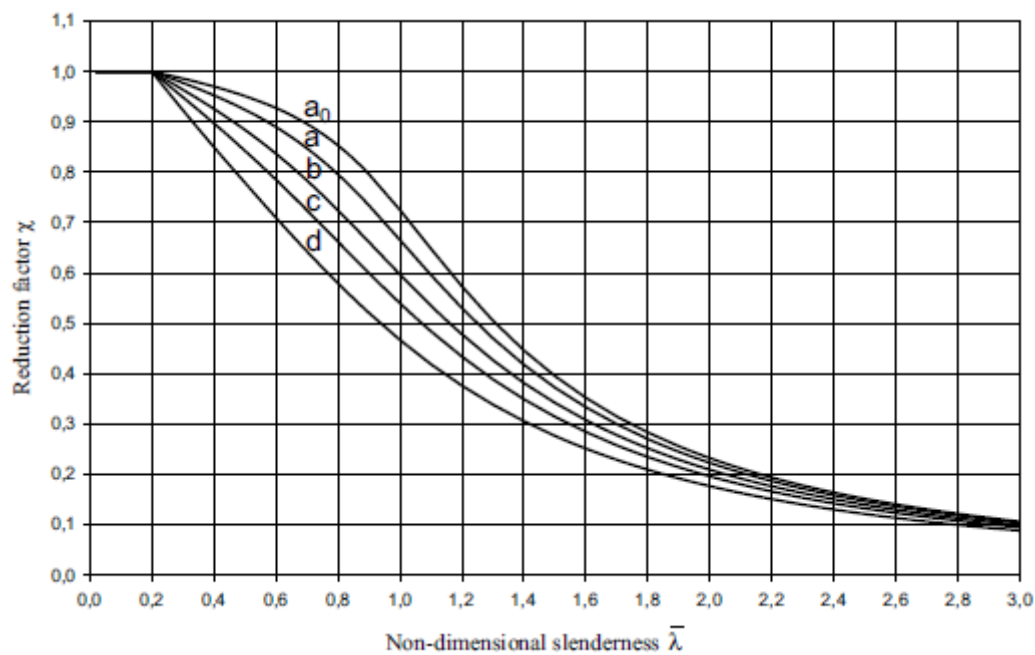


Figure 2.4 Buckling curves according to Eurocode 3.

2.5.3 Lateral torsional buckling

According to EN 1993-1-1 the design buckling resistance moment of a laterally unrestrained beam should be taken as:

$$M_{b,Rd} = \chi_{LT} W_y \frac{f_y}{\gamma_{M1}} \quad (2.15)$$

$W_y = W_{pl,y}$ for class 1 or 2 cross sections
 $W_y = W_{el,y}$ for class 3 cross sections
 $W_y = W_{eff,y}$ for class 4 cross sections

For the general case, the value of χ_{LT} for the appropriate non-dimensional slenderness λ_{LT} should be determined from:

$$\chi_{LT} = \frac{1}{\Phi_{LT} + \sqrt{\Phi_{LT}^2 - \beta \lambda_{LT}^2}} \text{ but } \begin{cases} \chi_{LT} \leq 1.0 \\ \chi_{LT} \leq \frac{1}{\bar{\lambda}_{LT}^2} \end{cases} \quad (2.16)$$

Where
$$\Phi_{LT} = 0.5[1 + \alpha_{LT}(\bar{\lambda}_{LT} - \bar{\lambda}_{LT,0}) + \beta \bar{\lambda}_{LT}^2] \quad (2.17)$$

$$\bar{\lambda}_{LT} = \frac{W_y f_y}{M_{cr}} \quad (2.18)$$

The following values for $\bar{\lambda}_{LT,0}$ and β are recommended:

$$\bar{\lambda}_{LT,0} = 0.4$$

$$\beta = 0.75$$

α_{LT} is an imperfection factor corresponding to the appropriate buckling curve, recommended values are given in Table 2.11. The buckling curves are presented in [2.5.2] Figure 2.4. M_{cr} is described in equations (2.19) and (2.20).

Table 2.11 Recommended values of imperfection factors for lateral torsional buckling curves.

Buckling curve	a	b	c	d
α_{LT}	0.21	0.34	0.49	0.76

The recommendations for buckling curves are given in Table 2.12.

Table 2.12 Recommended values for lateral torsional buckling curves.

Cross-section	Limits	Buckling curve
Rolled I-sections	$h/b \leq 2$	a
	$h/b > 2$	b
Welded I-sections	$h/b \leq 2$	c
	$h/b > 2$	d
Other cross-sections	-	d

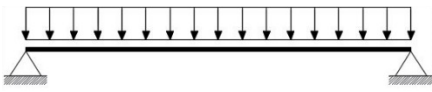

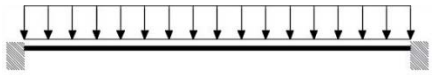

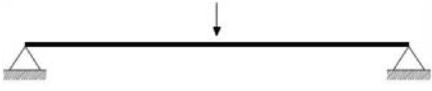

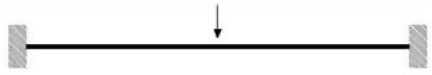

The elastic critical moment M_{cr} is calculated according to (2.19), derived from the buckling theory.

$$M_{cr} = C_1 \frac{\pi^2 EI_z}{(kL)^2} \left\{ \sqrt{\left(\frac{k}{k_w}\right)^2 \frac{I_w}{I_z} + \frac{(kL)^2 GI_t}{\pi^2 EI_z} + (C_2 z_g)^2} - C_2 z_g \right\} \quad (2.19)$$

The factor k refers to end rotation and should be taken as 1.0 if not less than 1.0 can be justified. The factor k_w refers to end warping and should be taken as 1.0 unless special provision for warping fixity is provided.

C_1 and C_2 are factors which depends on the section properties, support conditions and moment diagram. Table 2.13 gives values of C_1 and C_2 for a member which is transversally loaded.

Table 2.13 Values of C_1 and C_2 (for $k=1$)

Loading and support conditions	Bending moment diagram	C_1	C_2
		1.127	0.454
		2.578	1.554
		1.348	0.630
		1.683	1.645

If the bending moment diagram is linear or when the transverse load is applied in the shear center C_2 and z_g will be equal to zero and equation (2.19) can be simplified to equation (2.20).

$$M_{cr} = C_1 \frac{\pi^2 EI_z}{(kL)^2} \left\{ \sqrt{\frac{I_w}{I_z} + \frac{L^2 GI_t}{\pi^2 EI_z}} \right\} \quad (2.20)$$

Equation (2.15)-(2.20) show that the amount of influence of lateral torsional buckling on a beam is related to what cross section is used. If a cross section is kept constant while increasing the yield strength, the slenderness will increase and the reduction χ_{LT} will have a larger impact. Also, changing the cross section may change the cross section class, see [2.5.1].

2.5.4 Deflection

The governing variables that control the deflection of a beam is the geometry, length, magnitude of the applied load and the stiffness. With a decrease in cross section area the moment of inertia decreases and since the E -modulus always has a constant value,

this will directly influence the deflection of a beam, an example is shown in Figure 2.5. Equation (2.21)-(2.25) describes the deflections for the simply supported beam due to different load cases.

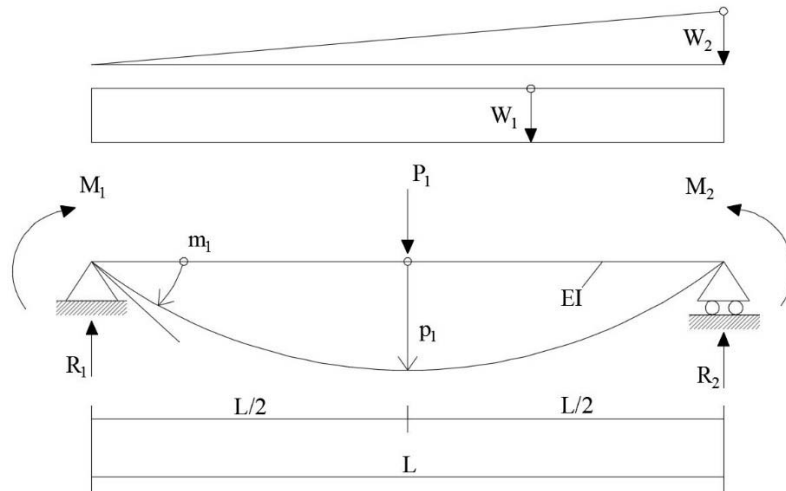


Figure 2.5 Simply supported beam and deflections.

$$p_1 = M_1 \frac{L^2}{16EI} \quad (2.21)$$

$$p_1 = M_2 \frac{L^2}{16EI} \quad (2.22)$$

$$p_1 = P_1 \frac{L^3}{48EI} \quad (2.23)$$

$$p_1 = W_1 \frac{5L^4}{384EI} \quad (2.24)$$

$$p_1 = W_2 \frac{L^4}{768EI} \quad (2.25)$$

2.6 Effects of an increased steel grade

There is a general impression that an increased steel grade will not optimize a structure in every way. Especially welding is an area where limitations are expected with HSS. This chapter describes more details regarding welding of steels and also studies made regarding effects on steels of different grades subjected to elevated temperatures.

2.6.1 Weldability

During welding, the temperature of the steel is increased which will influence the microstructure of the material (Kuoppa, et al., 2010). The zone affected is called the heat affected zone (HAZ), and is shown in Figure 2.6. How large the HAZ is depends on the cooling time, which itself depends on several factors such as heat input, thickness and type of welding. The HAZ should be as small as possible to maintain

ductility and strength. Defects that are dependent on the material could be for instance cold cracks or hot cracking.

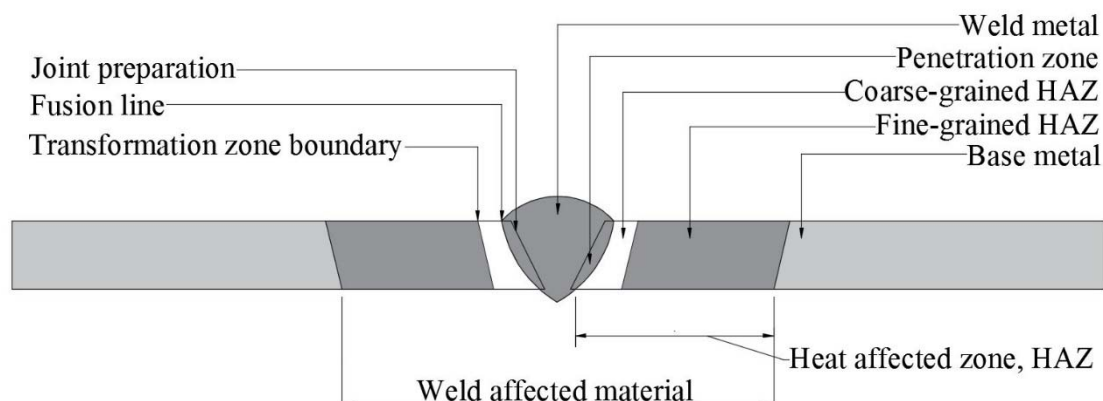


Figure 2.6 Heat affected zone of a weld (Lancaster, 1997)

Cold cracks occur for temperatures below 200 °C and are often very difficult to detect (Kuoppa, et al., 2010). They occur due to a brittle microstructure in combination with hydrogen and large stresses occurring during cooling of the weld. To determine the risk of cold cracks, the carbon equivalent value is a good guideline, see equation (2.1). Generally, a lower value means less risk of cold cracks.

Hot cracking occurs at much higher temperatures (above 1200 °C) (Kuoppa, et al., 2010). They are generally easier to detect than cold cracks but can still sometimes be invisible to the naked eye. A general recommendation to avoid hot cracking is that the height of the weld should not exceed the width of the weld. Also, the amount of carbon, phosphor and niob present in the weld affects the risk of hot cracking.

The microstructure of HSS is influenced during welding. A result of this is that the structural performance of the steel may be influenced. However, as QT and TM methods have been improved, lower carbon equivalents in combination with high toughness have made it possible to weld without a problem (Samuelsson & Schröter, 2005). Good welding properties combined with smaller plate thicknesses result in a reduced welding volume, labor and less costs. Welding of steel up grades up to S700 is regulated in SS-EN 1993-1-12.

When welding in HSS, filler material can be chosen as undermatching, matching or overmatching (Kuoppa, et al., 2010). Undermatching filler material is low alloy with lower strength than the base metal. Matching and overmatching filler materials have equal or higher strength than the base metal. Undermatching filler material is advantageously selected when welded joints is located in areas with low stress and/or when the weld is not transversally loaded. Under the right circumstances in fatigue-loaded joints, undermatching filler material could also be used to achieve more favourable weld geometries. Transversally loaded welded joints located in the most stressed areas, requires properties that complies with the base metal. Such welded joints should use matching and overmatching filler material. To fulfil that requirement, it is necessary to use adapted welding energies. The choice of filler material also depends on the product delivery condition. TM steel should normally be welded with matching or overmatching filler material while for QT steel, undermatching material is recommended. For QT steels with yield strength greater

than 500 MPa the major benefit of using undermatched filler material is increased toughness in the weld metal, reduced sensitivity to cracking and improved ductility in the joint.

In SS-EN 1993-1-12 it is stated that undermatched filler material used for steel grades greater than S460 up to S700, f_u should be replaced with the ultimate strength of the filler material, f_{eu} . Table 2.14 contains the substituted strength for electrodes.

Table 2.14 Ultimate strength, f_{eu} of electrodes.

Strength class	35	42	55	62	69
Ultimate strength, f_{eu} [MPa]	440	500	640	700	770

The weldability of HSS depends strongly on the delivery condition of the steel and the CEV, see [2.4]. Two common delivery conditions of HSS are TM and QT. According to (Willms, 2009), there are major differences between the steel types when working range of weldability is compared. Figure 2.7 show the difference in working range of structural steels. Three structural steels with different thickness are compared, S355J2 (80 mm), S500M (50 mm) and S690QL (30 mm). The typical behaviour of the steel show that working with QL steel requires both higher accuracy and higher pre-heating temperatures to obtain sufficient capacity in the weld. The TM steel has excellent working range properties, which provides the possibility of high safety and cost efficient welding, especially when performing on-site welding. Despite the differences between QT and TM, it is possible to weld in QT-steel with excellent results as long the user comply with the regulations and the steel manufacturers recommendations.

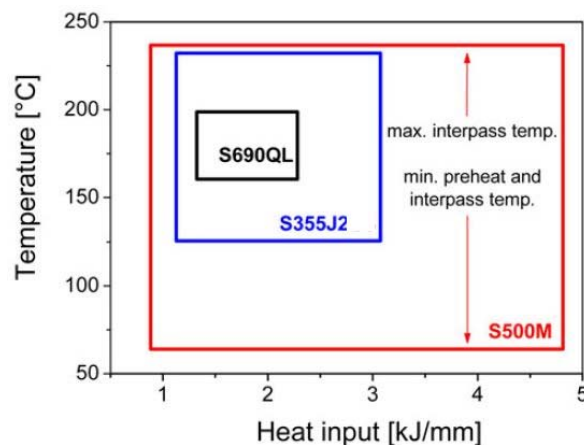


Figure 2.7 Comparison of typical working range for steel grades, S355J2, S500M and S690QL (Willms, 2009).

2.6.2 Properties of HSS on elevated temperatures

Design regarding fire resistance in steel construction is found in SS-EN 1993-1-2, which considers steel qualities up to S460. For higher steel grades, a limited amount of research have been made to establish if there are any differences. However, in 2012 (Qiang, et al., 2012) performed two studies for S460 and S690 steel and was able to draw some conclusions, the studies are presented below.

Study 1

This study made by (Qiang, et al., 2012) included both steady state and transient state tests of a quenched and tempered S690 steel. In the steady state test, specimens were heated up to a specific temperature and then loaded until failure. The heating rate was 50 °C/min and the temperatures were 100, 200, 300, 400, 500, 550, 600 and 700 °C. Two specimens were tested for each temperature. In the transient test, the specimens were exposed to a constant tensile load as the temperature increased until failure occurred. The heating rate was 10 °C /min and the tensile stress levels were 100, 200, 300, 400, 500, 600, 650, 700, 800, 850 and 900 MPa (Qiang, et al., 2012).

The elastic modulus decreases when steel is subjected to elevated temperatures, resulting in deteriorated material properties such as larger deformations and reduced load bearing capacities (Qiang, et al., 2012). The heat affected elastic modulus is represented by a reduction factor given by the ratio between the elastic modulus on some elevated temperature and the elastic modulus at an ambient temperature of 20 °C. The reduction factors and measured elastic modulus from the steady state test and transient state test, compared to what is recommended in Eurocode are given in Table 2.15.

Table 2.15 Reduction factors (RF) from steady state test, transient state test and Eurocode 3.

Temperature [°C]	Steady state		Transient state		Eurocode 3
	RF	E-modulus [MPa]	RF	E-modulus [MPa]	
20	1.000	204.69	1.000	205.89	1.000
100	1.000	204.59	0.982	202.27	1.000
200	0.875	179.15	0.869	178.87	0.900
300	0.839	171.82	0.841	173.24	0.800
400	0.775	158.61	0.736	151.46	0.700
500	0.685	140.13	0.647	133.15	0.600
600	0.372	76.11	0.370	76.24	0.310
700	0.141	28.85	0.099	20.48	0.130

Similar behavior for the yield strength occurs at elevated temperatures, high temperatures results in reduced yield strength (Qiang, et al., 2012). The reduction factor for yield strength is calculated in the same way as for the elastic modulus, i.e the ratio between the yield strength at some elevated temperature and on the ambient temperature of 20 °C. The reduction factors from the steady state test, transient state test and Eurocode 3 is given in Table 2.16.

Table 2.16 Reduction factors from steady state test, transient state test and Eurocode 3

Temperature [°C]	Steady state	Transient state	Eurocode 3
20	1.000	1.000	1.000
100	0.968	0.923	1.000
200	0.982	0.868	1.000
300	0.975	0.855	1.000
400	0.850	0.798	1.000
500	0.624	0.716	0.780
600	0.371	0.445	0.470
700	0.133	0.203	0.230

Table 2.15 and Table 2.16 show that the Eurocode which regulates steel up to S460 cannot always be applied on an S690 steel. The reduction factor for the E -modulus from Eurocode is generally conservative, but the reduction factor for the yield limit is not.

Study 2

In this study made by (Qiang, et al., 2012) evaluated the post fire mechanical properties of normalized rolled S460 steel and quenched and tempered S690 steel. The steady state method was used, where a tensile test was performed on the specimen which had been heated to a certain temperature and then cooled down to the ambient temperature. In the experiment, the S460 steel was heated up to 300, 400, 500, 600, 650, 700, 750, 800, 850, 900 and 1000 °C. The S690 steel was apart from these temperatures also heated up to 100 and 200 °C (Qiang, et al., 2012).

As for the previously presented study by (Qiang, et al., 2012), the residual factors were calculated in the same way for the elastic modulus and yield strength. The residual factors for elastic modulus and yield strength are shown in Figure 2.8 and Figure 2.9 respectively.

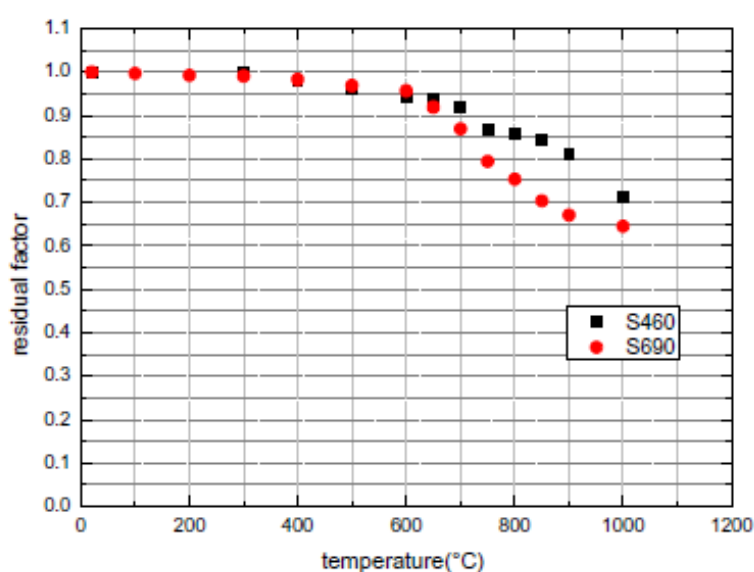


Figure 2.8 Elastic modulus residual factors (Qiang, et al., 2012)

Figure 2.8 shows that the steels can regain most of their elastic modulus when cooled down after exposed to temperatures below 600 °C. Beyond this point there is a loss of elastic modulus for both steel grades, where the S690 seems to degrade quicker.

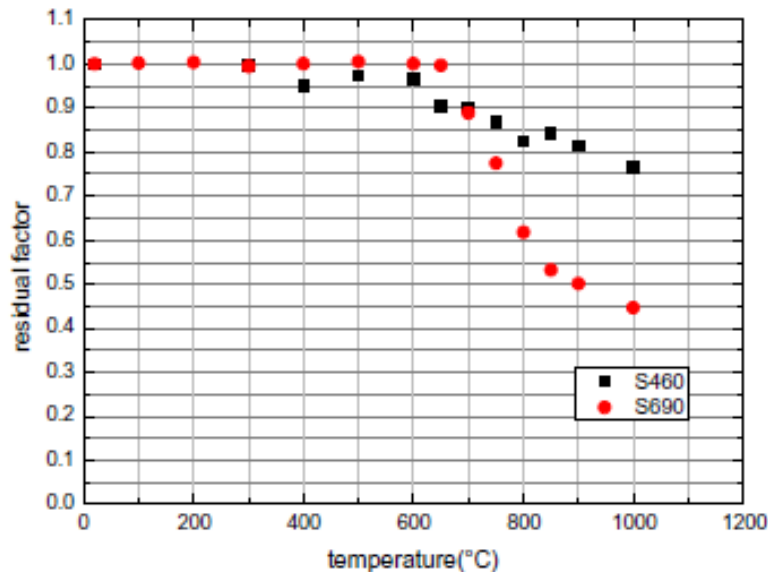


Figure 2.9 Yield strength residual factors (Qiang, et al., 2012).

As for the loss of elastic modulus, the yield strength is regained when the steels are cooled down from temperatures below 600 °C. After this, the S690 steel experiences a greater loss of yield strength compared to the S460 steel.

The conclusion from the second study made by (Qiang, et al., 2012) is that the steel grade has quite a significant influence on the post fire mechanical properties. For S460 and S690 steels it is concluded that they are not affected until they are exposed to a fire temperature above 600 °C. After this a drastic degradation of strength is seen (Qiang, et al., 2012).

2.7 High strength steel in existing structures

Regarding conventional structures, the use of HSS is very limited. There are however some examples where benefits of HSS have been used in bridges, arenas and other larger structures. This chapter contains some examples and studies, which presents the results of increased steel grades.

2.7.1 Truss structures

Friends Arena

The roof structure of Friends Arena in Solna, Sweden, is one example where various grades of HSS is used. In the beginning of the project, discussions whether the roof opening system should consist of steel or not was an important issue. The sense of an outdoor feeling was of great importance and the use of a light frame HSS structure solved that problem. It was therefore decided to use steel in the roof opening system.

The main trusses of the roof consists of three different HSS grades, where the top chord of the main trusses is made of S460, the U-shaped profile in the bottom chord is

made of S690 and the tension bars is made from S900 (Cederfeldt & Sperle, 2012). A 3D-model of a main truss is shown in Figure 2.10.

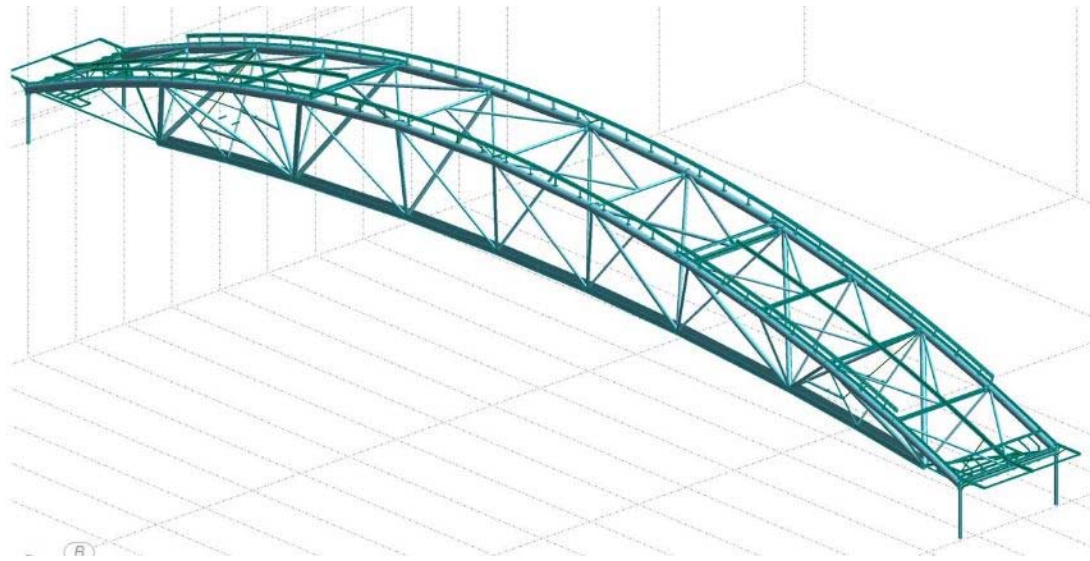


Figure 2.10 3D-model of one main truss in the roof structure of Friends Arena. The truss spans 162m, has a maximum height of 16m and a width of 15.3m. (Cederfeldt & Hansson, 2010).

A result of the implementation of HSS savings in weight and cost. The total amount of saved steel was 585 tons, or 12.8 % and the cost savings amounted to 2.2 million EUR by using HSS instead of conventional S355 steel (Cederfeldt & Sperle, 2012).

Airbus hangar, Frankfurt

In 2008, the Airbus hangar on Frankfurt airport was inaugurated. This building can hold up to five Airbus 380 at the same time, which demanded a large open space of 180 m by 120 m. To manage the span of 180 m, a special truss beam made from a modified type of S460ML was designed. To guarantee a yield strength of minimum 460 MPa for plates thicker than 120 mm, the TMCP S500ML steel was used (Willms, 2009). The hangar is shown in Figure 2.11.



Figure 2.11 Airbus hangar at Frankfurt Airport (Willms, 2009).

Sony Center, building F, Berlin

To meet the architectonic demands when designing Sony Center building F, usage of HSS was prerequisite. The function of the truss girders is to keep the apartment section of the building separated from a facade of an old hotel. The truss girders are made of welded box sections with S460ML plates with thickness up to 110 mm. In the nodes between the diagonals and the flanges areas, high stresses occurred. To manage the stress, steel details made of S690QL1 was used (Shröter, 2006). The building is shown in Figure 2.12.



Figure 2.12 HSS truss girders in Sony Center building F, Berlin (Anon., 2016).

2.7.2 Bridges

Bridges around the world have for several years used HSS which have been proven beneficial. Economical savings have been notified in several projects. In both Europe and the United states studies have been made to investigate where the benefits are notified using HSS in bridge construction. The studies are presented below.

COMBRI

The European Commission's Research Fund for Coal and Steel program has financed a research program called "Competitive steel and composite bridges by innovative steel plated structures – COMBRI". The study had a goal to make advances in future bridge design. Special focus was given to verify Eurocodes regarding plate buckling of steel plated structures. An outstanding result of the program was:

- The use of hybrid girders: the redesign of a S355 steel box girder, proposing a S460 and S690 steel hybrid girder, gives a reduction in cost of material of 10 % in spans and 25 % at the piers (Fundazioa, 2009).

HSS in the United States

In the United States the definition high performance steel (HPS) is used for steel grades with high yield limits, and is equal to the definition used in this report, high

strength steel. In 1994 the Federal Highway Administration (FHWA), the U.S. Navy and the American Iron and Steel Institute (AISI) launched a program to develop HPS for bridges. In “HIGH PERFORMANCE STEEL DESIGNERS GUIDE” written by the U.S. Department of Transportation, reflections and experiences by researchers, fabricators, manufacturers, owners and engineers working with HPS are described. The goal of the program was to gain more knowledge about HPS and how to best implement it in bridge construction (Lwin, 2002). The report includes a historical review of the usage of HPS in bridges, as well as material properties and design features. The steel considered is HPS 70W which corresponds to a yield strength of 485 MPa.

A numerous amount of bridges using HPS 70W are described briefly in the report, the first built in 1997. At about the same time the Martin Creek Bridge in Pennsylvania was designed, using HPS 70W for the girders and 50W, which corresponds to a yield strength of 345 MPa, for the cross frames. A comparison was made to if the bridge would be designed using only grade 50W. The result was that with the hybrid design, about 24 % reduction in steel weight and 10 % savings in cost, was accomplished. This experience, together with other experiences from HPS bridges built in Nebraska, Tennessee, Pennsylvania and New York concluded in a number of benefits using HPS in bridges, some of them are presented here (Lwin, 2002):

- Usage of HPS allows designers to use fewer lines of girders to reduce weight, use shallower girders to solve vertical clearance problem and also increase span lengths.
- Improved weldability of HPS eliminates hydrogen induced cracking, reduces the cost of fabrication by lower preheat requirement and improves the quality of weldment by using low hydrogen practices.
- Significantly higher fracture toughness of HPS minimizes brittle and sudden failures of steel bridges in extreme low service temperatures. Higher fracture toughness also means higher cracking tolerance, allowing more time for detecting and repairing cracks before the bridge becomes unsafe.
- HPS girders can be optimized by using a hybrid combination of HPS 70W in the negative moment top and bottom flanges and 50W or HPS 50W in other regions.
- Optimized HPS girders have shown to result in lower first cost and are expected to have lower life-cycle cost.

2.7.3 Tension rods

High strength steel is best utilized in applications where neither local buckling nor global buckling sets the limits for the material, such applications are tension rods (Ahlenius, et al., 1995). It is widely used in cables of suspension bridges, e.g. in the design of Hålogaland Bridge (under construction) where cables with a wire strength of 1770 MPa are used (Jensen & Matthew, 2009).

2.8 Example of experimental studies

In recent years there have been made several experimental studies on the behavior of structural elements such as columns, beams and plates with yield strengths ≥ 460 MPa.

In this chapter some of the experiment will be presented with focus on; which type of member was tested, how the tests were performed and the outcomes of the tests.

2.8.1 Columns

Three studies are presented where the buckling behavior of HSS is evaluated and compared to Eurocode 3.

Study 1

In “Experimental and numerical study on the behavior of axially compressed high strength steel columns with H-section” by (Wang, et al., 2012), six welded H-columns made from flame-cut steel plates were tested. Dimensions of the six columns are shown in Table 2.17.

Table 2.17 Measured dimensions of specimens (Wang, et al., 2012).

Specimen	B [mm]	H [mm]	t_w [mm]	t_f [mm]	λ
H-3-80-1	154.5	171.2	11.5	21.0	82.5
H-3-80-2	154.7	171.2	11.4	21.0	81.9
H-5-55-1	227.8	245.8	11.5	21.3	56.2
H-5-55-2	229.0	245.5	11.6	21.2	56.0
H-7-40-1	308.8	317.3	11.5	21.0	41.5
H-7-40-2	308.3	318.5	11.5	21.2	41.6

All the columns in the experimental part had a nominal yield strength of 460 MPa, a length of 3.0 m and were loaded with a centric axial force until failure occurred. The columns were pin supported at both ends, with the ability to rotate about the weak axis but restrained about the strong axis.

The results from the experimental part regarding residual stresses and geometrical imperfections were implemented in a nonlinear finite model. The model was then used to perform an extensive parametric study. The purpose of this study was to investigate how the design curves in Eurocode 3 and the Chinese codes for steel structures GB 50017-2003 corresponds with the results from the experimental- and numerical part in the experiment, and to find suitable design curves.

In the experimental study, some observations regarding the initial geometric imperfection between the tested columns were observed. It showed that columns with the same cross-sectional dimensions but different initial geometric imperfections had different capacities in bending stiffness and ultimate strength. The columns with smaller imperfections obtained higher bending stiffness and higher ultimate strength. This phenomena applies to the other two pairs of columns. By comparing the three set of tested columns it can be observed that columns with larger slenderness are more sensitive to geometrical imperfections. Figure 2.13, Figure 2.14 and Figure 2.15 show the different behavior of the three pairs of columns with respect to initial geometric imperfection.

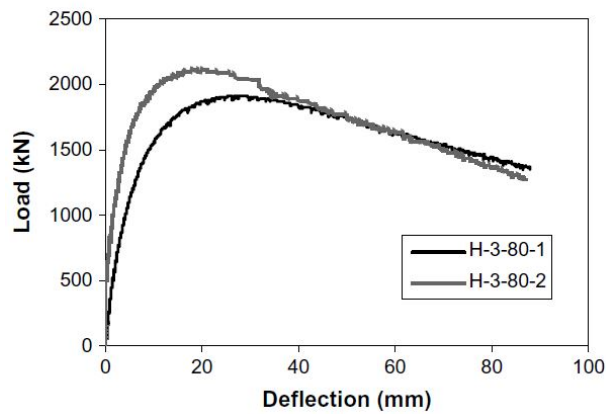


Figure 2.13 Load-deflection curve for columns with smallest dimensions (Wang, et al., 2012)

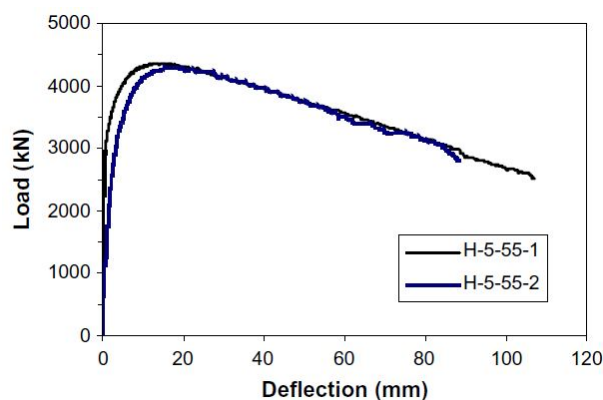


Figure 2.14 Load-deflection curve for columns with intermediate dimensions (Wang, et al., 2012).

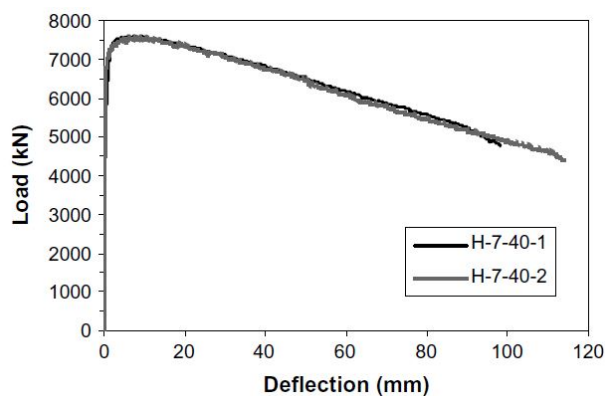


Figure 2.15 Load-deflection curve for columns with largest dimensions (Wang, et al., 2012).

In the parametric study based on the results from the experimental part, a Finite Element Method-model (FEM-model) consisting of 72 pin-ended columns was created to investigate the effect of residual stresses and the initial geometric imperfections. The columns were loaded with an axial compression force and the behavior both around the weak axis and the strong axis were analyzed. The columns were divided into three groups with a slenderness varying between 20 and 130.

Based on the experimental part and the numerical part the outcome of this study indicates that design curve b in Eurocode 3 corresponds better than the prescribed curve c for welded hollow section columns made from flamed cut Q460 HSS plates. Figure 2.16 show the relationship between the design curves in Eurocode 3 and the data from the tested columns. According to the test results, curve c underestimates the ultimate strength by 16.1 % in average. The study also shows that hollow section columns made from HSS are less sensitive to geometrical imperfections than columns made from conventional steel, this applies particular for columns with a non-dimensional slenderness of approximately 0.97.

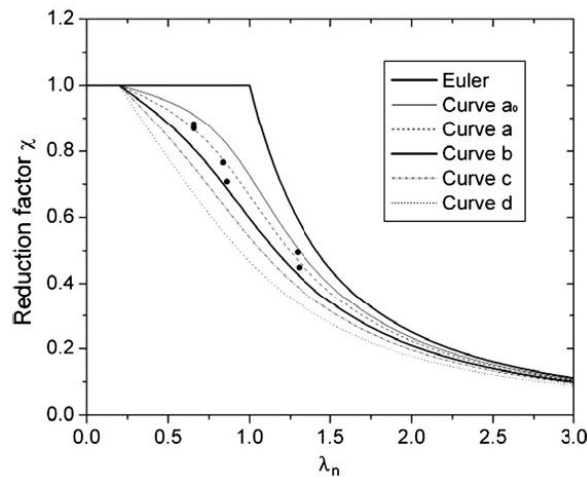


Figure 2.16 Relationship between design curves in Eurocode 3 and values measured from the tested columns (Wang, et al., 2012).

Study 2

In the study “Test and numerical study of ultra-high strength steel columns with end restraints” by (Shi, et al., 2012) eight welded end restrained I-section columns made from HSS were tested, four columns with a yield strength of 690 MPa and four columns with a yield strength of 960 MPa. The length of the columns varies between 1.3 m – 3.6 m. In essence, the study consisted of an experimental part and a numerical part. In the experimental part, eight columns, restrained about the minor axis subjected to an axial compression force, were loaded until failure occurred. The numerical part consists of 24 pin-ended columns modeled with a finite element software program. The properties of the 24 modeled columns were partly based on the results from the experimental part. The purpose of the study was to investigate the overall buckling behavior of the columns and compare the results with the design curves in Eurocode 3, the American specification ANSI/AISC and the Chinese design code GB50017-2003.

According to the study, the overall buckling behavior of the columns in the experimental part shows that the transverse deformations increase gradually with the increase of the compressional force, and the deformation continues to grow after the material has reach the ultimate value. Figure 2.17 displays load-displacement curves measured with three sensors (DT3, DT4 and DT5), the curves corresponds well to each other which indicates that pure flexural buckling without any torsional deformation occurs.

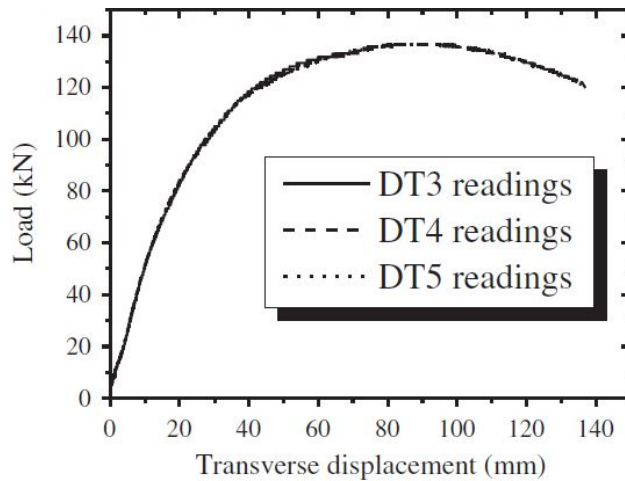


Figure 2.17 Load-displacement curves measured at the mid length of one column with yield strength of 690MPa (Shi, et al., 2012).

The results of the overall buckling capacity of the columns are based on design curve b in Eurocode 3. However, the outcomes of the test results are poor, only two of the tested columns have a buckling strength that exceeds the specifications in the design code for curve b. The main reason for this is because of the initial geometrical imperfection. The adopted value of the ratio of the imperfections in Eurocode 3 and GB50017-2003 is 1 ‰, the average value of the tested columns is 6.06 ‰ with the highest value as high as 10‰. Therefore, according to the report, a comparison between the tested columns and the design curves is not appropriate. The results of the tested columns can be seen in Figure 2.18.

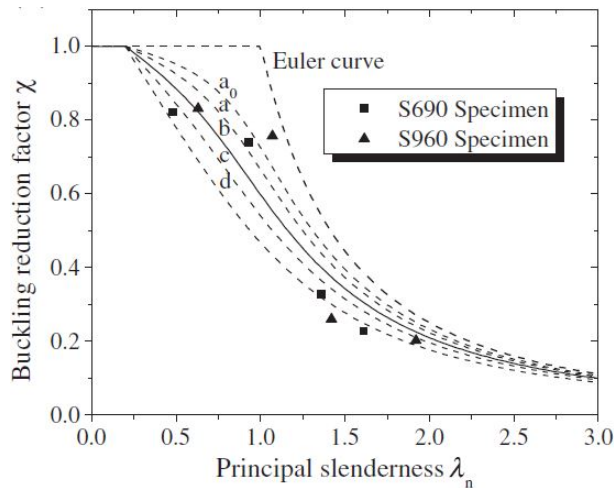


Figure 2.18 Calculated non-dimensional buckling strength from test compared with design curves in Eurocode 3 (Shi, et al., 2012).

The FEM-model was created and verified based on the results from the eight previously tested columns. After the verification of the FEM-model, 24 pin-ended columns with the same steel strength and dimensions as the eight columns were computed and investigated. To obtain a more reasonable comparison between the results of the Finite Element Analysis (FEA) and the design curves, the initial imperfection factor is set to 1 ‰. Residual stresses were not measured in the experimental part, but in the FEM-model compressive residual stresses were calculated and applied.

Based on the outcomes of the study, some conclusions were made. For welded I-section pin-ended columns made of S690 and S960, the non-dimensional buckling strength about the major axis is higher than the recommended design curve b in Eurocode 3 and GB50017-2003. According to the report, it is suggested to choose curve a and a₀ in Eurocode 3 and GB50017-2003 when designing welded I-section columns made from S690 and S960 with respect to buckling about the major axis. The comparison between the calculated buckling strength from the FEM-model and the design strength curves according to Eurocode 3 is shown in Figure 2.19.

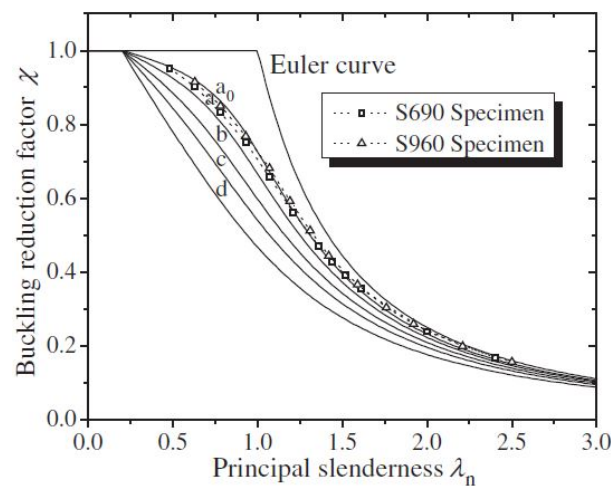


Figure 2.19 Comparison between design curves in Eurocode 3 and calculated values from the FEM-model (Shi, et al., 2012).

Study 3

In the study “Overall buckling behavior of 460 MPa high strength steel columns: Experimental investigation and design method” by (Huiyong, et al., 2012) twelve welded columns with a yield strength of 460 MPa were tested, five with a box-section geometry and seven with an I-section geometry. In the study a validated FEM-model based on the results from the present experimental part and from previous studies was used to evaluate a large number of columns. The purpose of the study was to investigate the overall buckling behavior of the columns and to compare the results with the design curves in Eurocode 3, the American specification ANSI/AISC and the Chinese design code GB50017-2003.

The columns in the experimental part are manufactured by flame-cut HSS plates. All the sections were designed as compact ones, i.e. they were supposed to fail due to overall buckling instead of local buckling. The dimensions of the columns were also restricted by the maximum load capacity of test equipment. The overall buckling behavior of the columns were investigated both around the major axis and the minor axis. The effect of initial imperfections such as initial bow and residual stresses were included in the experimental part of the study. The effect of load eccentricity were also considered.

Regarding the overall buckling behavior of the twelve tested columns, inelastic flexural overall buckling were the cause of failing. This occurred without any interaction of local buckling. The results from the buckling capacities of the various columns were then used to calculate the buckling factor to obtain values to be compared with the existing design codes.

Based from the test results of the experimental part, a FEM-model was created, verified and a test of 220 pin-ended columns were conducted. Residual stresses and a geometrical imperfection factor of 1 ‰ were implemented in the model. The values of the residual stresses were based from the calculations made in the experimental part and the geometrical imperfection of 1 ‰ were used to be consistent with the adopted value which Eurocode 3 and GB50017-2003 is based on.

The results regarding the overall buckling behavior of the columns from the experimental part compared with the design curves in Eurocode 3 are shown in Figure 2.20. For I-section columns, design curve b or c was adopted depending if rotation about major respective minor axis is considered. For the box-sections, design curve c was adopted. The results are scattered below and above the proposed design curves. The columns that lie beneath the curves does that mainly because the large initial geometrical imperfections. The researchers in this paper states that further numerical studies need to be done to get more reasonable and accurate data regarding the initial imperfections.

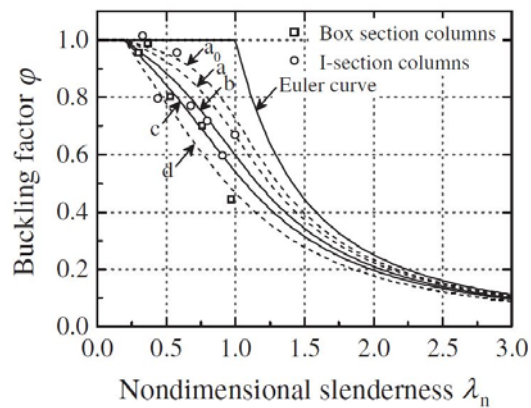


Figure 2.20 Experimental results compared with design curves in Eurocode 3 (Huiyong, et al., 2012).

The overall buckling behavior of the columns from the FE-analysis is compared with the design curves in Eurocode 3, the results are shown in Figure 2.21, Figure 2.22 and Figure 2.23. Based on the results from the FE-analysis some conclusions were made. It showed that I-section and box section columns made from welded flame-cut HSS plates have higher values than the corresponding design curves in the design codes. Compared to NSS, the non-dimensional buckling strength of HSS is substantially improved. The reason is the effect of imperfections is less severe than columns made from NSS. Based on the results in the study, it is suggested that the design curves could be selected in a different way, thus the curves in Eurocode 3 are slightly conservative.

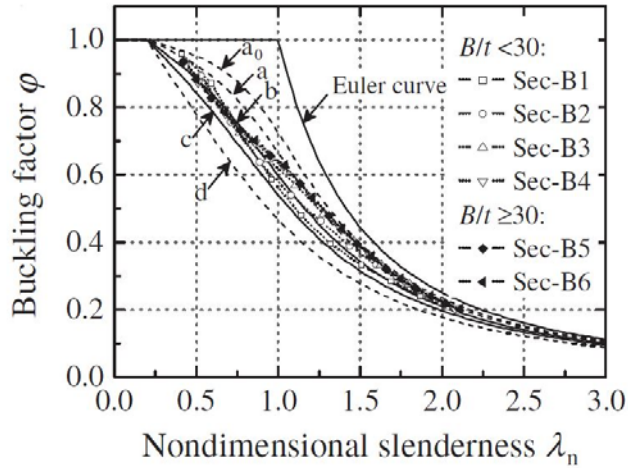


Figure 2.21 Comparison of design curves in Eurocode 3 with the FEA results for box section columns (Huiyong, et al., 2012)

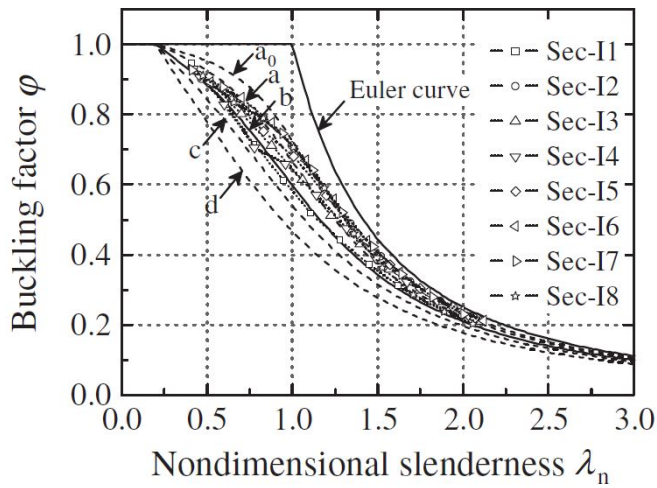


Figure 2.22 Comparison of design curves in Eurocode 3 with the FEA results for I-section columns, buckling around minor axis (Huiyong, et al., 2012)

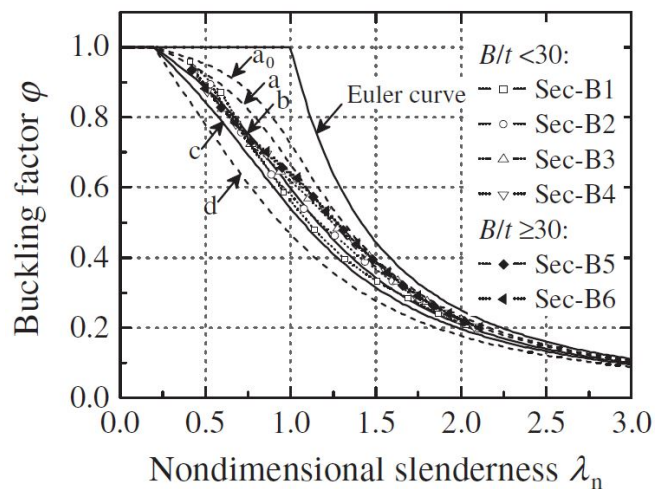


Figure 2.23 Comparison of design curves in Eurocode 3 with the FEA results for I-section columns, buckling around major axis (Huiyong, et al., 2012)

2.8.2 Beams

In a paper by (Hladnik, 1996) experimental and non-linear numerical analysis of the local stability of different beams was performed. The experimental part was carried out on ten beams with different flange slenderness which were loaded until failure. The non-linear numerical study was performed on six beams with different web slenderness. The purpose of the study was to evaluate and establish a more “accurate” slenderness limit for Class 3 cross section welded I-beams made of high strength steel (Hladnik, 1996).

The test beams were made of fine grained micro alloyed high strength steel with a nominal yield strength of 700 MPa (Hladnik, 1996). MAG welding was used to produce a 5 mm, 690 MPa, weld between the web and the flange. Lateral buckling was prevented for all beams except for the beam with the narrowest flange due to that numerical analysis showed that local buckling of the compressed flange and lateral buckling of the middle part of them beam would occur approximately at the same time. Two concentrated forces was applied to the beam which is illustrated in Figure 2.24 along with the dimensions of the beams and the position of the lateral supports.

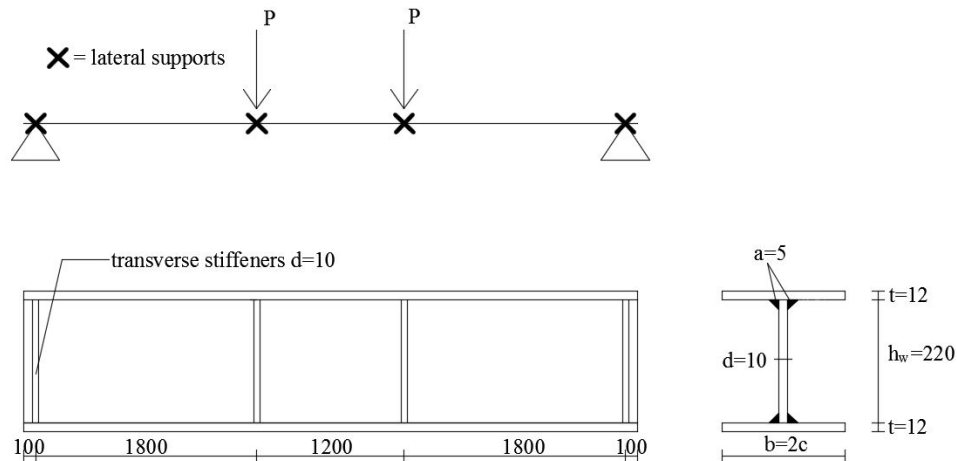


Figure 2.24 Static scheme and nominal dimensions (mm) of test beams (Hladnik, 1996).

Each test beam group (A-E) consists of two beams with the same nominal dimensions. All webs were in cross section class 1 according to EN 1993-1-1.

The geometrical imperfections are taken into account, see Figure 2.25, and are measured in the middle of the span. All values are illustrated in Table 2.18.

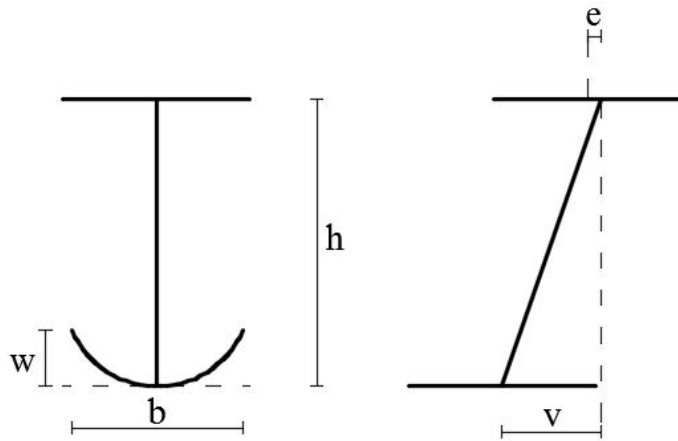


Figure 2.25 Geometrical imperfections (Hladnik, 1996).

Table 2.18 Measured geometrical imperfections (Hladnik, 1996).

Test beam	A1	A2	B1	B2	C1	C2
w [mm]	2.6	3.3	1.9	2.3	3.6	2.7
w/b	0.0087	0.0110	0.0070	0.0085	0.0143	0.0107
e_{max} [mm]	1.5	0.9	4.2	0.6	3.3	4.2
e_{max}/b	0.0050	0.0030	0.0155	0.0022	0.0131	0.0167
v [mm]	1.7	0.1	2.7	0.5	3.0	2.4
v/h_w	0.0077	0.0005	0.0121	0.0022	0.0135	0.0108
Test beam	D1	D2	E1	E2		
w [mm]	1.6	3.2	1.4	4.1		
w/b	0.0072	0.0145	0.0070	0.0206		
e_{max} [mm]	6.5	5.0	0.5	1.3		
e_{max}/b	0.0294	0.0226	0.0025	0.0065		
v [mm]	7.9	3.3	0.6	1.2		
v/h_w	0.0357	0.0149	0.0027	0.0054		

Test results

The beams were loaded until failure. All beams except for E1 and E2 collapsed due to local buckling of the compressed flange. Test beams E1 and E2 also experienced local buckling, but was also influenced by lateral buckling. The test results show that with an increasing slenderness of flanges $(b/t)\varepsilon$ the non-dimensional load carrying capacity and ductility decreases. The ultimate loads P_u and P_y as well as load factor γ_u^{exp} are illustrated in Table 2.19.

Table 2.19 Ultimate Loads and load factors of test beams (Hladnik, 1996).

Test beam	P_y [kN]	P_u [kN]	γ_u^{exp}
A1	427	389	0.91
A2	420	389	0.92
B1	376	391	1.04
B2	373	386	1.03
C1	335	359	1.07
C2	339	356	1.05
D1	320	358	1.12
D2	320	356	1.11
E1	286	311	1.08
E2	289	308	1.06

Where

P_u Ultimate load causing failure of test beam
 P_y Applied force that corresponds to the elastic resistance moment M_y
 γ_u^{exp} P_u/P_y Non-dimensional ultimate load carrying capacity of cross section

And

$M_y = W_{el} * f_{yc}^{flange}$
 W_{el} Elastic section modulus of the full cross section

In order to determine the influence of web slenderness, Hladnik performed a non-linear numerical analysis. The calculations considers the static scheme and nominal dimensions presented in Figure 2.24 as well as the geometrical imperfections and residual stresses presented in Figure 2.26.

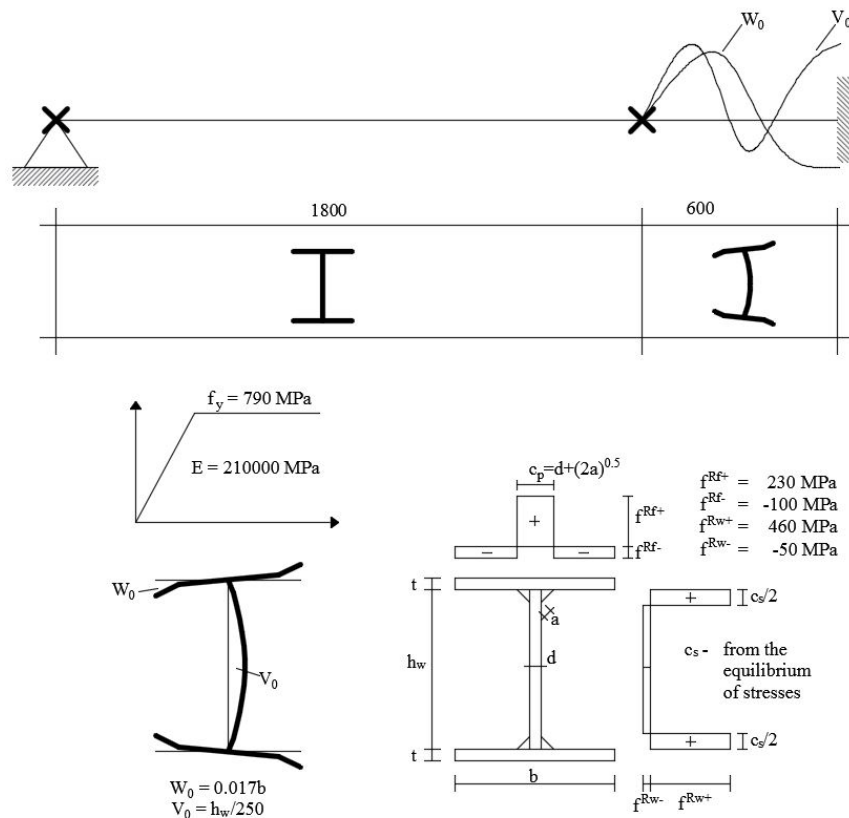


Figure 2.26 Geometrical imperfections and residual stresses considered in numerical analysis (Hladnik, 1996).

The analysis was verified by first calculating the influence of flange slenderness $(b/t)\epsilon$ and comparing this to the test results, see Figure 2.27. The test results and numerical results were considered to be in good correlation with each other.

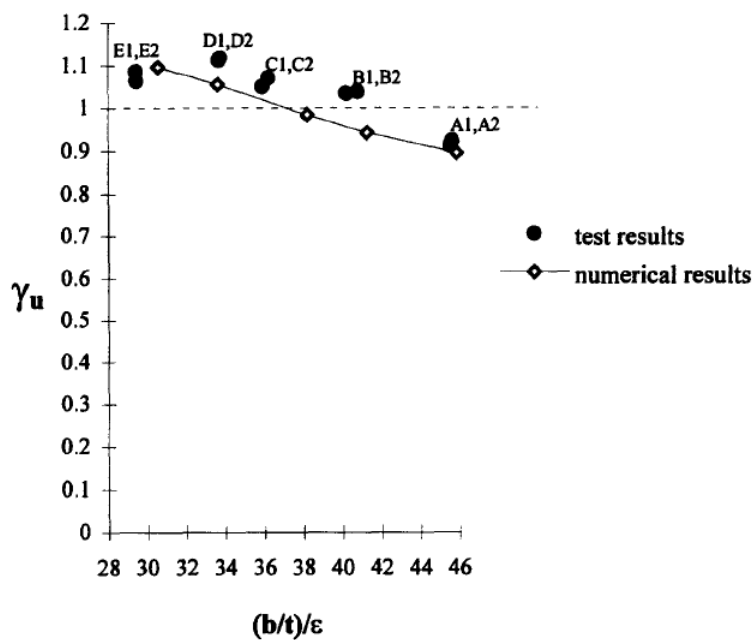


Figure 2.27 Non-dimensional ultimate carrying capacity of test beams in relation to the slenderness of flange for test results and numerical results (Hladnik, 1996).

After this verification the web dimensions of the test beams from group A,D and E were modified, other dimensions remained as before. The web depths calculated was of 200, 350, 500, 700 and 900 mm. The non-dimensional limit carrying capacity in relation to the web slenderness $(h_w/d)\epsilon$ is shown in Figure 2.28. It was concluded that with increasing web slenderness the limit carrying capacity is decreased.

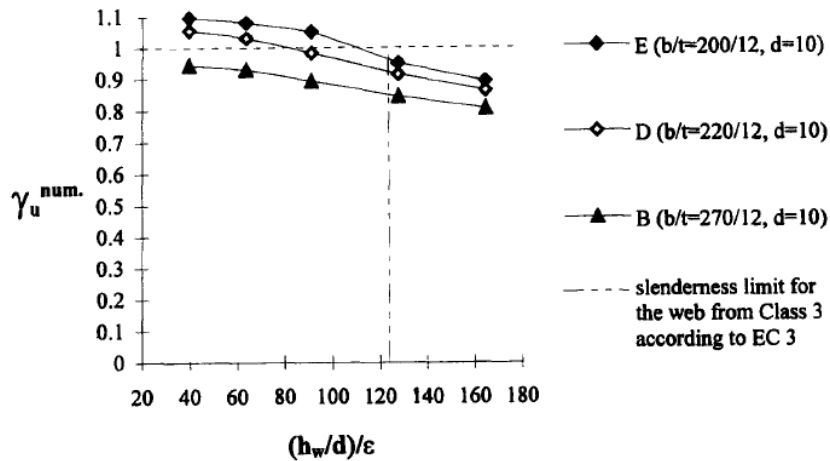


Figure 2.28 The influence of web slenderness on ultimate carrying capacity of a cross section (Hladnik, 1996).

Conclusions from test

The final conclusions made by (Hladnik, 1996) was that welded I-beams made of HSS loaded in bending to a great extent are influenced by the flange and web interaction. Also, it is established that the results obtained from both the experiment and numerical study would relate to cross sections made of mild structural steel. The greatest difference with regard to local stability is the higher intensity of compressive residual stresses in flanges, which results in a relatively lower load carrying capacity for mild steels (Hladnik, 1996).

3 Conclusions from literature study

The literature study shows that high strength steel is slowly making its way into the construction industry, even if the process is very slow. 20 years ago, steel grades with a yield limit of 275 MPa were considered standard but with today's standards this would be considered as "low strength steel". Today a steel with a yield limit of 355 MPa would be considered as standard, and it proves that the construction industry is slowly but surely is adopting higher steel grades. However, considering for how long HSS steel have been around, it can also be recognized that the construction industry is conservative.

Steels with yield strengths up to 700 MPa are today regulated in Eurocode 3. One may reflect upon why higher grades of steel are not used in any larger extent in structures today. Few manufacturers produce standard profiles for beams and columns with yield strengths above 420 MPa. This may be because the demand is low for members with higher resistance than this. Another way of thinking about it is that due to the low production of standard profiles of higher steel grades, no demand is generated. With more research illustrating where HSS is best implemented in structures, the production would increase and profiles would make its way into the building construction market. In the following chapters some conclusions are drawn regarding the way of implementing HSS in different structural elements.

3.1 Columns

It is obvious that a higher steel strength results in a higher buckling resistance if the cross section is kept constant. It is considered to be most beneficial to use HSS in relatively stub columns. Longer and more slender elements in HSS will not result in as much savings in material usage and cost compared to conventional steel columns. It is however interesting to evaluate further which lengths would be most beneficial and would be best suited to implement in a building structure.

The first study in [2.8.1] show that columns with smaller dimensions are more sensitive to imperfections. More slender columns of higher steel grades may carry the same load as less slender columns made by NSS. However the initial imperfections and unintended eccentricity have a larger influence and the accuracy during production and erection of these elements becomes more important.

3.2 Beams

The general perception of using HSS in beams is that there is little or no gain due to the fact that the E -modulus is equal and deflection is often decisive. By knowledge gained through the literature study and conversations with experienced structural engineers, we understand that this has been quickly realized. No extra stiffness is gained by increasing the steel strength and the same cross section is needed in order to avoid extra deflections.

Bridge structures and larger roof spans have benefited using HSS. Long span hybrid bridge girders reduces the self-weight of the structure to the extent that it is better to use compared to only NSS girders. Considering building construction, welded profiles

are generally not used for steel beams because they are generally more expensive. Therefore hybrid beams is considered to be less appropriate in buildings compared to bridge design.

3.3 Standard profiles

During the literature study no information regarding standard profiles in HSS was found. Since the demand of rolled profiles in HSS is so low, no manufacturers have produced any standard sections. Further research on rolled sections made of HSS is recommended to establish the best method for implementation in conventional structures.

3.4 Fire resistance

The studies presented in section [2.6.2] shows that more research is needed to evaluate and regulate the fire resistance of HSS. Eurocode today have rules for steels up to S460, but even for these steel grades questions are raised concerning their accuracy. The HSS tested proves that HSS loses load bearing capacity during a fire, just as conventional steels do. However the post fire load bearing capacity is greatly influenced on what steel grade is used. The studies show that an increase of steel grade seems to affect the post load bearing capacity in a negative way. This is however only noticed if the steels are heated to more than 600 °C, and then cooled down.

3.5 Weldability

There are methods and guidelines that enable welding in HSS with excellent results regardless if the delivery condition of the steel is QT or TM. But there are major differences between welding in QT and TM. Since TM steel has lower carbon content than both NSS and QT steel makes welding in TM steel is considerably easier and more cost efficient when for example lower preheating temperatures can be used.

3.6 Continuation of thesis

The literature study has given a general perception of different steels and how they are used today. The thesis aims to investigate members of different steel grades subjected to axial and transversal loading. Therefore possible limitations regarding fire resistance, weldability and the fact that there may be no standard profiles in HSS, will not be more thoroughly studied. This is something that has been presented and discussed and some general thoughts have been given. However the continuing part of the thesis will present analyses which studies the influence of high strength steel on structural members subjected to transversal and axial loading compared to normal strength steel.

4 Members subjected to transversal loads

In order to investigate the difference in behaviour between different steel grades, 18 different standard IPE beams were evaluated according to Eurocode 3. Moment capacities with and without respect to lateral torsional buckling (LT-buckling) as well as deflections for different lengths are presented. All beams are single span, simply supported and fully utilized. Calculations are carried out using the programming software MATLAB. Four different beams are presented below; IPE80, IPE180, IPE330 and IPE600. A cross calculation of the IPE330 beams is shown in Appendix A.

4.1 Moment resistance

The moment capacities for the beams are calculated as presented in [2.5.3], equation (2.15) but the effect of lateral-torsional buckling, χ_{LT} , is not taken into account. Increasing the yield strength and cross section dimensions will result in a greater moment resistance, see Table 4.1.

Table 4.1 Moment Resistance for IPE 80, IPE 180, IPE 330, IPE 600.

f_y [MPa]	355	420	460	500	620	690
	M_{Rd} [kNm]					
IPE 80	8.2	9.7	10.7	11.6	14.4	16.0
IPE 180	58.9	69.7	76.4	83.0	102.9	114.5
IPE 330	285.4	337.7	369.8	402.0	498.5	554.8
IPE 600	1246.0	1474.0	1615.0	1755.0	2176.0	2422
Relation to S355	1.00	1.18	1.30	1.41	1.75	1.94

The increase of moment resistance is directly proportional to the increase of f_y , which can be seen in (2.15).

4.2 Lateral torsional buckling resistance ratio

The moment resistance with respect to lateral torsional buckling ratio for all beams are calculated with the method described in [2.5.3]. For each length a ratio is calculated as the resistance for the HSS divided by the resistance for the conventional S355 steel, see Figure 4.1.

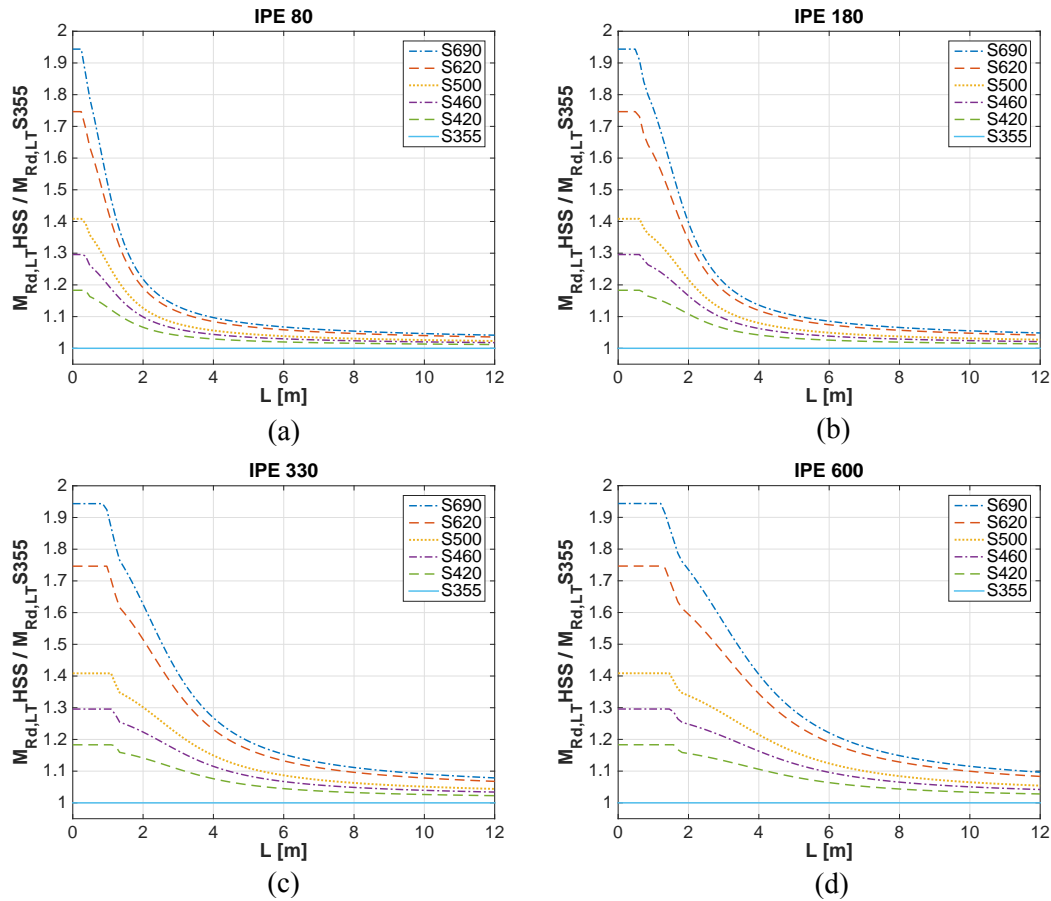


Figure 4.1 Lateral torsional buckling resistance ratios for IPE 80 (a), IPE 180 (b), IPE 330 (c) and IPE 600 (d).

As the figure illustrates, HSS are to a greater extent influenced of an increasing length of the beam. The largest benefits in ratios are seen in relatively short spans and large sections i.e. the greatest benefits are seen for non-slender beams.

4.3 Deflection

The deflection of the beams is calculated with the method described in [2.5.4]. The calculated fully utilized moment is used as the load to calculate the deflections and the results are illustrated in Figure 4.2 (a).

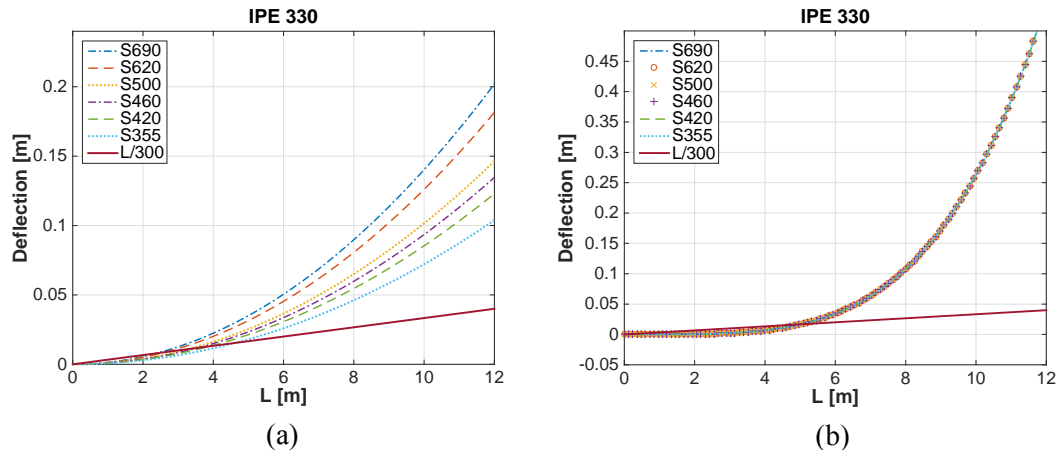


Figure 4.2 Deflections for fully utilized IPE 330 beam (a), Deflection for a uniform distributed loaded IPE 330(b).

The straight solid line in Figure 4.2 represents a deflection limit of $\frac{L}{300}$. Since the deflection of a beam depends on the geometry and the E -modulus, the use of steel with higher yield strength will not have any positive effect on the deflection for any given load case. Therefore, using HSS in beams will result in poor material utilization. Figure 4.2 (a) illustrates that an IPE 330 beam made of S355 can be fully utilized and fulfill the $\frac{L}{300}$ demand up to 4.5 m, while the S690 beam only can be spanned for about 2m before the deflection limit is reached. The irrelevance of the steel grade regarding deflection can be seen by simply looking at the governing deflection equations, which was presented in [2.5.4]. The equation for a deflection due to a uniformly distributed load is again shown in (4.1).

$$p_1 = W_1 \frac{5L^4}{384EI} \quad (4.1)$$

Regardless if a beam made of S690 steel has a higher moment resistance than the same beam made of S355, they will both have the same deflection for the same load. Figure 4.2 (b) show the deflection between different steel grades for an equal loaded IPE 330 beam. The steel grade has no impact, it is only the stiffness that matters, which is the same for equally sized beams. This means that if a load on a beam is doubled on two beams made of different steel grades, the deflection will be doubled and equal for both beams. This is shown in Appendix A.

5 Members subjected to axial loading

In this chapter, the behaviour of fully utilized columns subjected to pure compression made from HSS was investigated with respect to local buckling. The columns considered are hot rolled with a quadratic cross section. In order to see the effects of implementing HSS, the analyzed columns were compared with columns made from NSS. Three different analyses were performed on the columns, Analysis 1, Analysis 2 and Analysis 3, described in detail in [5.1.3]. The software used in this study was MATLAB.

All columns in this study were investigated at four different load levels; 500, 1000, 2000 and 4000 kN. The choice of the load level span was based on common values of flexural buckling resistance for hot rolled quadratic columns according to design tables from (TIBNOR AB, 2011).

5.1 MATLAB script

The MATLAB script essentially consists of two parts. The first part calculates the buckling resistance for a wide range of cross sections using (5.1) and (5.2). The second part is an iterative process to find an optimized steel area i.e. the smallest possible steel area. This optimized steel area is related to a predefined buckling load. In order to make the results from this study comparable, the optimized areas was calculated for both NSS and HSS.

$$N_{b,Rd} = \frac{\chi A f_y}{\gamma_{M1}} \quad \text{For class 1,2 and 3 cross-sections} \quad (5.1)$$

$$N_{b,Rd} = \frac{\chi A_{eff} f_y}{\gamma_{M1}} \quad \text{For class 4 cross-sections} \quad (5.2)$$

For each length the optimized steel area of each steel grade was divided with the optimized steel area for the normal strength S355 steel, see (5.3).

$$Ratio = \frac{A_{HSS}}{A_{NSS}} \quad (5.3)$$

In the first part of the calculation the script loops through different dimensions, yield strengths and column lengths. The range of the thicknesses and the widths in the script is based on values from design tables from (TIBNOR AB, 2011). The widths and thicknesses for the investigated columns are summarized in Table 5.1.

Table 5.1 Range of dimensions for quadratic columns.

	Quadratic
width [mm]	40-400
thickness [mm]	3-16

The widths and the thicknesses are stored in vectors, see (5.4) and (5.5). Each width is combined with each thickness to calculate the cross sectional constants, A , I and i for every combination. These constants are stored in matrices; see (5.6) which is an example of the matrix structure for the cross sectional area. The number of steps chosen as input for the dimensions governs the size of the selection of cross sections in each analysis. Table 5.2 summarizes the selection of cross sections based on the number of chosen steps.

Table 5.2 The relationship between number of steps in the dimension vectors and the selection of cross sections.

Steps	Widths	Thicknesses	Selection of cross sections
10	10	10	100
50	50	50	2500
100	100	100	10000
400	400	400	160000

The yield strengths and column lengths are stored in vectors in the same way as the dimensions vectors, but with another configuration regarding the number of steps, see (5.7) and (5.8). In this study, 6 different yield strengths were investigated, 355, 420, 460, 500, 620 and 690 MPa. The column lengths span between 0m – 12m. When all constants are combined, a 4-dimensional matrix is created containing the buckling resistance associated with a cross section, a yield strength and a column length. The structure of this matrix is illustrated in Figure 5.1.

$$\mathbf{b}_{(j)} = [b_1 \ b_2 \ \dots \ b_j] \quad \text{where } j = n \text{ steps} \quad (5.4)$$

$$\mathbf{t}_{(k)} = [t_1 \ t_2 \ \dots \ t_k] \quad \text{where } k = n \text{ steps} \quad (5.5)$$

$$\mathbf{A}_{(jk)} = \begin{bmatrix} b_1, t_1 & b_1, t_2 & \ddots & b_1, t_k \\ b_2, t_1 & b_2, t_2 & \ddots & b_2, t_k \\ \vdots & \vdots & \ddots & \vdots \\ b_j, t_1 & b_j, t_2 & \ddots & b_j, t_k \end{bmatrix} \quad \text{where } jk = n \text{ steps} \times n \text{ steps} \quad (5.6)$$

$$\mathbf{f}_{y(s)} = [355 \ 420 \ 460 \ 500 \ 620 \ 690] * MPa \quad (5.7)$$

$$\mathbf{L}_{(m)} = [L_1 \ L_2 \ \dots \ L_m] \quad \text{where } m = 13 \quad (5.8)$$

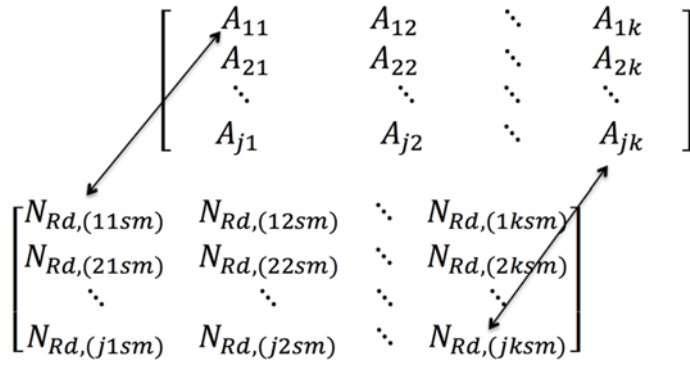


Figure 5.1 The structure and the relationship between the 4D buckling resistance matrix and the cross section matrix.

The purpose of the second part of the script is to find the smallest possible steel area for every yield strength and column length that corresponds to a predefined buckling resistance. To find the smallest area, the script runs a loop that searches through the selection of cross sections. The loop contains a condition, which ensures that the column with the smallest steel area with a buckling resistance closest to the predefined buckling loads, N_{Ed} is found, see (5.9). This could be explained by studying equation (5.10), which is a modified variant of (5.1), where A is the selection of cross sectional areas written in matrix form, see (5.6) and $N_{b,Rd}$ is the calculated buckling resistance for each column. When the columns with the smallest possible steel areas is found, the scrip extracts all the corresponding properties of interest for these particular columns, such as reductions factors, slenderness, dimensions and weights. The complete MATLAB script is shown in Appendix E.

$$N_{b,Rd} \geq N_{Ed} \quad (5.9)$$

$$A = \frac{N_{b,Rd} \gamma_{M1}}{\chi f_y} \quad (5.10)$$

5.1.1 Cross section approximation

The cross sections of the quadratic columns in this study were calculated with sharp corners compared to the true shape of hot rolled quadratic columns, which corners are rounded, see Figure 5.2. This approximation was made to obtain fair, comparable results in the analyses, because the data regarding the corner radius differs between steel manufacturers. The consequence of this approximation was that columns with sharp corners obtain slightly higher buckling resistance due to greater cross section area and moment of inertia. Table 5.3 summarizes the buckling resistance and differences between the approximated value and the true value from a construction table by (TIBNOR AB, 2011). The cross section of the column is illustrated in Figure 5.2. To verify the behaviour of this approximation for other cross sections, the buckling resistance difference for a 3.6m long column with a square 200x200 mm² cross section with a material thickness of 8mm, see Table 5.4. The results of the larger column, confirms that a slightly higher buckling resistance occurs for the sharp cornered cross section.

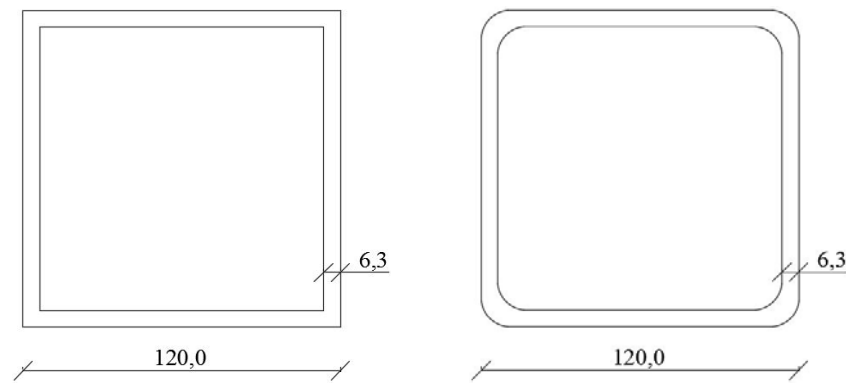


Figure 5.2 Cross section with sharp corners and with rounded corners.

Table 5.3 Differences in buckling resistance for different steel grades between a 3.6 m long, 120 mm wide and 6.3 mm thick column with rounded corners and with sharp corners.

	S355	S420	S460	S500	S620	S690
Rounded corners [kN]	653.1	699.2	781.8	798.9	833.4	846.5
Sharp corners [kN]	667.4	715.3	800.4	818.3	854.4	868.1
Difference	2.15%	2.25%	2.33%	2.37%	2.46%	2.48%

Table 5.4 Differences in buckling resistance for different steel grades between a 3.6m long 200 mm wide and 8 mm thick column with rounded corners and with sharp corners.

	S355	420	S460	S500	S620	S690
Rounded corners [kN]	1918.3	2215.0	2519.7	2706.2	3222.0	3489.1
Sharp corners [kN]	1940.7	2241.5	2549.2	2738.4	3262.5	3534.6
Difference	1.15%	1.18%	1.16%	1.18%	1.24%	1.29%

Table 5.3 and Table 5.4 illustrate that there is a difference between cross sections with rounded corners and cross sections with sharp corners. The differences will also increase with higher yield strengths. However, the differences are generally small and it will not affect the calculations because columns with sharp corners are used consistently through this study. This verification was made to ensure that no major deviations occurred by this simplification.

5.1.2 Script verification

To verify the accuracy of the program a reference column was tested with different step sizes in the loop. The number of steps in the loop varies between 50-1000 steps. The 2.1 m long reference column has a buckling resistance of 908.6 kN and measures 120 mm in width and 6.3 mm in thickness, see Figure 5.3. This load was set as the input load in the MATLAB script. After each run of the script, columns with the buckling resistances related to the smallest cross sections areas closest to the input load were stored in Table 5.5. These columns have the same length as the reference column but other dimensions as the steel grades differ.

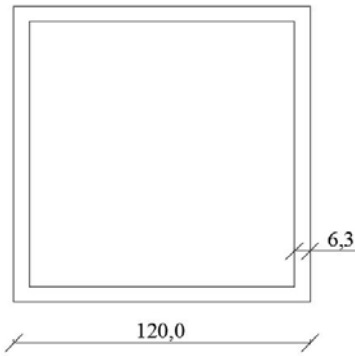


Figure 5.3 Reference column tested for script verification

Table 5.5 Design buckling resistance for different step size of a 2.1 m long hot rolled quadratic column.

f_y [MPa]	355	420	460	500	620	690
Number of steps	$N_{b,Rd}$ [kN]					
50	914.8	921.6	909.4	931.3	938.3	950.6
100	926.7	910.6	917.4	911.4	921.5	910.3
200	909.1	919.5	913.4	910.4	915.7	919.4
300	911.4	913.0	916.8	912.8	913.8	912.2
400	912.0	909.7	910.9	910.1	912.8	909.4
500	908.6	913.4	913.4	914.0	912.2	913.1
600	909.3	911.5	910.5	912.0	908.7	910.6
1000	909.3	909.8	909.9	910.2	909.2	909.1

The error of the different step sizes between the input load of 908.6 kN and the buckling resistances related to the smallest cross sections areas was calculated, the difference in percentage is summarized in Table 5.6.

Table 5.6 Deviation between buckling resistance obtained from MATLAB for a 120 mm wide and 6.3 mm thick hot rolled column.

f_y [MPa]	355	420	460	500	620	690
Number of steps						
50	0.68%	1.41%	0.09%	2.44%	3.17%	4.42%
100	1.96%	0.22%	0.96%	0.31%	1.40%	0.19%
200	0.06%	1.19%	0.53%	0.19%	0.78%	1.18%
300	0.30%	0.48%	0.89%	0.46%	0.57%	0.39%
400	0.37%	0.12%	0.25%	0.16%	0.46%	0.09%
500	0.00%	0.53%	0.52%	0.59%	0.40%	0.49%
600	0.07%	0.31%	0.21%	0.37%	0.01%	0.22%
1000	0.07%	0.14%	0.14%	0.18%	0.07%	0.05%

From Table 5.6, the deviation in buckling resistance for the number of steps between 50 and 300 is considered to be too large. When the number of steps is increased from 400 steps up to 1000 steps, the error becomes smaller and the deviation between the different yield strengths decreases as well. The choice of 400 steps is based on the size of the error, but also the script running time. The computational time is of some interest, because the script will be run several times in this study.

To verify the MATLAB script, the buckling resistance of two different hot rolled columns with rounded corners was independently cross checked with hand calculations, see Appendix B. The verification was carried out by comparing the buckling resistance from the MATLAB script with hand calculations. To ensure that the correct value of the buckling resistances was calculated, they were compared with values from the corresponding column taken from a design table (TIBNOR AB, 2011). The hand calculations were made with the software Mathcad Prime and the results of the verification is summarized in Table 5.7.

Table 5.7 Verification of the MATLAB script by comparison between buckling resistances obtained from MATLAB, Mathcad and true values from design by TIBNOR¹⁾.

L [m]	$N_{b,Rd}$			Difference	
	MATLAB	Mathcad	True value ¹⁾	MATLAB/Mathcad	MATLAB/True value ¹⁾
2.1	892.9	892.9	894.0	0.00%	0.12%
3.0	766.9	766.9	768.0	0.00%	0.15%
5.0	410.4	410.4	411.0	0.00%	0.14%
7.0	227.1	227.1	227.0	0.00%	0.14%

Table 5.7 shows that the buckling resistances calculated in MATLAB and calculations carried out in Mathcad Prime was equal. They were also very similar to values obtained from TIBNOR. The conclusion is that the script is considered to be accurate.

5.1.3 Analysis 1, 2 and 3

To capture the different behaviour when implementing HSS in hot rolled quadratic columns, the study is divided into three different analyses. The difference between the analyses is how they approach the limit of cross section class 4. The properties and limitations of cross section class 1, 2, 3 and 4 is described in [2.5.1].

5.1.4 Analysis 1

In *Analysis 1*, columns in cross section class 1, 2 and 3 are of interest while columns in cross section class 4 are removed from the script. Matrices with the same structure as presented in (5.6) are created for the cross sectional classes. Figure 5.4 illustrates an example of two 10x10 matrices for the S355 and S690 steel grades. Each number represent the cross section class for a specific column which corresponds to a width and thickness. The region inside the borders represents cross sections that are removed from the script.

355

690

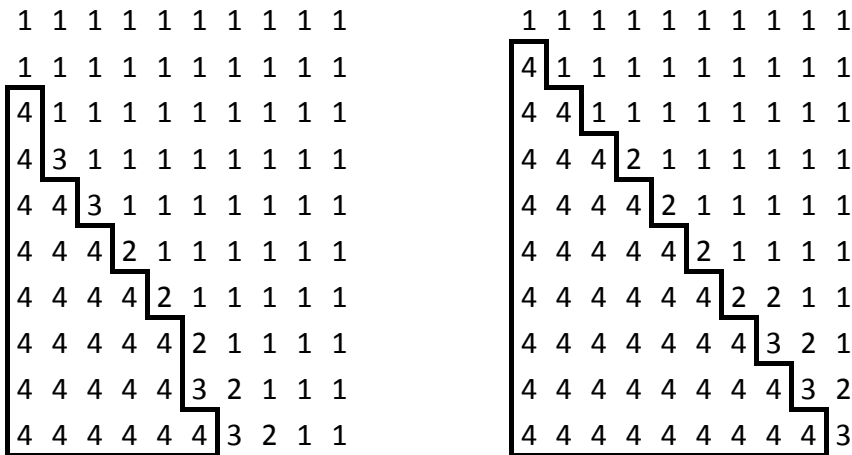


Figure 5.4 Cross section class matrix for a loop with 10 steps. Each number represents the cross section class for a specific column made of S355 and S690 steel.

5.1.5 Analysis 2

In Analysis 2, columns in cross section class 1, 2, 3 and 4 are considered. The load carrying capacity of cross sections in class 4 is calculated with a reduced area, see equation (5.2). Matrices with the same structure as presented in (5.6) are created for the cross sectional classes. Figure 5.5 illustrates an example of two 10x10 matrices for the S355 and S690 steel grades. Each number represent the cross section class for a specific column which corresponds to a width and thickness. The region inside the borders represents cross sections that are calculated with a reduced area.

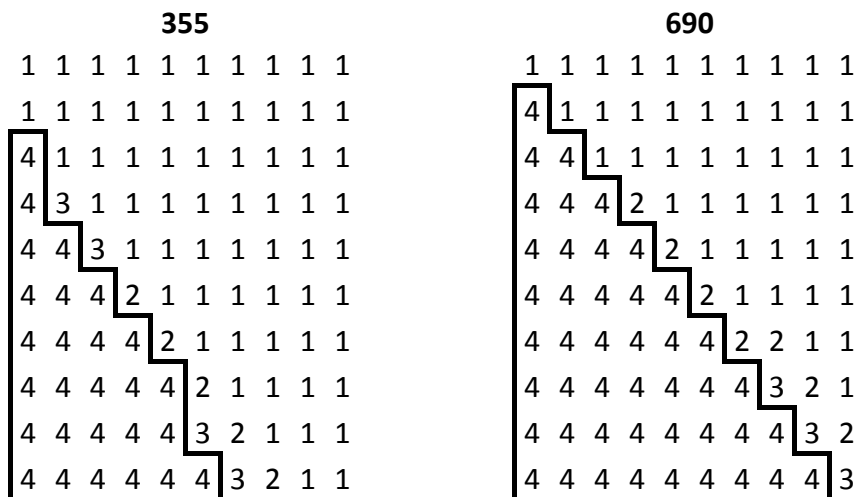


Figure 5.5 Cross section class matrix for a loop size with 10 steps. Each number represents the cross section class for a specific column made of S355 and S690 steel.

5.1.6 Analysis 3

In Analysis 3, the limit of cross section class 4 is ignored. Local buckling is considered not to be an issue due to measures taken to prevent it. This can be achieved by for example corrugating the web and thereby decrease the c-distance and increase the stiffness of the cross sections, see Figure 5.6.

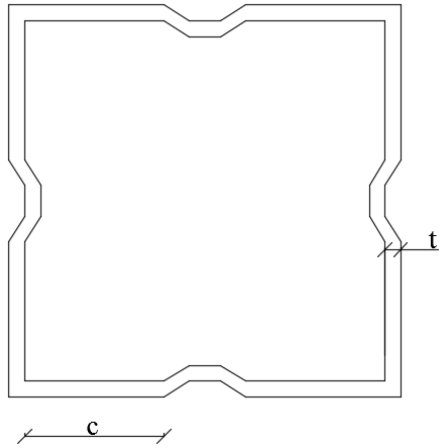


Figure 5.6 Cross sections with corrugated web which has an increased stiffness compared to normal square cross sections.

The load carrying capacity of cross sections in class 4 is calculated in the same way as cross sections in class 1, 2 and 3, see equation (5.1). Figure 5.7 illustrates an example of two 10x10 matrices for the S355 and S690 steel grades where all cross sections are considered. Each number represents the cross section class for a specific column which corresponds to a width and thickness.

355										690									
1	1	1	1	1	1	1	1	1	1	1	1	1	1	1	1	1	1	1	1
1	1	1	1	1	1	1	1	1	1	4	1	1	1	1	1	1	1	1	1
4	1	1	1	1	1	1	1	1	1	4	4	1	1	1	1	1	1	1	1
4	3	1	1	1	1	1	1	1	1	4	4	4	2	1	1	1	1	1	1
4	4	3	1	1	1	1	1	1	1	4	4	4	4	2	1	1	1	1	1
4	4	4	2	1	1	1	1	1	1	4	4	4	4	4	2	1	1	1	1
4	4	4	4	2	1	1	1	1	1	4	4	4	4	4	4	2	2	1	1
4	4	4	4	4	2	1	1	1	1	4	4	4	4	4	4	4	3	2	1
4	4	4	4	4	3	2	1	1	1	4	4	4	4	4	4	4	4	3	2
4	4	4	4	4	4	3	2	1	1	4	4	4	4	4	4	4	4	4	3

Figure 5.7 Cross section class matrix for a loop size with 10 steps. Each number represents the cross section class for a specific column made of S355 and S690 steel.

5.2 Results

Chapter [5.2.1] through [5.2.5] show the results obtained from *Analysis 1*, *Analysis 2* and *Analysis 3*.

5.2.1 Analysis 1

Figure 5.8 displays the optimized steel area ratio between the S355 steel and the HSS grades according to *Analysis 1*. The straight solid line represents the ratio of the optimized areas for NSS, and is therefore equal to 1. The other curves represents the optimized steel areas for the HSS related to the optimized areas for the NSS. Curves

below the straight line implies that columns made from HSS have a smaller steel area compared to a columns made of NSS. Each of the four graphs represents the load levels, 500 kN, 1000 kN, 2000 kN and 4000 kN.

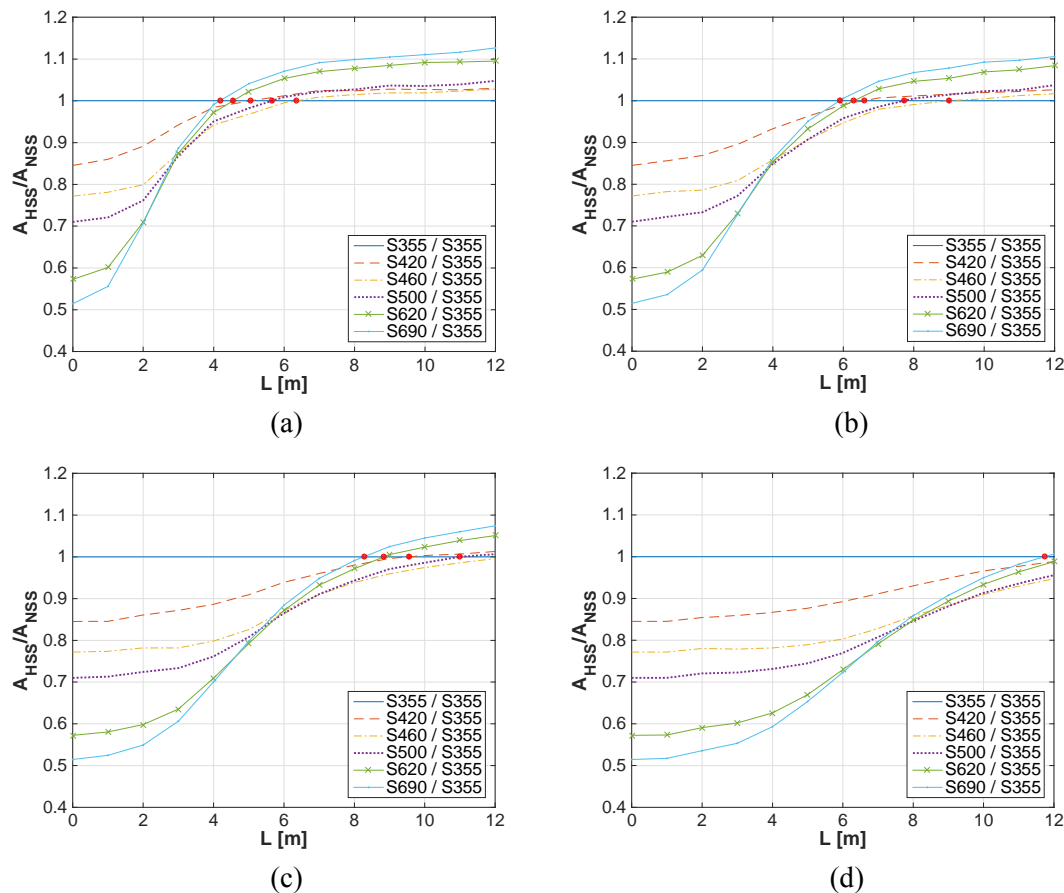


Figure 5.8 Relation between the smallest steel area possible for steel grades S420 – S690 and the smallest steel area possible for a S355 steel according to analysis 1. The areas regard quadratic columns with buckling resistance of 500 kN (a), 1000 kN (b), 2000 kN (c) and 4000 kN (d).

The outcome from this analysis show two significant effects of an implementation of HSS in hot rolled quadratic columns with cross sections which are below the limit of cross section class 4.

The most obvious result from *Analysis 1* was that columns made from HSS were and were not beneficial. The dots in Figure 5.8 represents the inflection points, which indicates when HSS were beneficial or not. At these points, results showed that a critical non-dimensional slenderness occurred which was more or less the same for each steel grade regardless column length and/or buckling resistance. Table 5.8 summarizes the critical non-dimensional slenderness values corresponding to the inflection points in Figure 5.8. With the critical non-dimensional slenderness, results showed that less slender columns generally benefit more from HSS, these columns had a lower non-dimensional slenderness value than the critical value. Columns that not benefit from HSS were slenderer and had a higher non-dimensional slenderness value than the critical value. Results from this analysis also showed that columns subjected to larger loads were more beneficial for a wider range of column lengths.

Table 5.8 Critical non-dimensional slenderness values for different steel grades.

	S420		S460		S500		S620		S690	
	$\bar{\lambda}$	L [m]	$\bar{\lambda}$	L [m]	$\bar{\lambda}$	L [m]	$\bar{\lambda}$	L [m]	$\bar{\lambda}$	L [m]
500 [kN]	1.25	5.04	1.54	6.36	1.54	5.66	1.58	4.55	1.61	4.17
1000 [kN]	1.20	6.58	1.54	9.00	1.51	7.73	1.56	6.30	1.61	5.89
2000 [kN]	1.21	9.55	-	-	1.51	11.00	1.55	8.84	1.61	8.27
4000 [kN]	-	-	-	-	-	-	-	-	1.61	11.73

The second observation from *Analysis 1* was the differences between the optimized steel areas for the HSS grades. The results show that the highest steel grade of S690, goes from having the most beneficial cross sections for shorter columns when the slenderness were low, to have the least beneficial cross sections at higher slenderness which occurred for longer columns. This phenomenon is not load dependent in the same manner when HSS are compared with NSS. The behaviour applies to all the HSS grades. One difference that is seen is the curve of the S420 steel ratio. This curve has a slightly different trend compared to the other HSS. This is explained by the fact that S420 steel is calculated with another buckling curve than the other HSS grades.

The behaviour of when HSS is not beneficial to implement, described in the first observations is related to the available selection of cross sections in the MATLAB script. Table 5.9 summarizes the number of available columns in cross section class 1, 2, 3 and the difference between the steel grades. The table shows that for example the steel grade S690 has 26 015 fewer available cross sections than the S355 steel. The differences of available columns are consequences of the governing equations (5.11) and (5.12) when determining whether the cross sections are in class 4 or not.

Table 5.9 The number of columns in cross section class 4 for each steel grade.

Steel grade	S355	S420	S460	S500	S620	S690
Selection of columns	160000	160000	160000	160000	160000	160000
Number of columns in class 1, 2 and 3	119763	113964	110616	107407	98519	93748
Number of columns in class 4	40237	46036	49384	52593	61481	66252
Difference between NSS and HSS	-	5799	9147	12356	21244	26015

$$\varepsilon = \sqrt{\frac{235}{f_y}} \quad \text{Where } f_y \text{ is the yield strength in MPa} \quad (5.11)$$

$$\frac{c}{t} \leq 42\varepsilon \quad (5.12)$$

Where $c = b - 2t$
 b = width
 t = thickness

The reason why S355 has a greater selection of cross sections than steel with higher yield strength is based on the fact that an increased yield strength decreases the limit value of cross section class 4, thus decreases the number of available cross section for steel with higher yield strengths. Table 5.10 summarizes the value of ε and the limit value of cross section class 4 for different steel grades.

Table 5.10 Values of ϵ and limits for cross section class 4 for different steel grades.

	S355	S420	S460	S500	S620	S690
ϵ	0.81	0.75	0.71	0.69	0.62	0.58
42ϵ	34.17	31.42	30.02	28.79	25.86	24.51

The circumstances when HSS was not beneficial compared to NSS can be visualized by looking at the behaviour when the selection of an optimized steel area was calculated for a 10 m column with a buckling resistance of 500 kN for the steel grades S355 and S690. Table 5.11 through Table 5.14 shows how the selection was made. The matrices in the tables are downscaled versions of the matrices in the MATLAB script and measures 10 by 10 instead of 400 by 400, but the principle is the same. Due to the limit value for cross sections class 4 seen in Table 5.10, columns made from HSS was strongly governed by the $\frac{c}{t}$ ratio, where the S690 was most affected. This implies that columns made from steel with higher yield strengths demanded greater steel areas in order to fulfil the limitation of cross section class 3. This can be observed by comparing the $\frac{c}{t}$ ratios in Table 5.11 and Table 5.12 with the limit values for cross section class 4 in Table 5.10. Table 5.13 and Table 5.14 show the optimized steel area for S355 and S690 respectively.

Table 5.11 $\frac{c}{t}$ ratios for the selection of cross section for S355. Highlighted region represents cross sections in class 4 (removed in script). Values within the boundary represents columns with a buckling resistance of 500 kN or greater. The $\frac{c}{t}$ ratio corresponding to the optimized steel area*).

11.33	7.00	4.79	3.45	2.56	1.91	1.43	1.05	0.75	0.50
24.67	16.00	11.58	8.91	7.11	5.83	4.86	4.10	3.50	3.00
38.00	25.00	18.38	14.36	11.67	9.74	8.29	7.15	6.24	5.50
51.33	34.00	25.17	19.82	16.23	13.65	11.71	10.20	8.99	8.00
64.67	43.00	31.96*	25.27	20.78	17.57	15.14	13.25	11.74	10.50
78.00	52.00	38.75	30.73	25.34	21.48	18.57	16.31	14.49	13.00
91.33	61.00	45.55	36.18	29.90	25.39	22.00	19.36	17.24	15.50
104.67	70.00	52.34	41.64	34.46	29.30	25.43	22.41	19.98	18.00
118.00	79.00	59.13	47.09	39.01	33.22	28.86	25.46	22.73	20.50
131.33	88.00	65.92	52.55	43.57	37.13	32.29	28.51	25.48	23.00

Table 5.12 $\frac{c}{t}$ ratio for the selection of cross section for S690. Highlighted region represents cross sections in class 4 (removed in script). Values within the boundary represents columns with a buckling resistance of 500 kN or greater. The $\frac{c}{t}$ ratio corresponding to the optimized steel area*).

11.33	7.00	4.79	3.45	2.56	1.91	1.43	1.05	0.75	0.50
24.67	16.00	11.58	8.91	7.11	5.83	4.86	4.10	3.50	3.00
38.00	25.00	18.38	14.36	11.67	9.74	8.29	7.15	6.24	5.50
51.33	34.00	25.17	19.82	16.23	13.65	11.71	10.20	8.99	8.00
64.67	43.00	31.96	25.27	20.78*	17.57	15.14	13.25	11.74	10.50
78.00	52.00	38.75	30.73	25.34	21.48	18.57	16.31	14.49	13.00
91.33	61.00	45.55	36.18	29.90	25.39	22.00	19.36	17.24	15.50
104.67	70.00	52.34	41.64	34.46	29.30	25.43	22.41	19.98	18.00
118.00	79.00	59.13	47.09	39.01	33.22	28.86	25.46	22.73	20.50
131.33	88.00	65.92	52.55	43.57	37.13	32.29	28.51	25.48	23.00

Table 5.13 Selection of cross sectional areas for S355. Highlighted region represents cross sections in class 4 (removed in script). Values within the boundary represents columns with a buckling resistance of 500 kN or greater. Optimized cross sectional area*).

0.0004	0.0006	0.0008	0.0010	0.0011	0.0012	0.0013	0.0014	0.0015	0.0015
0.0009	0.0013	0.0017	0.0021	0.0025	0.0029	0.0032	0.0035	0.0038	0.0041
0.0014	0.0021	0.0027	0.0033	0.0039	0.0045	0.0051	0.0056	0.0061	0.0067
0.0019	0.0028	0.0036	0.0045	0.0053	0.0061	0.0069	0.0077	0.0085	0.0092
0.0024	0.0035	0.0046*	0.0057	0.0067	0.0078	0.0088	0.0098	0.0108	0.0118
0.0028	0.0042	0.0055	0.0068	0.0081	0.0094	0.0107	0.0119	0.0131	0.0143
0.0033	0.0049	0.0065	0.0080	0.0095	0.0110	0.0125	0.0140	0.0155	0.0169
0.0038	0.0056	0.0074	0.0092	0.0109	0.0127	0.0144	0.0161	0.0178	0.0195
0.0043	0.0063	0.0083	0.0103	0.0123	0.0143	0.0163	0.0182	0.0201	0.0220
0.0048	0.0070	0.0093	0.0115	0.0137	0.0159	0.0181	0.0203	0.0224	0.0246

Table 5.14 Selection of cross sectional areas for S690. Highlighted region represents cross sections in class 4 (removed in script). Values within the boundary represents columns with a buckling resistance of 500 kN or greater. Optimized cross sectional area*).

0.0004	0.0006	0.0008	0.0010	0.0011	0.0012	0.0013	0.0014	0.0015	0.0015
0.0009	0.0013	0.0017	0.0021	0.0025	0.0029	0.0032	0.0035	0.0038	0.0041
0.0014	0.0021	0.0027	0.0033	0.0039	0.0045	0.0051	0.0056	0.0061	0.0067
0.0019	0.0028	0.0036	0.0045	0.0053	0.0061	0.0069	0.0077	0.0085	0.0092
0.0024	0.0035	0.0046	0.0057	0.0067*	0.0078	0.0088	0.0098	0.0108	0.0118
0.0028	0.0042	0.0055	0.0068	0.0081	0.0094	0.0107	0.0119	0.0131	0.0143
0.0033	0.0049	0.0065	0.0080	0.0095	0.0110	0.0125	0.0140	0.0155	0.0169
0.0038	0.0056	0.0074	0.0092	0.0109	0.0127	0.0144	0.0161	0.0178	0.0195
0.0043	0.0063	0.0083	0.0103	0.0123	0.0143	0.0163	0.0182	0.0201	0.0220
0.0048	0.0070	0.0093	0.0115	0.0137	0.0159	0.0181	0.0203	0.0224	0.0246

The circumstances when HSS was beneficial compared to NSS can be visualized by looking at the behaviour when the selection of an optimized steel area was calculated for a column with a length of 4 m and a buckling resistance of 4000 kN for the steel grades S355 and S690. Table 5.15 through Table 5.18 shows how the selection was made. It was not only the $\frac{c}{t}$ ratio that governed the selection for the optimized columns, but also the difference in the number of columns that manage to resist the predefined buckling resistance between different steel grades. The results showed that steel with higher yield strength affects the buckling resistance more beneficially than steel with lower strength. This resulted in a greater variety of cross sections, and cross sections with smaller steel areas as the steel grades increase.

Table 5.15 $\frac{c}{t}$ ratio for the selection of cross section for S355. Highlighted region represents cross sections in class 4 (removed in script). Values within the boundary represents columns with a buckling resistance of 4000 kN or greater. The $\frac{c}{t}$ ratio corresponding to the optimized steel area*).

11.33	7.00	4.79	3.45	2.56	1.91	1.43	1.05	0.75	0.5
24.67	16.00	11.58	8.91	7.11	5.83	4.86	4.10	3.50	3
38.00	25.00	18.38	14.36	11.67	9.74	8.29	7.15	6.24	5.5
51.33	34.00	25.17	19.82	16.23	13.65	11.71	10.20	8.99	8
64.67	43.00	31.96	25.27	20.78	17.57	15.14	13.25	11.74	10.5
78.00	52.00	38.75	30.73	25.34	21.48	18.57	16.31	14.49	13
91.33	61.00	45.55	36.18	29.90	25.39	22.00*	19.36	17.24	15.5
104.67	70.00	52.34	41.64	34.46	29.30	25.43	22.41	19.98	18
118.00	79.00	59.13	47.09	39.01	33.22	28.86	25.46	22.73	20.5
131.33	88.00	65.92	52.55	43.57	37.13	32.29	28.51	25.48	23

Table 5.16 $\frac{c}{t}$ ratio for the selection of cross section for S690. Highlighted region represents cross sections in class 4 (removed in script). Values within the boundary represents columns with a buckling resistance of 4000 kN or greater. The $\frac{c}{t}$ ratio corresponding to the optimized steel area*).

11.33	7.00	4.79	3.45	2.56	1.91	1.43	1.05	0.75	0.50
24.67	16.00	11.58	8.91	7.11	5.83	4.86	4.10	3.50	3.00
38.00	25.00	18.38	14.36	11.67	9.74	8.29	7.15	6.24	5.50
51.33	34.00	25.17	19.82	16.23	13.65	11.71	10.20	8.99	8.00
64.67	43.00	31.96	25.27	20.78	17.57*	15.14	13.25	11.74	10.50
78.00	52.00	38.75	30.73	25.34	21.48	18.57	16.31	14.49	13.00
91.33	61.00	45.55	36.18	29.90	25.39	22.00	19.36	17.24	15.50
104.67	70.00	52.34	41.64	34.46	29.30	25.43	22.41	19.98	18.00
118.00	79.00	59.13	47.09	39.01	33.22	28.86	25.46	22.73	20.50
131.33	88.00	65.92	52.55	43.57	37.13	32.29	28.51	25.48	23.00

Table 5.17 Selection of cross sectional areas for S355. Highlighted region represents cross sections in class 4 (removed in script). Values within the boundary represents columns with a buckling resistance of 4000 kN or greater. Optimized cross sectional area*).

0.0004	0.0006	0.0008	0.0010	0.0011	0.0012	0.0013	0.0014	0.0015	0.0015
0.0009	0.0013	0.0017	0.0021	0.0025	0.0029	0.0032	0.0035	0.0038	0.0041
0.0014	0.0021	0.0027	0.0033	0.0039	0.0045	0.0051	0.0056	0.0061	0.0067
0.0019	0.0028	0.0036	0.0045	0.0053	0.0061	0.0069	0.0077	0.0085	0.0092
0.0024	0.0035	0.0046	0.0057	0.0067	0.0078	0.0088	0.0098	0.0108	0.0118
0.0028	0.0042	0.0055	0.0068	0.0081	0.0094	0.0107	0.0119	0.0131	0.0143
0.0033	0.0049	0.0065	0.0080	0.0095	0.0110	0.0125*	0.0140	0.0155	0.0169
0.0038	0.0056	0.0074	0.0092	0.0109	0.0127	0.0144	0.0161	0.0178	0.0195
0.0043	0.0063	0.0083	0.0103	0.0123	0.0143	0.0163	0.0182	0.0201	0.0220
0.0048	0.0070	0.0093	0.0115	0.0137	0.0159	0.0181	0.0203	0.0224	0.0246

Table 5.18 Selection of cross sectional areas for S690. Highlighted region represents cross sections in class 4 (removed in script). Values within the boundary represents columns with a buckling resistance of 4000 kN or greater. Optimized cross sectional area*).

0.0004	0.0006	0.0008	0.0010	0.0011	0.0012	0.0013	0.0014	0.0015	0.0015
0.0009	0.0013	0.0017	0.0021	0.0025	0.0029	0.0032	0.0035	0.0038	0.0041
0.0014	0.0021	0.0027	0.0033	0.0039	0.0045	0.0051	0.0056	0.0061	0.0067
0.0019	0.0028	0.0036	0.0045	0.0053	0.0061	0.0069	0.0077	0.0085	0.0092
0.0024	0.0035	0.0046	0.0057	0.0067	0.0078*	0.0088	0.0098	0.0108	0.0118
0.0028	0.0042	0.0055	0.0068	0.0081	0.0094	0.0107	0.0119	0.0131	0.0143
0.0033	0.0049	0.0065	0.0080	0.0095	0.0110	0.0125	0.0140	0.0155	0.0169
0.0038	0.0056	0.0074	0.0092	0.0109	0.0127	0.0144	0.0161	0.0178	0.0195
0.0043	0.0063	0.0083	0.0103	0.0123	0.0143	0.0163	0.0182	0.0201	0.0220
0.0048	0.0070	0.0093	0.0115	0.0137	0.0159	0.0181	0.0203	0.0224	0.0246

5.2.2 Analysis 2

Figure 5.9 displays the optimized steel area ratio between the S355 steel and the HSS grades according to *Analysis 2*. The straight solid line represents the ratio of the optimized areas for NSS, and is therefore equal to one. The other curves represents the optimized steel areas for the HSS related to the optimized areas for the NSS. All curves are below the straight line which implies that columns made from HSS have a smaller steel area than a column made from NSS. Each of the four graphs represents the load levels, 500 kN, 1000 kN, 2000 kN and 4000 kN.

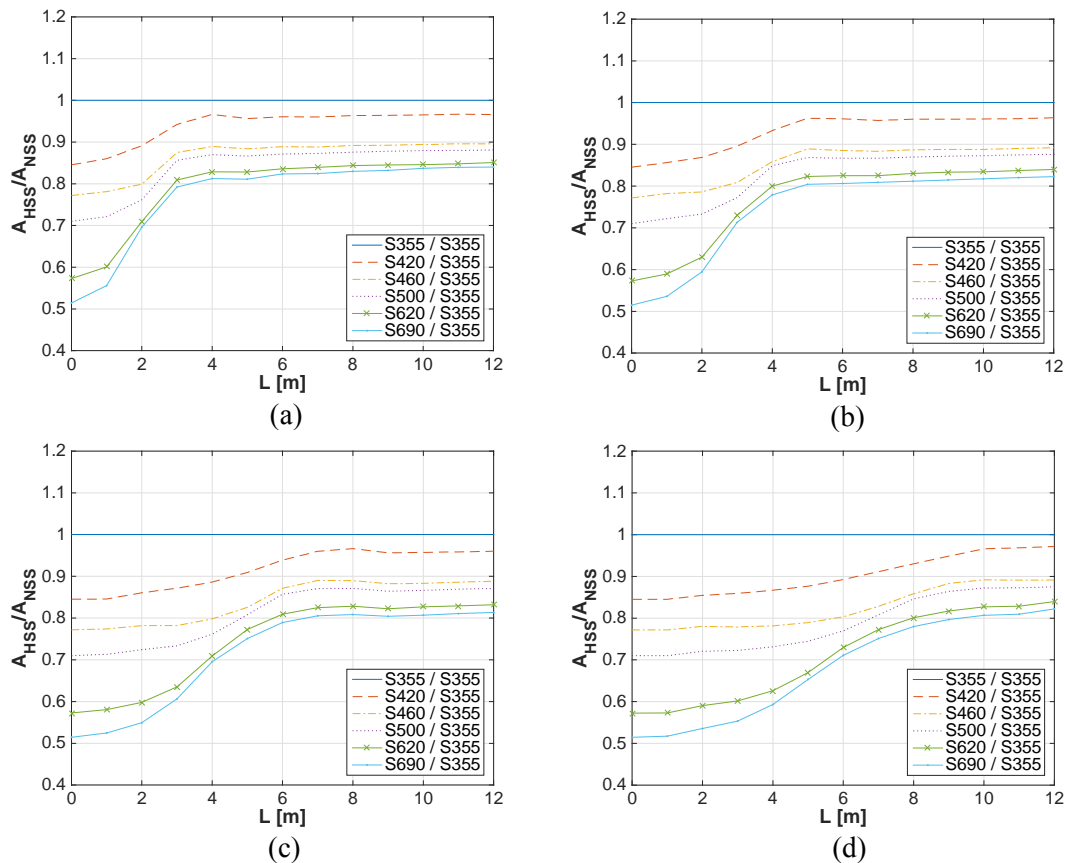


Figure 5.9 Relation between the smallest steel area possible for steel strengths 420 – 690MPa and the smallest steel area possible for a 355MPa steel strength according to analysis 2. The areas regard quadratic columns with buckling resistance of 500 kN (a), 1000 kN (b), 2000 kN (c) and 4000 kN (d).

The first and most obvious observation from this analysis was that implementation of HSS will always be beneficial for column regardless of yield strength, column length or buckling resistance. However, there were differences of how great the benefits were and when the benefits occurred. The S690 steel always showed the most favourable results. The other HSS grades were also favourable compared to the NSS, but with a descending rate, the least favourable steel grade was the S420. This behaviour was consistent throughout *Analysis 2*. The smallest gain from implementing HSS occurred for the longest columns at any buckling resistance. However, when the buckling loads were increased, longer columns showed a beneficial behaviour too. The highlighted values in Table 5.19 capture this behaviour, it shows that for a 2 m long column with a buckling resistance of 500 kN and a 6m long column with a buckling resistance of 4000 kN made from S690 steel almost had an equal steel area reduction of 30 %. The other values summarized in Table 5.19 represents the steel area reductions for column lengths 2m, 6m and 10m according to *Analysis 2*. This table corresponds to the results in Figure 5.9.

Table 5.19 Steel area reductions possible with HSS for a hot rolled quadratic column with a design buckling resistance of 500 kN, 1000 kN, 2000 kN and 4000 kN for the lengths 2, 6 and 10 m.

L [m]	N _{Rd} [kN]	Smallest steel area [%]					
		S355	S420	S460	S500	S620	S690
2	500	0	11	20	24	29	30
	1000	0	13	21	27	37	41
	2000	0	14	22	28	40	45
	4000	0	15	22	28	41	46
6	500	0	4	11	13	16	18
	1000	0	4	11	13	18	19
	2000	0	6	13	14	19	21
	4000	0	11	20	23	27	29
10	500	0	4	11	12	15	17
	1000	0	4	11	13	17	18
	2000	0	4	12	13	17	19
	4000	0	3	11	13	17	19

The result from this analysis showed also that the relative ratio between the optimized steel areas for columns made from HSS was consistent through the analysis. However, one observation was made, it showed that increased buckling resistances resulted in displaced curves, i.e. larger buckling capacities entailed larger relative ratios between HSS grades for a wider range of column lengths. This can be seen in Figure 5.9, where the curves are ‘pushed’ more to the right for increasing loads. What this means is that a critical non-dimensional slenderness where HSS is no longer beneficial is achieved at longer column lengths when the buckling load is increased.

In Figure 5.9 area ratios are presented for different buckling loads. For a buckling load of 500 kN an area ratio of 90 % is achieved at approximately 2 m for the S420 steel. The same area ratio but for a buckling load of 4000 kN is achieved at approximately 6 m. The non-dimensional slenderness for both of them is however equal. This is shown in Figure 5.10 where the intersections of the lines represents positions where the different steel grades have equal slenderness and equal area reductions are possible.

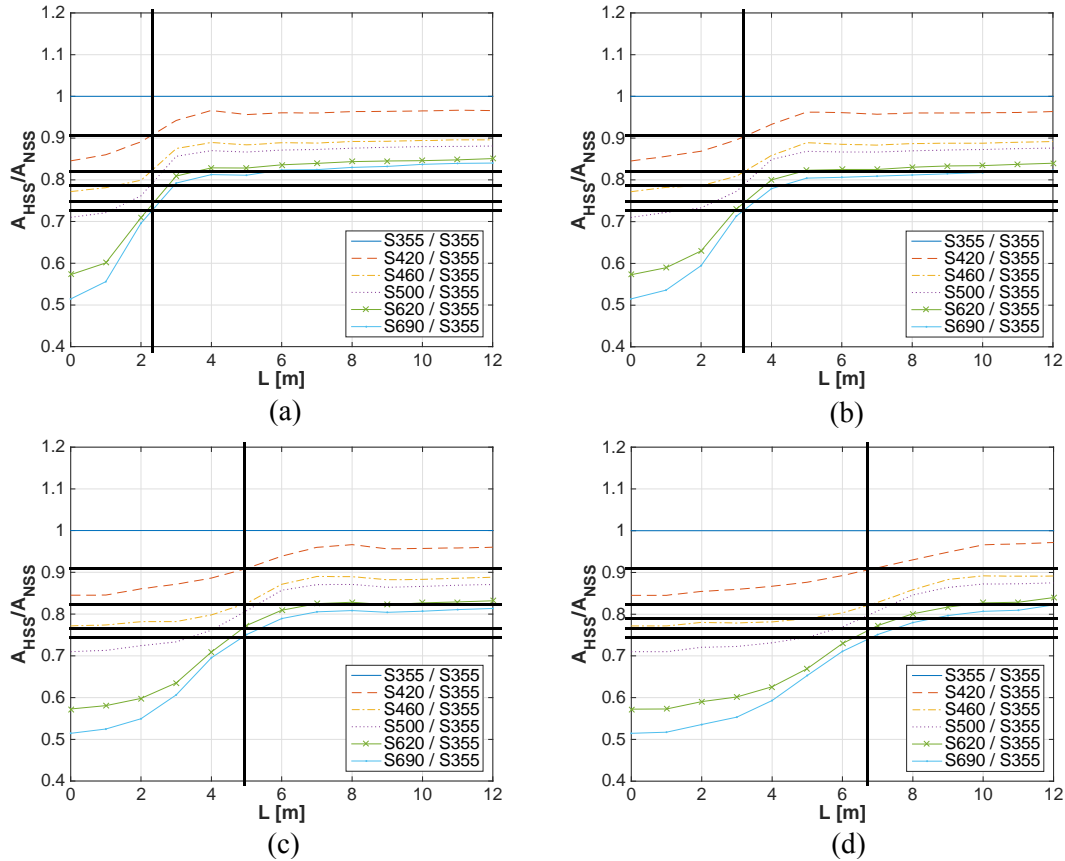


Figure 5.10 Illustration of positions where the non-dimensional slenderness is equal for the steel grades S420, S460, S500, S620 and S690. The intersections for each steel grades represents columns with equal slenderness.

The area benefits when using HSS can therefore be concluded to be dependent on the non-dimensional slenderness independently on what the buckling load is. Table 5.20 shows the non-dimensional slenderness for the steel grades S420, S460, S500, S620 and S690 at different buckling loads. It is seen that they are equal at different lengths where they also have the same area reduction.

Table 5.20 Non-dimensional slenderness for different steel grades at different lengths where they result in the same area reduction compared to S355 steel according to analysis 2.

	$\frac{A_{HSS}}{A_{NSS}}$	500 kN		1000 kN		2000 kN		4000 kN	
		L [m]	$\bar{\lambda}$	L [m]	$\bar{\lambda}$	L [m]	$\bar{\lambda}$	L [m]	$\bar{\lambda}$
S420	0.91	2.2	0.67	3.2	0.67	5.0	0.67	6.3	0.67
S460	0.82	2.2	0.77	3.2	0.77	5.0	0.77	6.3	0.77
S500	0.79	2.2	0.83	3.2	0.83	5.0	0.83	6.3	0.83
S620	0.74	2.2	1.00	3.2	1.00	5.0	1.00	6.3	1.00
S690	0.72	2.2	0.92	3.2	0.92	5.0	0.92	6.3	0.92

Table 5.20 shows that equal non-dimensional slenderness occur at different lengths depending on what buckling load the column is design for. The conclusions is that

HSS is beneficial to use up to a certain non-dimensional slenderness. For an S690 steel an area reduction of approximately 30 % compared to S355 is possible up to a slenderness of 0.92. So for example, if an S690 steel is more than 30 % costly than an S355 steel, it is not beneficial to implement it for columns that exceed a non-dimensional slenderness of 0.92.

The main reason that all columns made from HSS were more or less beneficial compared to NSS in this analysis was that none of the columns were removed from the calculations i.e. the total selection of cross sections were considered. With all columns taken into consideration, the script was able to find HSS cross sections with a smaller area than cross sections made from NSS even though that all columns in cross section class 4 were calculated with an effective area.

Table 5.21 through Table 5.24 exemplifies how the script selects the optimized steel area for a 10m column with a buckling resistance of 500 kN for the steel grades S355 and S690. The matrices in these tables are downscaled versions of the matrices in the MATLAB script but the principles are the same. From these tables it clearly shows that the $\frac{c}{t}$ ratio for the optimized column was considerably higher for both S355 and S690 compared to the limit values of cross section class 4 according to Table 5.10 and thus the smallest steel area were found for columns in cross section class 4. The underlying cause behind that behaviour was that the limit values of cross section class 4 according to Table 5.10 are not the governing factor when the selection of the optimized columns was made. The governing factor in this analysis was instead the difference in the number of columns that were able to resist the predefined buckling load. The results showed that columns with higher yield strength had a greater selection of these columns and therefore, the steel areas became smaller.

Table 5.21 $\frac{c}{t}$ ratio for the selection of cross section for S355. Highlighted region represents cross sections in class 4 (removed in script). Values within the boundary represents columns with a buckling resistance of 500 kN or greater. The $\frac{c}{t}$ ratio corresponding to the optimized steel area*).

11.33	7.00	4.79	3.45	2.56	1.91	1.43	1.05	0.75	0.50
24.67	16.00	11.58	8.91	7.11	5.83	4.86	4.10	3.50	3.00
38.00	25.00	18.38	14.36	11.67	9.74	8.29	7.15	6.24	5.50
51.33	34.00	25.17	19.82	16.23	13.65	11.71	10.20	8.99	8.00
64.67	43.00	31.96	25.27	20.78	17.57	15.14	13.25	11.74	10.50
78.00	52.00*	38.75	30.73	25.34	21.48	18.57	16.31	14.49	13.00
91.33	61.00	45.55	36.18	29.90	25.39	22.00	19.36	17.24	15.50
104.67	70.00	52.34	41.64	34.46	29.30	25.43	22.41	19.98	18.00
118.00	79.00	59.13	47.09	39.01	33.22	28.86	25.46	22.73	20.50
131.33	88.00	65.92	52.55	43.57	37.13	32.29	28.51	25.48	23.00

Table 5.22 $\frac{c}{t}$ ratio for the selection of cross section for S690. *Highlighted region represents cross sections in class 4 (removed in script). Values within the boundary represents columns with a buckling resistance of 500 kN or greater. The $\frac{c}{t}$ ratio corresponding to the optimized steel area*).*

11.33	7.00	4.79	3.45	2.56	1.91	1.43	1.05	0.75	0.50
24.67	16.00	11.58	8.91	7.11	5.83	4.86	4.10	3.50	3.00
38.00	25.00	18.38	14.36	11.67	9.74	8.29	7.15	6.24	5.50
51.33	34.00	25.17	19.82	16.23	13.65	11.71	10.20	8.99	8.00
64.67	43.00	31.96	25.27	20.78	17.57	15.14	13.25	11.74	10.50
78.00	52.00	38.75	30.73	25.34	21.48	18.57	16.31	14.49	13.00
91.33*	61.00	45.55	36.18	29.90	25.39	22.00	19.36	17.24	15.50
104.67	70.00	52.34	41.64	34.46	29.30	25.43	22.41	19.98	18.00
118.00	79.00	59.13	47.09	39.01	33.22	28.86	25.46	22.73	20.50
131.33	88.00	65.92	52.55	43.57	37.13	32.29	28.51	25.48	23.00

Table 5.23 Selection of cross sectional areas for S355. *Highlighted region represents cross sections in class 4 (removed in script). Values within the boundary represents columns with a buckling resistance of 500 kN or greater. Optimized cross sectional area*).*

0.0004	0.0006	0.0008	0.0010	0.0011	0.0012	0.0013	0.0014	0.0015	0.0015
0.0009	0.0013	0.0017	0.0021	0.0025	0.0029	0.0032	0.0035	0.0038	0.0041
0.0014	0.0021	0.0027	0.0033	0.0039	0.0045	0.0051	0.0056	0.0061	0.0067
0.0019	0.0028	0.0036	0.0045	0.0053	0.0061	0.0069	0.0077	0.0085	0.0092
0.0024	0.0035	0.0046	0.0057	0.0067	0.0078	0.0088	0.0098	0.0108	0.0118
0.0028	0.0042*	0.0055	0.0068	0.0081	0.0094	0.0107	0.0119	0.0131	0.0143
0.0033	0.0049	0.0065	0.0080	0.0095	0.0110	0.0125	0.0140	0.0155	0.0169
0.0038	0.0056	0.0074	0.0092	0.0109	0.0127	0.0144	0.0161	0.0178	0.0195
0.0043	0.0063	0.0083	0.0103	0.0123	0.0143	0.0163	0.0182	0.0201	0.0220
0.0048	0.0070	0.0093	0.0115	0.0137	0.0159	0.0181	0.0203	0.0224	0.0246

Table 5.24 Selection of cross sectional areas for S690. Highlighted region represents cross sections in class 4 (removed in script). Values within the boundary represents columns with a buckling resistance of 500 kN or greater. Optimized cross sectional area*).

0.0004	0.0006	0.0008	0.0010	0.0011	0.0012	0.0013	0.0014	0.0015	0.0015
0.0009	0.0013	0.0017	0.0021	0.0025	0.0029	0.0032	0.0035	0.0038	0.0041
0.0014	0.0021	0.0027	0.0033	0.0039	0.0045	0.0051	0.0056	0.0061	0.0067
0.0019	0.0028	0.0036	0.0045	0.0053	0.0061	0.0069	0.0077	0.0085	0.0092
0.0024	0.0035	0.0046	0.0057	0.0067	0.0078	0.0088	0.0098	0.0108	0.0118
0.0028	0.0042	0.0055	0.0068	0.0081	0.0094	0.0107	0.0119	0.0131	0.0143
0.0033*	0.0049	0.0065	0.0080	0.0095	0.0110	0.0125	0.0140	0.0155	0.0169
0.0038	0.0056	0.0074	0.0092	0.0109	0.0127	0.0144	0.0161	0.0178	0.0195
0.0043	0.0063	0.0083	0.0103	0.0123	0.0143	0.0163	0.0182	0.0201	0.0220
0.0048	0.0070	0.0093	0.0115	0.0137	0.0159	0.0181	0.0203	0.0224	0.0246

5.2.3 Analysis 1 and 2 – influence of cross section class

By combining the plots from *Analysis 1* and *2* it is possible to see when the change of cross section class appears. Figure 5.11 show the plots from *Analysis 1* and *2* in the same figure, for the steel grade S690. The first part of the curves are from *Analysis 1* and *Analysis 2*. Up until a certain length, the ratio according to *Analysis 1* and *Analysis 2* are equal. At a certain length, which represents equal non-dimensional slenderness, there is a separation of the curves which illustrates where the analysis separate which means there is a transition from class 3 to class 4.

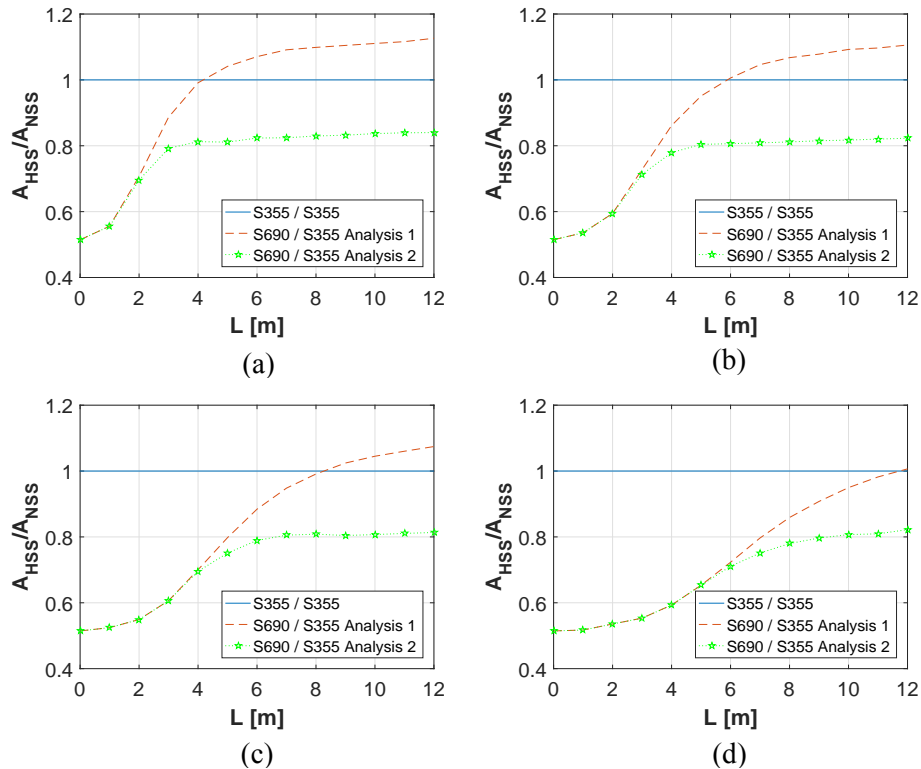


Figure 5.11 Transition between cross section class 3 and 4 for an S690 quadratic column loaded with 500 kN (a), 1000 kN (b), 2000 kN (c) and 4000 kN (d).

The curve separation is dependent on the non-dimensional slenderness. For each steel grade, also S355, the separation takes place at a non-dimensional slenderness of approximately 1, see Table 5.25. This is true regardless what buckling load the column is designed for. The study does not say that much about HSS. It only shows that steel columns that have a non-dimensional slenderness above 1 benefit in cross sectional steel area by exceeding the limit of cross section class 4.

Table 5.25 Non-dimensional slenderness for each steel grade where the separation between cross section class 3 and 4 takes place.

	500kN	1000kN	2000kN	4000kN
S355	0.99	1.02	1.04	1.02
S420	0.97	1.01	1.01	1.01
S460	0.99	0.99	1.03	1.02
S500	0.96	0.99	1.00	1.03
S620	1.01	1.01	1.01	1.00
S690	0.95	0.99	1.03	0.99

5.2.4 Analysis 3

Figure 5.12 displays the optimized steel area ratio between the S355 steel and the HSS grades for *Analysis 3*. The straight solid line represents the optimized steel area for NSS, the other curves represent the optimized steel areas for the HSS. Curves below the straight line implies that columns made from HSS have a smaller steel area

than a column made from NSS. Each of the four graphs represents the load levels, 500 kN, 1000 kN, 2000 kN and 4000 kN.

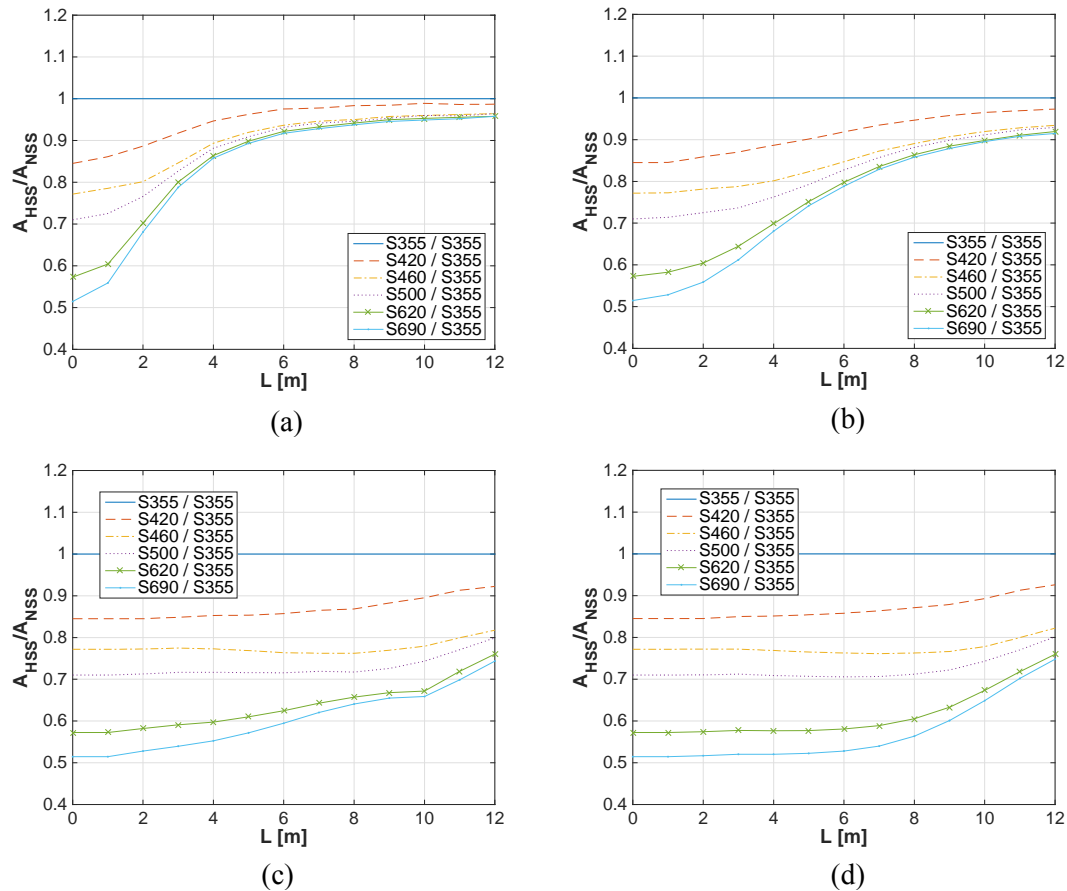


Figure 5.12 Relation between the smallest steel area possible for steel strengths 420 – 690MPa and the smallest steel area possible for a 355MPa steel strength. The areas regard quadratic columns with buckling resistance of 500 kN (a), 1000 kN (b), 2000 kN (c) and 4000 kN (d).

The first and most obvious observation from this analysis was that implementation of HSS will always be beneficial for column regardless of yield strength, column length or buckling resistance. However, there were differences of how great the benefits were and when the benefits occurred. Results showed that an increasing yield strength gave higher benefits. The least favourable steel grade was the S420. This behaviour was consistently throughout Analysis 3.

Regarding the column non-dimensional slenderness, the results from this analysis showed that less slender columns in general were more beneficial when HSS was implemented irrespective of the buckling resistance. The behavior can be explained in the same way as in *Analysis 2*. For each steel grade, the same area reductions are seen for an equal slenderness. With increasing buckling loads, these values of slenderness will occur at different lengths. Figure 5.13 shows the area relations between HSS and S355 steel for the loads 500 kN and 1000 kN along with the non-dimensional slenderness values for each steel grade.

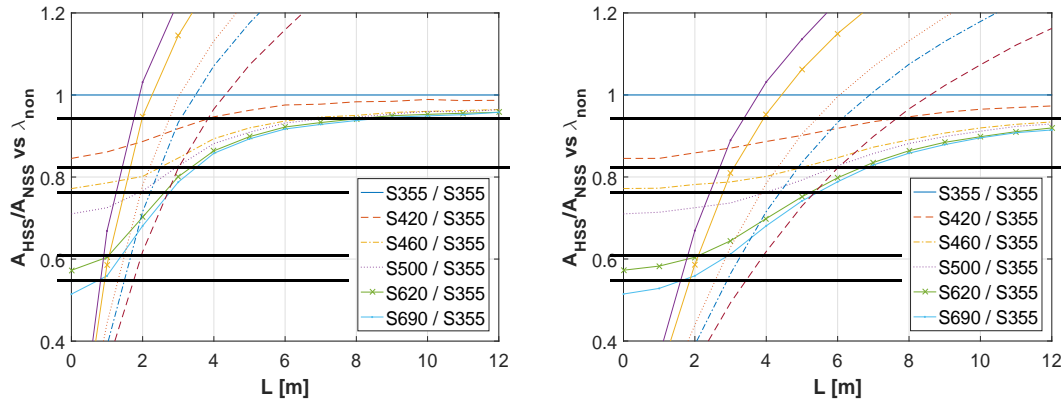


Figure 5.13 Area relation between HSS and S355 steel according to analysis 3. Also non-dimensional slenderness for the optimized cross sections in HSS according to analysis 3.

From Figure 5.13 it can be seen that the same non-dimensional slenderness occurs at different lengths depending on the buckling load. The conclusion is that HSS is beneficial to use up to a certain slenderness. In *Analysis 3* an S690 steel gave an area reduction of approximately 45% at a slenderness of 0.55. So for example if the S690 steel is 45 % more expensive it is not beneficial to implement it for columns with a non-dimensional slenderness that exceeds 0.55.

The main reason that all columns made from HSS always were more or less beneficial compared to NSS in this analysis was the fact that in *Analysis 3*, cross section class 4 was not considered. This means that equations (5.13) and (5.14) that governs the limit value of cross section class 4 was ignored. The result of this was that none of the columns were removed from the calculations i.e. the total selection of cross sections could be considered. The governing factor in this analysis was instead the difference in the number of columns that were able to resist the predefined buckling resistance. The results showed that columns with higher yield strength had a greater selection of these columns and therefore, the steel areas became smaller.

$$\varepsilon = \sqrt{\frac{235}{f_y}} \quad \text{Where } f_y \text{ is the yield strength in MPa} \quad (5.13)$$

$$\frac{c}{t} \leq 42\varepsilon \quad (5.14)$$

Where $c = b - 2t$
 $b = \text{width}$
 $t = \text{thickness}$

5.2.5 Summary of analysis

In order to summarize the results from *Analysis 1*, *Analysis 2* and *Analysis 3* two plots are presented in Figure 5.14. The plot in (a) illustrates the optimized areas for quadratic columns made by S690 steel and S355 steel from all three analysis. The plot in (b) illustrates the optimized area ratios from all three analysis. The figure represents columns with a design buckling capacity of 1000 kN. It is important to remember that

in each analysis, optimized cross sections in HSS are compared to optimized cross sections in NSS. This means that the solid line with a value of 1 in (b) represents 3 different lines. These three lines originates from S355 divided with S355 from *Analysis 1*, *Analysis 2* and *Analysis 3*. They are all equal to one but originates from different S355 relations.

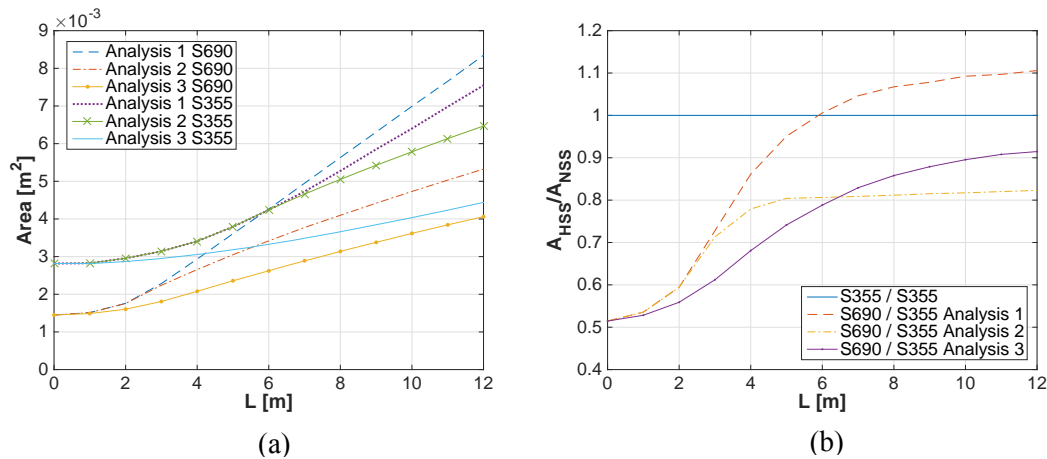


Figure 5.14 Optimized steel areas according to analysis 1, 2 and 3 for the steel grades S355 and S690 (a). Optimized steel area relation between S690 and S355 steel (b). The plots considers a buckling resistance of 1000 kN.

From Figure 5.14 conclusions from the analysis performed can be drawn. Firstly, the optimized steel areas in S690 seen in (a) were smallest in *Analysis 3*, a little larger in *Analysis 2*, and largest in *Analysis 1*. This was true for independently of the non-dimensional slenderness of the column. The fact that *Analysis 3* resulted in the smallest areas was expected due to the fact that it was assumed that cross sections were prevented to buckle which means that fully utilized areas could be chosen. In *Analysis 2* the cross sections which were in class 4 were reduced which resulted in larger areas.

Also with an S355 steel the smallest areas were possible in *Analysis 3*. With this steel grade, *Analysis 1* and 2 had the same optimized steel areas up until approximately 6m where they both had the same non-dimensional slenderness of 1.0. This can be seen in both figure (a) and (b). Beyond this length, S355 cross sections in cross section class 4 were able to be less slender and have smaller cross sectional areas than the ones demanded to stay in cross section class 3.

The solid line in figure (a) represents optimized cross sections which were prevented to buckle locally. If this is achieved, columns made of S355 steel are able to have a smaller cross sectional area than the S690 steel in *Analysis 1* and *Analysis 2* at approximately 4 m and 5.5 m respectively. To modify an S355 cross section can therefore be more beneficial than to increase the steel grade. An example calculation of this is shown in Appendix C.

Figure 5.14 (b) tells us that the order of optimized steel area ratios are not the same as the order of steel areas seen in (a). At a length slightly above 6 m the ratio from *Analysis 3* gets less beneficial than the ratio from *Analysis 2*. This means that beyond this length, cross sections which are prevented to buckle do not benefit as much from

an S690 steel as cross sections which are in class 4 but not prevented to buckle. Even so, the actual areas were always smaller according to *Analysis 3*.

The actual dimensions of the optimized cross sections for a 4 m long column with a buckling resistance of 1000 kN are presented in Table 5.26.

Table 5.26 Widths, thicknesses, areas and non-dimensional slenderness of optimized cross sections regarding steel areas for a 4 m long column with a design buckling resistance of 1000 kN according to analysis 1, 2 and 3.

	Analysis 1		Analysis 2		Analysis 3	
	S355	S690	S355	S690	S355	S690
b [mm]	178.0	141.1	178.0	164.5	257.4	176.2
t [mm]	4.9	5.4	4.9	4.1	3.0	3.0
Area [mm²]	3409	2936	3409	2656	3053	2079
$\bar{\lambda}$	0.74	1.32	0.74	0.93	0.92	1.03

The 4 m long column benefit from the S690 steel in all three analyses, where the optimized columns in *Analysis 3* was most beneficial. The possible steel area reductions are shown in Table 5.27.

Table 5.27 Possible area reduction for a 4 m long column when increasing the steel grade from S355 to S690 according to analysis 1, 2 and 3.

	Analysis 1	Analysis 2	Analysis 3
Area reduction	11%	22%	32%

At 4m, a quadratic column benefit from HSS according to all three analysis. However the cross sections are wider in *Analysis 2* and *Analysis 3* compared to *Analysis 1*. The S690 steel area in *Analysis 3* is 2079 mm² and in *Analysis 2* it is 2656 mm². The cross section in *Analysis 3* is however 12 mm wider compared to *Analysis 2*. The same behaviour is seen between *Analysis 1* and *Analysis 2* where the width is greater in *Analysis 2* compared to *Analysis 1*. Cross sections decrease in steel areas by smaller thicknesses, but increase in widths in order to have enough buckling resistance.

The actual dimensions of the optimized cross sections for a 10 m long column with a buckling resistance of 1000 kN are presented in and Table 5.28.

Table 5.28 Widths, thicknesses and areas of optimized cross sections regarding steel areas for a 10 m long column with a design buckling resistance of 1000 kN according to analysis 1, 2 and 3.

	Analysis 1		Analysis 2		Analysis 3	
	S355	S690	S355	S690	S355	S690
b [mm]	243.9	218.6	282.7	298.9	339.5	304.4
t [mm]	6.7	8.3	5.2	8.3	3.0	3.0
Area [mm²]	6400	6992	5789	4731	4039	3616
$\bar{\lambda}$	1.35	2.12	0.97	1.35	0.95	1.48

The 10 m long column does not benefit from HSS in all analysis. The area reductions are shown in Table 5.29. It is shown that *Analysis 2* resulted in the largest steel area reduction. The actual areas are however smaller in *Analysis 3*, see Figure 5.14.

Table 5.29 Possible area reduction for a 10 m long column when increasing the steel grade from S355 to S690 according to analysis 1, 2 and 3.

	Analysis 1	Analysis 2	Analysis 3
Area reduction	-9%	18	10

Table 5.28 and Table 5.29 show that the largest area reduction was seen in *Analysis 2*. However, the steel area was smallest in *Analysis 3*. This means that beyond a critical slenderness it is more beneficial to modify S355 cross sections so that they do not buckle than to increase the steel grade.

5.2.6 Column analysis - Final conclusions

Three different analyses were carried out where different approaches was used regarding the cross section classes. The difference between steel grades was achieved by always comparing optimized cross sections in HSS to optimized cross sections in NSS.

Analysis 1 and *Analysis 2* showed that the cross section class has a major impact on the fact if HSS is beneficial compared to NSS. Columns which are demanded to be below the limit of cross section class 4 benefit from an increased steel grade to a certain non-dimensional slenderness. There is a non-dimensional slenderness limit for each steel grade where S355 steel is more beneficial than HSS. If however columns are allowed to be over the limit of cross section class 4, area reductions are always seen with HSS. How large the benefits are is related to the non-dimensional slenderness. Therefore the price becomes interesting. If the price of different HSS is known, it can be concluded what non-dimensional slenderness is maximum in order to get a lower cost with HSS than NSS.

In *Analysis 3*, cross sections were considered to not buckle locally by modifications made to the cross section, an example was shown in Figure 5.6. The result of this is of course that a higher steel grades demands a smaller steel area when using HSS compared to NSS. If it is beneficial or not to replace NSS with HSS is again dependent on the price and non-dimensional slenderness. If the price is known, a non-dimensional slenderness which is maximum to lower the cost can be concluded.

The smallest steel areas were always seen in analysis 3. However, these cross sections would need to be modified in order to prevent local buckling. After a certain non-dimensional slenderness, cross sections made by S355 steel and prevented to buckle were able to have smaller areas than cross sections made by S690 steel but not prevented to buckle. This means that it could be more beneficial to modify existing cross sections in S355 steel instead of increasing the steel grade.

Final conclusion of the three analysis performed is that the greatest steel area reduction was possible when the non-dimensional slenderness of columns is as small as possible. There is a critical non-dimensional slenderness for each steel grade where

HSS is no longer beneficial. What this critical non-dimensional slenderness is, depends on the price of the HSS.

6 Case study

Between 2012 and 2015 Prioritet Serneke Arena was erected just outside of Gothenburg. The building was initiated to provide Gothenburg with a new multisport arena with e.g. an indoor football field, two handball courts and a 1000m ski run. Integra Engineering AB was the main designer for the foundation and structure.

The building can be considered to consist of two parts. One part consists of a relatively conventional structure with columns and beams while the other part is made by truss frames which are connected with tension chords. The load bearing structure for both parts is made of S355 steel. In total the building consists of more than 1500 beams, 1200 columns and a number of truss structures of different sizes and lengths. A 3D-model of the steel structure is shown in Figure 6.1.

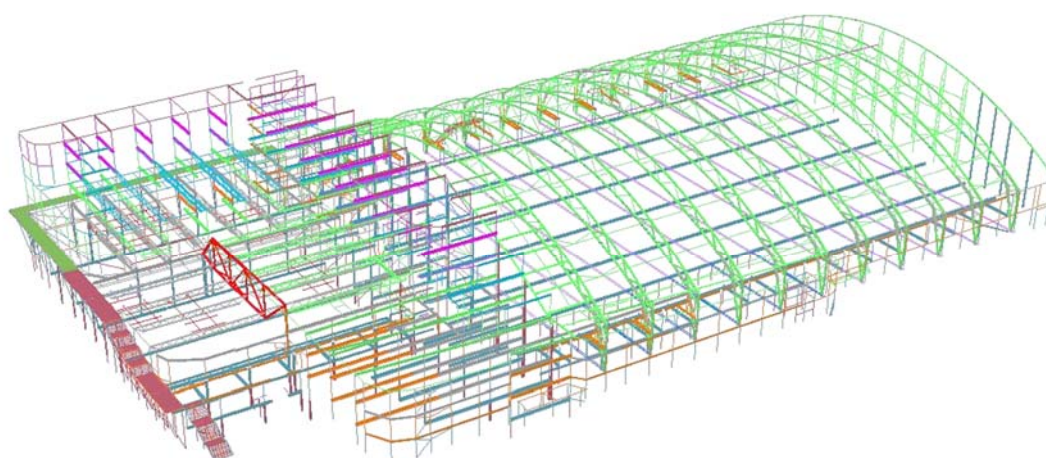


Figure 6.1 Steel structure of Prioritet Serneke Arena.

The results presented in chapter [4] and [5] are general results regarding differences between HSS and NSS and possible steel area reductions. The structure in Figure 6.1 was chosen because it holds a large variety of columns and it has both a part which is considered conventional and one that is more like the structure of an arena.

It has already been concluded that beams do not benefit that much when increasing the steel strength, see chapter [4]. However the analysis made in chapter [5] show benefits regarding steel area reduction when increasing the steel grade in hot rolled quadratic columns. Therefore this case study was initiated. The case study aims to study three optimizations, listed below.

Steel area optimization:

Investigate possible weight reductions by implementing HSS and obtaining smallest steel areas in all hot rolled quadratic columns, see Figure 6.2. Existing cross sections were compared to optimized cross sections in steel grades S355 up to S690. Also, in order to get just results regarding material behavior, the smallest area of the steel grades S420 up to S690 were compared to the smallest area that is possible of the S355 columns. This means that two comparisons were made. One result is weight reductions possible by a direct implementation in the structure. The other is where optimized cross sections in HSS replace optimized cross sections in NSS. Two

weights of the S355 steel will therefore be presented, both the weight of the existing columns and also the weight of optimized cross sections in S355 steel. This was done in order to see both the difference in material behavior between steel grades and the effect of directly implementing HSS in the existing structure.

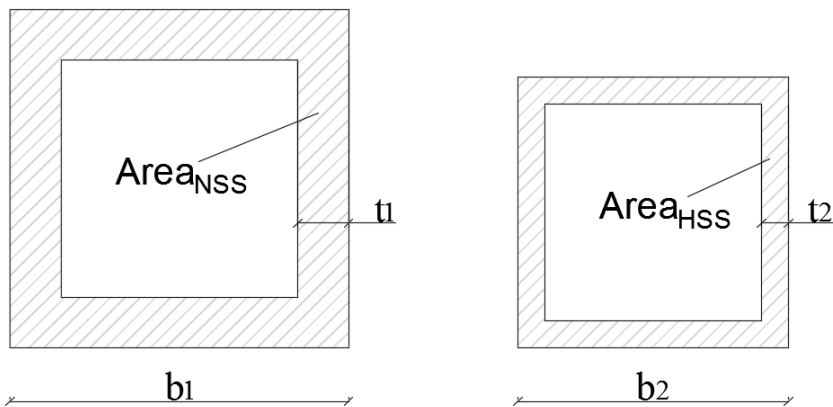


Figure 6.2 The area of interest in the optimization is the steel area. Is HSS beneficial regarding the steel area in quadratic columns?

Thickness optimization:

Investigate the possible thickness reduction while keeping the same width as the existing columns by implementing HSS in all hot rolled quadratic columns in the structure. This entails that all the columns in this optimization had the same column area while the thickness differs, see Figure 6.3. In this investigation there was no optimization for the S355 columns, weights of the optimized columns were compared to weights of the existing columns.

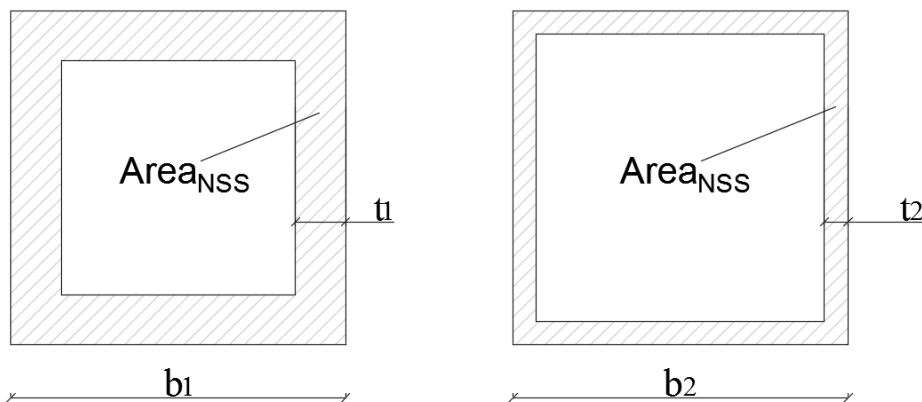


Figure 6.3 Is HSS beneficial regarding the thickness in quadratic columns? The widths b_1 and b_2 are equal.

Column area optimization:

Investigate the possible column area reduction by implementing HSS in all hot rolled quadratic columns in the structure, Figure 6.3. The smallest circumference was of interest for each HSS. In this investigation all the HSS columns were compared to existing S355 columns and to optimized S355 columns. Two weights of the S355 steel cross sections will therefore be presented, both the weights of the optimized cross section and the weights of the existing cross sections in S355 steel. This was done in order to see both the difference in material behavior between steel grades and the effect of directly implementing HSS in the existing structure.

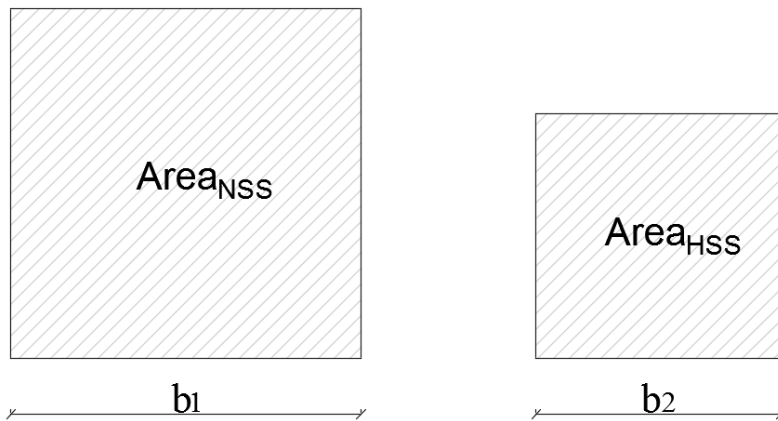


Figure 6.4 Is HSS beneficial regarding the circumference of quadratic columns?

6.1 Columns in structure

Out of the 1200 columns in Prioritet Serneke Arena, 885 are hot rolled and have a quadratic cross section. The columns vary in length where, according to the model, the shortest one is 40 mm and the longest 23.1 m. Lengths below 500 mm are not really considered as columns, but are still accounted for in the MATLAB script. This was done due to the fact that they are considered to be subjected to pure compression and could just as well be replaced with HSS. The number of quadratic columns with the corresponding dimensions are summarized in Table 6.1.

Table 6.1 Number of quadratic hot rolled columns and dimensions in Prioritet Serneke Arena.

t [mm]	4	5	6.3	8	10	12.5	16
HxB [mm]							
60	46	3					
80	2	11	1				
90		78	1				
100	3	27	43	11	4		
120		9	148	15	78		
140			6		13		
150			18	51	43		
160			4		7		
200			5	60	30	1	38
250				2	5	4	1
300					67	27	8
350						1	14

All the columns used in Prioritet Serneke Arena with their corresponding lengths were imported to the MATLAB script, described in [5.1]. The script was modified by instead of setting the input load manually, it was set as the calculated design buckling resistance of each column in Table 6.1. The script outputs new possible cross sections able to resist this load.

The study shows a comparison between HSS and NSS which are subjected to pure compression and fully utilized. No horizontal loads such as wind or accidental loads are taken into account. Therefore the results presented shows the trend HSS would have on the columns in the structure. They cannot be directly applicable on the structure.

All the columns were investigated according to *Analysis 2*, described in [5.1.3]. The analysis was used to investigate the optimization approaches *Steel area optimization*, *Thickness optimization* and *Column area optimization*, which was described in [6]. The HSS considered were S420, S460, S500, S550, S620 and S690. To see the differences between steel grades, comparison of weights between steel grades was carried out. In each approach the weight per meter of the optimized cross sections were calculated according to equation (6.1).

$$Weight = \rho A_s \quad (6.1)$$

Where

$\rho = 7850 \text{ kg/m}^3$ Density of steel
 A_s Steel area

In order to investigate the columns in the structure, weights and weight savings for the entire building will be presented. Also, weights and weight savings for the most common cross section which is 120 mm wide and 6.3 mm thick is presented with different steel grades. The cross section is shown in Figure 6.5.

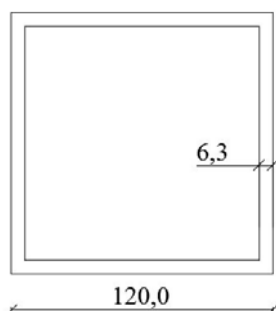


Figure 6.5 Most common cross section found in Prioritet Serneke Arena.

Columns with the cross section as presented in Figure 6.5 have lengths varying between 59 mm and 6980 mm. Of the 148 columns made of this cross section, 12 are 4010 mm, 18 are 3330 mm and 26 are 310 mm long. These lengths was investigated thoroughly. The 4010 mm and 3330 mm long columns were chosen because they are considered as ‘normal’ and vary common lengths in conventional structure. The short 310mm long column was chosen to see results also for these lengths which could be used in for example smaller trusses.

The longest columns in the structure are 23.1 m. The cross section of these are shown in Figure 6.6. In order to see if HSS is beneficial for very long columns, this column was also investigated thoroughly.

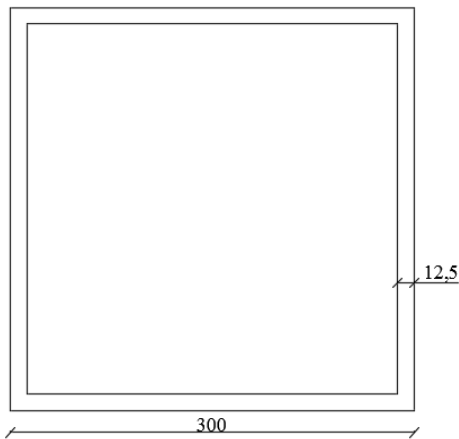


Figure 6.6 Cross section of the longest column in the structure

6.2 Steel area optimization

The weights and weight savings that is possible with this approach according to analysis 2 are shown in Table 6.2.

Table 6.2 Weights and weight savings by implementing HSS in the quadratic columns in Prioritet Serneke Arena according to analysis 2. ¹⁾ Reference column from Prioritet Serneke Arena. ²⁾ Optimized S355 column.

	S355 ¹⁾	S355 ²⁾	S420	S460	S500	S550	S620	S690
			Optimized cross sections					
Weight [kg]	175166	147776	136093	124766	120572	116534	112194	108841
Saving¹⁾ [kg/m]	0	27391	39073	50400	54594	58632	62972	66325
Saving¹⁾ [%]	0	16	22	29	31	33	36	38
Saving²⁾ [kg]		0	11682	23009	27203	31241	35582	38934
Saving²⁾ [%]		0	8	16	18	21	24	26

Table 6.2 shows that a weight reduction is possible by implementing HSS in the structure. If directly implementing optimized cross sections in the structure a maximum weight reduction of 38 % is possible. This is possible with the S690 steel. When comparing an optimized S355 cross section to optimized cross sections in HSS a maximum reduction of 26 % is possible with an S690 steel.

The weights and weight savings of the 120 mm wide and 6.3 mm thick column are shown in Table 6.3.

Table 6.3 Weights and weight savings for a hot rolled 120 mm wide and 6.3 mm thick column made of different steel grades according to analysis 2. ¹⁾ Reference column from Prioritet Serneke Arena. ²⁾ Optimized S355 column.

L [m]		S355 ¹⁾	S355 ²⁾	S420	S460	S500	S550	S620	S690
4.01	Weight [kg/m]	22.5	18.0	17.3	15.9	15.6	15.2	14.8	14.4
	Saving ¹⁾ [kg/m]	0.0	4.5	5.2	6.5	6.9	7.3	7.7	8.0
	Saving ¹⁾ [%]	0	20	23	29	31	32	34	36
	Saving ²⁾ [kg/m]		0.0	0.6	2.0	2.4	2.7	3.2	3.5
	Saving ²⁾ [%]		0	4	11	13	15	18	20
	Width [mm]	120	145.6	151.0	146.5	144.7	149.2	149.2	150.1
	Thickness [mm]	6.3	4.0	3.7	3.6	3.5	3.3	3.2	3.1
3.33	Weight [kg/m]	22.5	19.3	17.8	16.4	16.2	15.8	15.3	14.9
	Saving ¹⁾ [kg/m]	0.0	3.2	4.7	6.1	6.3	6.7	7.2	7.6
	Saving ¹⁾ [%]	0	14	21	27	28	30	32	34
	Saving ²⁾ [kg/m]		0.0	1.4	2.9	3.1	3.5	4.0	4.4
	Saving ²⁾ [%]		0	7	15	16	18	21	23
	Width [mm]	120	150.1	139.2	131.1	127.5	136.5	135.6	135.6
	Thickness [mm]	6.3	4.2	4.2	4.1	4.2	3.8	3.7	3.6
0.31	Weight [kg/m]	22.5	22.5	19.0	17.4	16.0	14.5	12.9	11.6
	Saving ¹⁾ [kg/m]	0.0	0.0	3.5	5.1	6.5	8.0	9.6	10.9
	Saving ¹⁾ [%]	0	0	15	23	29	35	43	49
	Saving ²⁾ [kg/m]		0.0	3.5	5.1	6.5	8.0	9.6	10.9
	Saving ²⁾ [%]		0	15	23	29	35	43	49
	Width [mm]	120	157.3	111.3	66.6	88.7	92.3	93.2	100.5
	Thickness [mm]	6.3	4.7	5.7	9.8	6.2	5.3	4.6	3.8

Table 6.3 show that the 4.01 m and 3.33 m long columns was able to have a weight reduction of 20 % and 23 % respectively when comparing optimized cross sections. The column with a length of 4.01 m had a steel area reduction of 36 % when comparing optimized cross sections to the existing cross section. This was possible with the S690 steel. The optimized cross sections would however have a larger width than the existing column, see Figure 6.7.

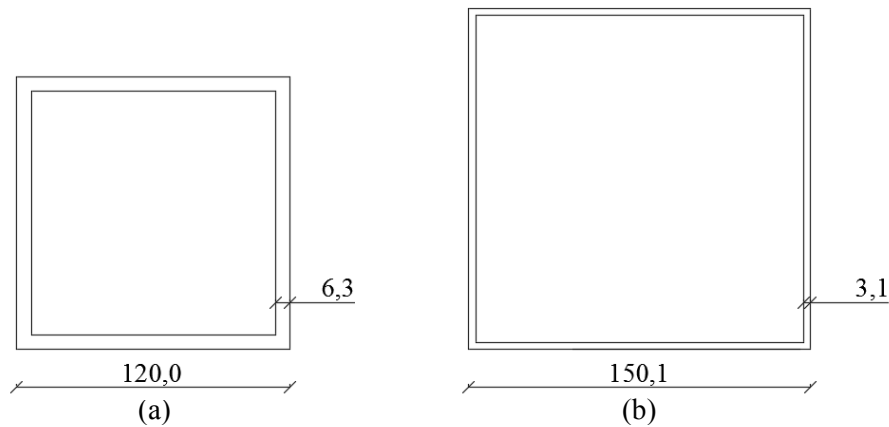


Figure 6.7 Cross section of existing S355 column (a) and the optimized cross section regarding steel area made of S690 steel (b). The cross sections regards the column length 4.01 m.

There is a breakpoint in length for each cross section where the cross section needs to be wider in order to benefit from HSS. The breakpoint for the cross section presented in Figure 6.7 (a) is at about 2.5 m. After this length columns with a cross section that is 120 mm wide and 6.3 mm thick still benefit from HSS but they will need to be wider to get the maximum benefits. Calculation of this is shown in Appendix D.

The shortest column of 310 mm had the same weight reduction both when comparing the optimized cross sections to the existing cross section and when comparing optimized cross sections in HSS to the optimized cross section in S355 steel. The existing column was not able to be more optimized than the cross section that is used today. The weight reduction for the 310 mm long column could be as much as 49%.

The results show that cross sections can vary quite much in width. The S690 steel always results in the best weight savings. If the cross section is smaller in width or not vary from column to column, for example the 4.01 m long column gets wider and thinner, see Figure 6.8.

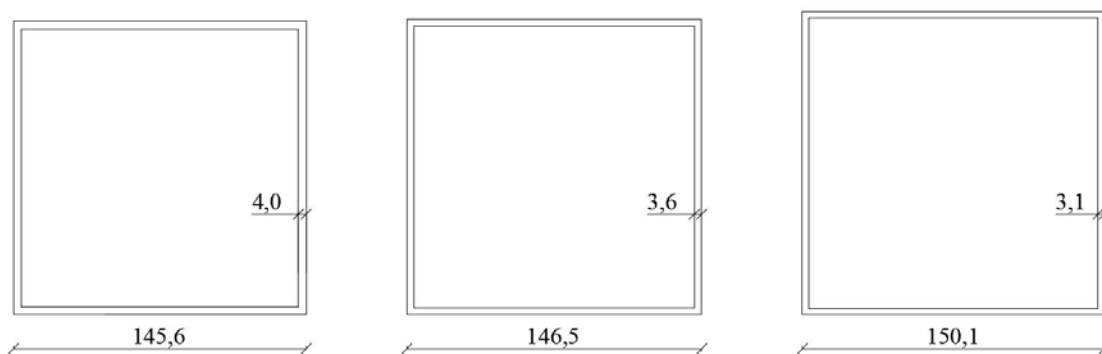


Figure 6.8 Optimized cross sections regarding steel area with the same design buckling resistance as an S355 120 mm wide and 6.3 mm thick column with a length of 4010 mm. The steel grades of the cross sections are S355 (a), S460 (b) and S690 (c).

The analysis show that also the longest column in the structure was able to have an area reduction with higher steel grades, see Table 6.4.

Table 6.4 Weights and weight savings for a hot rolled 300 mm wide and 12.5 mm thick column made of different steel grades according to analysis 2. ¹⁾ Reference column from Prioritet Serneke Arena. ²⁾ Optimized S355 column.

L [m]	S355 ¹⁾	S355 ²⁾	S420	S460	S500	S550	S620	S690
23.1	Weight [kg/m]	112.8	67.4	66.6	62.7	62.3	61.9	61.1
	Saving ¹⁾ [kg/m]	0.0	45.4	46.2	50.2	50.6	51.0	51.8
	Saving ¹⁾ [%]	0	40	41	44	45	45	46
	Saving ²⁾ [kg/m]		0.0	0.8	4.8	5.2	5.6	6.4
	Saving ²⁾ [%]		0	1	7	8	8	9
	Width [mm]	300	400	400	400	400	400	400
	Thickness [mm]	12.5	5.4	5.4	5.1	5.0	5.0	4.9

Table 6.4 show that a direct implementation of an optimized cross section of S690 steel would reduce the weight of the existing column with as much as 46 %. Because cross section class 4 is allowed, this optimized cross section would however be very thin and very wide, see Figure 6.9. Even if the weight reduction was this high, noticeable is that just by optimizing the existing column and still using S355 steel, a reduction of 40 % is possible. To see the difference between HSS and NSS it is better to look at the comparison made between optimized cross sections. This shows that a weight reduction of 9 % is possible when increasing the steel grade from S355 to S690.

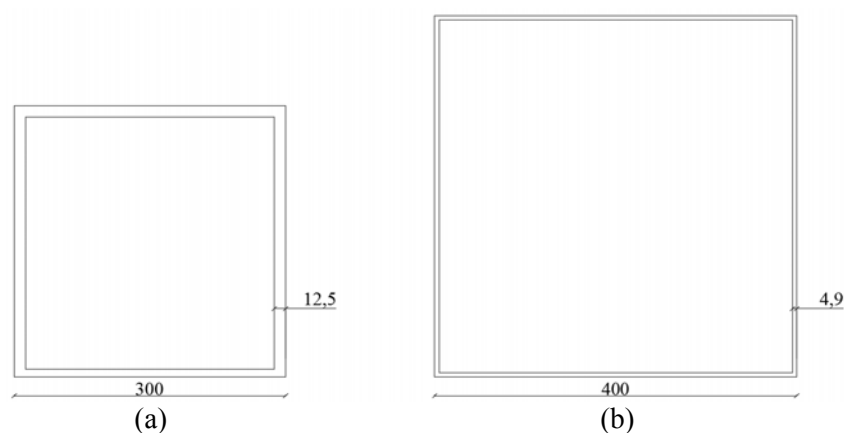


Figure 6.9 Cross section of existing S355 column (a) and optimized cross section regarding steel area, made of S690 steel (b).

Due to the fact that cross section class 4 is allowed, the 23 m long column reduce its weight by being as wide as possible and at the same time very thin. By comparing optimized cross sections a weight reduction of 9 % is possible when increasing the steel grade from S355 to S690. The optimized cross sections regarding steel area for S355, S460 and S690 are shown in Figure 6.10.

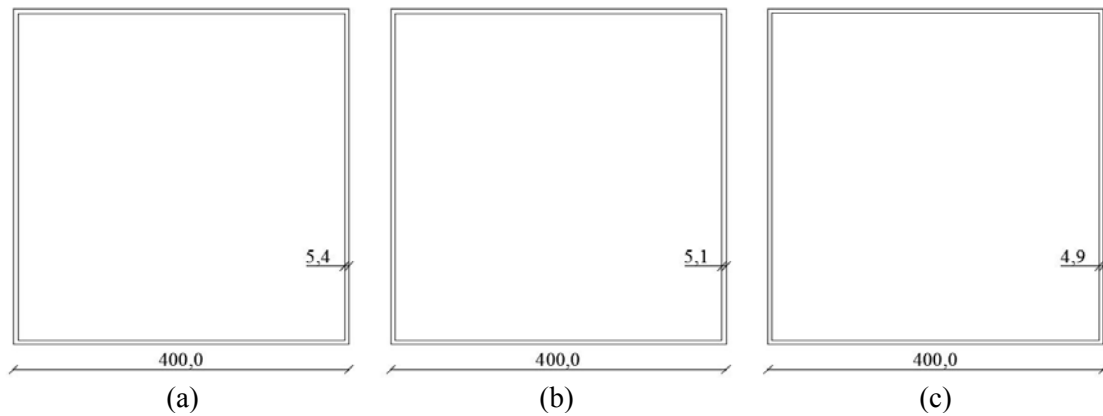


Figure 6.10 Optimized cross sections regarding steel area with the same design buckling resistance as a S355 300 mm wide and 12.5 mm thick column with a length of 23.1 m. The steel grades of the cross sections are S355 (a), S460 (b) and S690 (c).

The $\frac{c}{t}$ ratio for cross sections (a), (b) and (c) Figure 6.10 are:

$$(a) \quad \frac{c}{t} = 72$$

$$(b) \quad \frac{c}{t} = 76$$

$$(c) \quad \frac{c}{t} = 80$$

The limit for cross section class 4 can be seen in Table 6.5

Table 6.5 Cross section class 3 limit and slenderness for S460 and S690 steel.

	S460	S690
42ε	30.0	24.5
λ₁	67	55

It can be concluded that the cross optimized sections are very thin and well above the limit for cross section class 4. The effective areas of the cross sections are only 55 %, 47 % and 38 % for column (a), (b) and (c) respectively but even so, they are sufficient to resist the load necessary.

The results were as expected after the analysis was made in [5.2.2]. The plots in Figure 5.9 show the same tendency as Table 6.3 and Table 6.4 does. With increasing steel grades there is an increase in area reduction and therefore a weight reduction. How large the weight reduction is able to be, is dependent on the non-dimensional slenderness of the columns, where less slender columns benefit more from HSS.

Steel area optimization - Conclusions

According to analysis 2, there is a possible weight saving when increasing the steel grades of the quadratic columns in the structure. If a direct implementation were to be performed, a weight reduction of 38 % would be possible. This would however often

mean that wider cross sections would be needed. When this is true and not true depends on the lengths of the columns and the reference cross section in the existing columns. Every cross section have a breakpoint in length where HSS could mean a reduction in weight but where wider cross sections would be needed. In analysis 2 this breakpoint is at about 2.5 m for the 120 mm wide and 6.3 mm thick cross section. Also, by just optimizing the cross sections and keeping the steel grade as S355, a weight reduction of 16 % would be possible.

By instead comparing optimized cross sections in HSS to optimized cross sections in S355, the columns of the structure could be reduced in weight with 26 %. For all columns, whatever length they may have, the weight savings increase by increasing steel grade. However for the less slender columns, a greater weight saving is possible compared to more slender columns.

6.3 Thickness optimization

The weights and weight savings possible with this approach according to analysis 2 is presented in Table 6.6.

Table 6.6 Weights and weight savings by implementing HSS cross sections with an optimized thickness in the quadratic columns in Prioritet Serneke Arena according to analysis 2.

	S355	S420	S460	S500	S550	S620	S690
Weight [kg]	175166	161661	147920	144039	140685	137096	134211
Saving [kg]	0	13505	27247	31127	34481	38070	40955
Saving [%]	0.0	7.7	15.6	17.8	19.7	21.7	23.4

Table 6.6 proves that by letting the cross sections necessary to be in cross section class 4, weight savings are possible by an increased steel grade. With the S690 steel, a 23% weight reduction would be possible of the quadratic columns in the structure.

Also here, the lengths of the columns play an important role when determining how great the weight savings can be. The weight reductions of the 120 mm wide and 6.3 mm thick column, see Table 6.7, for the lengths 4.01 m, 3.33 m and 0.31 m are shown in Table 6.7.

Table 6.7 Weights and weight savings for a hot rolled 120 mm wide column with different thicknesses and steel grades according to analysis 2.

L [m]		S355	S420	S460	S500	S550	S620	S690
4.01	Weight [kg/m]	22.5	21.4	19.2	18.9	18.6	18.3	18.1
	Saving [kg/m]	0.0	1.1	3.2	3.6	3.9	4.1	4.4
	Saving [%]	0	5	14	16	17	18	19
	Width [mm]	120	120	120	120	120	120	120
	Thickness [mm]	6.3	6.0	5.3	5.2	5.2	5.1	5.0
3.33	Weight [kg/m]	22.5	20.6	18.1	17.4	17.0	16.4	16.2
	Saving [kg/m]	0.0	1.9	4.4	5.0	5.5	6.1	6.3
	Saving [%]	0	8	19	22	24	27	28
	Width [mm]	120	120	120	120	120	120	120
	Thickness [mm]	6.3	5.7	5.0	4.8	4.7	4.5	4.5
0.31	Weight [kg/m]	22.5	19.0	17.4	16.0	14.8	14.4	13.8
	Saving [kg/m]	0.0	3.5	5.0	6.5	7.7	8.1	8.7
	Saving [%]	0	15	22	29	34	36	39
	Width [mm]	120	120	120	120	120	120	120
	Thickness [mm]	6.3	5.3	4.8	4.4	4.1	3.9	3.8

Table 6.7 show that a weight reduction is always noticed by an increased steel grade. The largest benefits are seen on the 0.31 m long column which can have a reduction of 39 %. With longer and longer columns, benefits are still appearing but with a decreasing rate. The 3.33 m and 4.01 m long columns were able to be reduced by 28 % and 19 % respectively if implementing S690 steel. The longest column which is 23.1 m long and the weight savings possible for this are shown in Table 6.8. It can be concluded that weight savings are still possible but not to the same extent as for the short columns.

Table 6.8 Weight and weight savings for a quadratic hot rolled 300 mm wide column with different thicknesses and steel grades.

L [m]		S355	S420	S460	S500	S550	S620	S690
23	Weight [kg/m]	112.8	112.1	108.5	108.2	107.9	107.6	107.3
	Saving [kg/m]	0.0	0.7	4.4	4.7	5.0	5.2	5.5
	Saving [%]	0	1	4	4	4	5	5
	Width [mm]	300	300	300	300	300	300	300
	Thickness [mm]	12.5	12.4	12.0	12.0	11.9	11.9	11.9

Thickness optimization - Conclusions

According to analysis 2, there is a possible weight saving when keeping the same width of cross sections but changing the thicknesses. For the entire structure of Prioritet Serneke Arena a weight reduction of the hot rolled columns of 23 % was possible when using S690 steel instead of S355. Weight reductions are noticed for all columns, both less and more slender. However, again, the rate of weight reduction reduces with increasing slenderness of the columns.

6.4 Column area optimization

The weights and weight savings possible for all quadratic columns in the structure with this approach according to analysis 2 are presented in Table 6.9.

Table 6.9 Weights and weight savings with by implementing HSS cross sections with an optimized column area in the quadratic columns in Prioritet Serneke Arena according to analysis 2. 1) Reference column from Prioritet Serneke Arena. 2) Optimized S355 column.

	S355 ¹⁾	S355 ²⁾	S420	S460	S500	S550	S620	S690
Optimized cross sections								
Weight [kg]	175166	218111	211142	203163	201252	199217	197174	196180
Saving¹⁾ [kg]	0	-42944	-35976	-27997	-26086	-24051	-22008	-21013
Saving¹⁾ [%]	0.0	-24.5	-20.5	-16.0	-14.9	-13.7	-12.6	-12.0
Saving²⁾ [kg]		0	6969	14947	16859	18894	20936	21931
Saving²⁾ [%]		0.0	3.2	6.9	7.7	8.7	9.6	10.1

Table 6.9 shows that the comparison made between optimized cross sections in HSS and optimized cross sections in S355 steel would result in a weight reduction of 10.1 % if implementing S690 steel. However if directly implementing these optimized cross sections instead of the existing columns in the structure, the weight of the structure would increase. Optimized column area cross sections made from S690 steel would weigh 12 % more than the existing S355 columns. They would though have a smaller column area, this can be seen by looking at the common columns with lengths 4.01 m, 3.33 m, 0.31 m and 23.1 m. Table 6.10 and Table 6.11 show optimized cross sections regarding column area and the weight of these columns which have different lengths.

Table 6.10 Weight, column area and dimensions for a hot rolled 120 mm wide and 6.3 mm thick column made of different steel grades with optimized surface area. ¹⁾ Reference column from Prioritet Serneke Arena. ²⁾ Optimized S355 column.

L [m]		S355 ¹⁾	S355 ²⁾	S420	S460	S500	S550	S620	S690
4.01	Weight [kg/m]	22.5	38.2	38.4	38.1	37.8	37.5	37.2	36.9
	Area [m ²]	0.014 4	0.009 0	0.008 9	0.008 5	0.008 5	0.008 5	0.008 5	0.008 5
	Width [mm]	120.0	95.0	94.1	92.3	92.3	92.3	92.3	92.3
	Thickness [mm]	6.3	15.3	15.6	15.9	15.7	15.6	15.4	15.3
3.33	Weight [kg/m]	22.5	37.3	37.0	36.1	35.7	35.3	34.9	36.1
	Area [m ²]	0.014 4	0.008 4	0.008 2	0.007 9	0.007 9	0.007 9	0.007 9	0.007 7
	Width [mm]	120	91.4	90.5	88.7	88.7	88.7	88.7	87.8
	Thickness [mm]	6.3	15.7	15.8	15.7	15.5	15.3	15.1	16.0
0.31	Weight [kg/m]	22.5	22.5	19.3	17.6	16.2	14.9	13.3	12.1
	Area [m ²]	0.014 4	0.003 8	0.003 0	0.002 7	0.002 4	0.002 1	0.001 8	0.001 7
	Width [mm]	120.0	61.7	54.4	51.7	49.0	46.3	42.7	40.9
	Thickness [mm]	6.3	15.6	16.0	15.4	15.4	15.2	15.7	14.6

Table 6.11 Weight, column area and dimensions for a hot rolled 300 mm wide and 12.5 mm thick column made of different steel grades with optimized surface area. ¹⁾ Reference column from Prioritet Serneke Arena. ²⁾ Optimized S355 column.

L [m]		S355 ¹⁾	S355 ²⁾	S420	S460	S500	S550	S620	S690
23	Weight [kg/m]	112.8	132.6	131.6	130.8	130.5	130.0	130.8	130.6
	Area [m ²]	0.09	0.0784	0.0784	0.0769	0.0769	0.0769	0.0764	0.0764
	Width [mm]	300.0	280.0	280.0	277.3	277.3	277.3	276.4	276.4
	Thickness [mm]	12.5	16.0	15.9	15.9	15.9	15.8	16.0	16.0

Table 6.10 and Table 6.11 show that both when comparing optimized cross sections made of different steel grades, and also the existing cross section in the structure a column area reduction is seen for all columns. How much the area is able to be reduced depends on the length of the columns.

By comparing the optimized areas to each other, it can be concluded that the shortest column which is 310 mm long is able to be reduced to an area of 0.0016 m² when using S690 steel instead of an area of 0.0038 m² when using S355 steel. The optimized cross sections regarding column area for this column is shown in Figure 6.11.

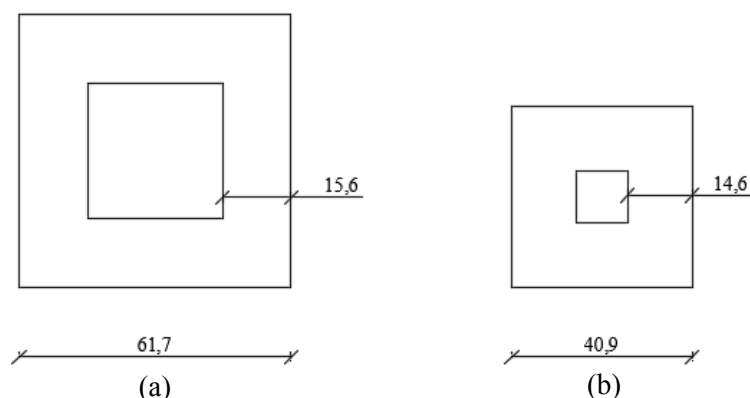


Figure 6.11 Optimized column area cross sections of a 310 mm long column in steel grade S355 (a) and S690 (b).

The longest column which is 23.1m was able to have an optimized area reduction from 0.0784 m² to 0.0764 m² when increasing the steel grade from S355 to S690, the cross sections of these areas are shown in Figure 6.12.

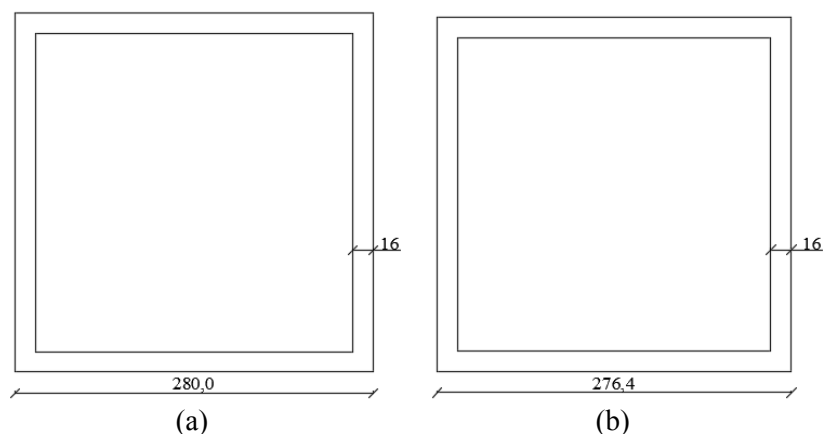


Figure 6.12 Optimized column area cross sections of a 23 m long column in steel grade S355 (a) and S690 (b).

If instead comparisons are done between the existing reference columns in the structure, and the optimized cross sections, other conclusions can be drawn. Table 6.10 shows the results which originates from the reference column that is 120 mm wide and 6.3 mm thick. For every length of this column, a column area reduction is possible by using higher steel grades. Also here, the possible reduction increase with decreasing length of columns. In order to compensate for the reduced width the thickness increases. Figure 6.13 show the existing reference column and the optimized cross sections for the column lengths 4.01 m, 3.33 m and 0.31 m.

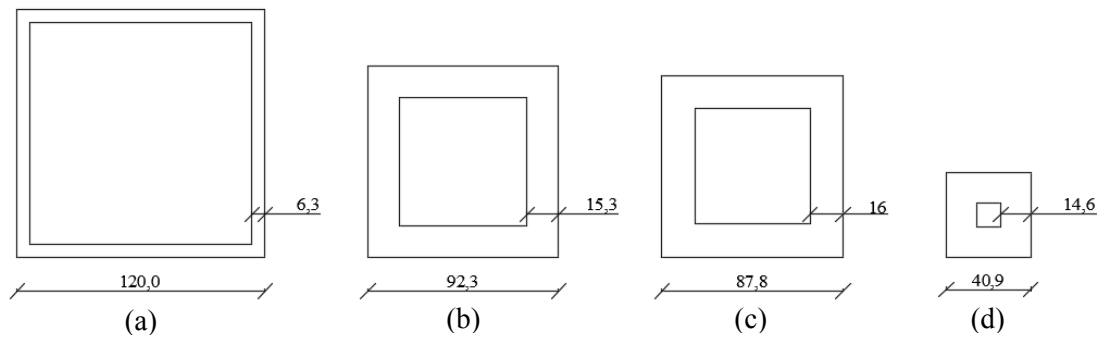


Figure 6.13 Reference column in the existing structure (a), optimized column area cross sections in S690 steel for the lengths 4010 mm (b), 3330 mm (c) and 310 mm (d).

The shorter columns have a very high thickness to width relation. However with longer columns the optimized areas have more reasonable dimensions. Figure 6.14 show the cross section of the existing 23 m long column and the optimized S690 column.

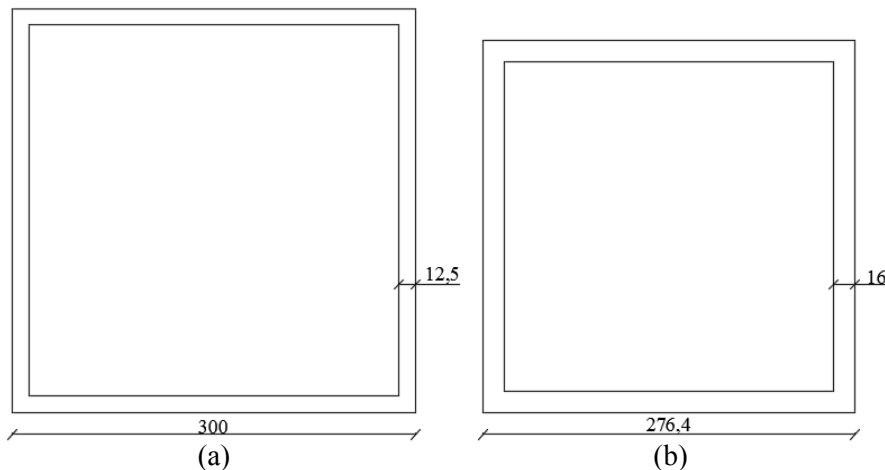


Figure 6.14 Reference column in the existing structure (a) and optimized column area cross section in S690 steel for a 23086 mm long column.

Column area optimization – Conclusions

The outcome of this approach is that it is possible to get a reduced column circumference by implementing HSS, both in comparison with the reference column and with an optimized NSS column. However, the consequence of the reduced area is that the cross section will compensate for the reduced width by an increased thickness. This often entails heavier columns than the reference column and in some cases cross sections with very stocky dimensions. Except for the very short columns the optimized cross sections have a much higher weight than the ones that are placed in the structure today.

6.5 Recommendation

In Prioritet Serneke Arena there are 885 hot rolled quadratic columns. It has been concluded that HSS is best suited in less slender columns.

How the results should be used depends on what is most important for the design. If it is prioritized to keep the steel consumption as low as possible, a steel area reduction resulting in 38 % less weight of the columns is possible. If the cost of S690 steel is maximum 38 % more than S355, a reduced cost could be achieved.

The results also show that columns can be made with smaller widths by increasing the steel grade. If directly implementing optimized cross sections the whole structure was able to use smaller cross sections. However a weight increase of 12 % would occur for the columns if they were replaced with S690 steel. Cross sections compensated for the reduced widths by an increased thicknesses which gave these higher weights. But if this is of interest for the designer, it would be possible using HSS.

If columns in the structure were to be replaced, it may be of interest to keep the widths, and only save material by decreasing the thicknesses. This is possible according to the results obtained from the thickness optimization. Commonly used columns vary in length between 2.5 m and 5.0 m. This was also seen in the arena, where 61 % of the analysed columns were of these lengths. With this method, the quadratic columns in the structure with lengths between 2.5 m and 5 m could experience a weight reduction of 32 %, see Table 6.12.

Table 6.12 Weights and weight savings by implementing HSS cross sections with an optimized thickness in the quadratic columns with lengths varying between 2.5 m and 5.0 m in Prioritet Serneke Arena according to analysis 2.

	S355	S420	S460	S500	S550	S620	S690
Weight [kg]	75360	67227	59825	57343	55153	52923	51184
Saving [kg]	0	8133	15534	18017	20206	22437	24176
Saving [%]	0.0	11	21	24	27	30	32

7 Discussion

In this chapter, the outcomes from the different parts of the thesis are discussed.

7.1 Member subjected to transversal load

The outcome from the bending analysis of IPE beams showed that increasing the steel grades for IPE resulted in both higher moment resistance and lateral torsional buckling resistance, where less slender beams were more beneficial regarding LT-buckling. However, LT-buckling is not always considered to be decisive in practice, since the compressed upper flange is often restrained via roof plates, floor elements, or less common by restraints.

Regarding the deflection analysis, results showed that HSS was not beneficial if deflection is the governing limitation. This can be directly derived from the deflection equations, where the yield strength variable is not part of the equations. This means that two equally loaded beam with same dimensions made from different steel grades will have the same deflection. However, there are circumstances when deflection is not the governing limitation, and for those cases it could be beneficial to implement HSS instead of conventional S355 steel.

7.2 Member subjected to axial loading

From the literature study it was concluded that columns made from HSS could be beneficial. Therefore an investigation of columns was conducted. To capture the differences of behaviour between columns made from HSS and those made from S355, three analyses were carried out with respect to minimum steel area. The differences between the analyses were how the influence of cross section class was considered.

It can be concluded that the limit between cross sections class 3 and cross section class 4 affects the benefits of HSS. When the cross section classes governed the columns, a critical non-dimension slenderness value was found. This value indicated when the HSS grades became non-beneficial. If however columns are allowed to be in cross section class 4, columns made from HSS will always need a smaller cross sectional area to resist the same load as a column made from NSS. Noticeable is that the steel area needed of an optimized HSS column in cross section class 4 do not tend to be equal to the steel area of the optimized column in NSS regardless how slender they get. Each steel area relation for each steel grade decreases up to a certain length. The curves then evens out and stay approximately the same even for more slender columns.

The same behaviour did not occur for columns that were prevented to buckle by a modification of the cross section. These columns benefit more from NSS than those that are designed with an effective cross sectional area, to a certain slenderness. After this, they tend to get closer to the optimized steel area of the NSS. This means that if columns are prevented to buckle, HSS is not as beneficial as for columns that are designed with an effective cross sectional area. The actual areas will however be smaller for the cross sections that are prevented to buckle. This makes it more

appropriate to after a certain non-dimensional slenderness modify cross sections in S355 instead of increasing the steel grade.

7.3 Case study

The quadratic hot rolled columns of Prioritet Serneke Arena have been investigated with regard to weight reduction and area differences when implementing HSS instead of the existing S355 steel. Only *Analysis 2* was conducted in the case study because it was considered being more relevant to include all 4 cross section classes.

The results show that an increased steel grade would have made differences on the structure. What these differences would be depended on what is desired and what is prioritized. If the total amount of steel should be kept as low as possible, the results regarding steel optimization should be considered. The total weight of all the quadratic columns could accord this been reduced by 38 %. The dimensions of the columns would however change, especially in widths. When columns passes a certain length, HSS cross sections are optimized in weight by increasing in width and decrease in thickness. What length this is, is dependent on the existing reference column that is to be replaced.

The investigation regarding thickness optimization, where the optimized columns kept the width constant would reduce the total weight of the columns in the structure by 23 %. This weight reduction is smaller compared to the columns with the smallest steel area. However, this approach could be more equitable than the smallest steel area investigation due to the differences in width in that approach, which would impact and change the conditions for the structure.

From these two investigations, the results showed that the optimized columns could become thin, some cross section as thin as 3 mm. The consequences with such thin cross sections will affect the fire resistance, and that will affect how the fire protection must be designed. However, this has not been further investigated, but could be a limitation when hot rolled quadratic columns are optimized.

The results from the case study also show that columns can be made with smaller widths by increasing the steel grade, this would impact the column area i.e. how much space the column would claim in a building. This could be beneficial from an architectural perspective, where columns can be made narrower and give a building a more spacious impression. The result showed that all investigated columns in the structure became narrower. However, the consequences of this were that the columns needed to compensate to be able to resist the same load by an increased thickness. This resulted that some of the columns got heavier than the existing column and/or got dimensions that became unrealistic.

Important to emphasize is that all calculations made to optimize the columns in the structure were based on the assumption that all these columns were subjected to a centric axial compression force. In the reality, some of the existing columns in the structure were probably designed to resist other load effects, such as wind loads, accidental loads etc. The consequence of this assumption could be that the weight savings may be misleading. This mainly concerns the case when optimized columns

made from HSS were directly compared to the non-optimized existing columns in the structure.

8 Conclusions

In this Master thesis, a broad investigation was conducted regarding whether HSS could be a beneficial alternative to conventional S355 steel in building structures. The literature study was carried out in order to gain information and to understand the generally behaviour of HSS. The information from the literature study formed the basis of the parametric and the case study. Based on the results and the discussion, following conclusions were made:

- Beams governed by a deflection limit do not benefit from HSS.
- HSS gets more beneficial with a decreasing non-dimensional slenderness of columns.
- HSS columns subjected to larger loads were more beneficial for a wider range of column lengths and thus more suited to use in applications where large buckling resistances are needed.
- HSS would reduce weights, steel consumption and column areas compared to NSS.
- It can, depending on the slenderness, be more beneficial to modify cross sections in S355 so they do not buckle instead of increasing the steel grade.
- The case study showed that the weight of existing columns in the structure of Prioritet Serneke Arena could have been reduced in weight with 38% by using HSS.
- If the price is known for different HSS grades, it can be concluded what non-dimensional slenderness of columns that is maximum in order to lower the costs.

8.1 Further studies

Based on the results from this Master Thesis, it would be useful to investigate the background of the $\varepsilon = \sqrt{\frac{235}{f_y}}$ factor. This factor strongly governs the limitation of the cross section classes and it became more severe for steel with higher strengths. During this thesis it was hard to find background information regarding this factor and therefore, an interesting research objective could be to investigate this more in detail.

In this thesis, hot rolled quadratic columns were optimized regarding the smallest steel area to investigate if HSS could be a beneficial alternative to NSS. There are other types of columns and analyses that could be interesting to investigate. An interesting approach could be to replace existing hot rolled quadratic columns in a structure with cold formed quadratic columns, because the major differences between hot rolled columns and cold formed columns is the different buckling curves and that cold formed columns are generally less expensive. The objective for a study could be to investigate if the higher yield strength can compensate for the lower buckling curve and thus be able to reduce the costs.

The literature study gave a general impression of HSS and how it has been used until today. Some information was gathered regarding HSS at elevated temperatures. It was

however considered important to carry out more tests and evaluate if HSS behaves different than conventional steels in situations where extreme temperatures occurs.

In further studies a cost analysis could be carried out. By considering the cost parameter, it would be possible to study if implementing HSS could be a beneficial alternative to NSS in another perspective. The lack of relevant price information was the reason that this was excluded in this thesis.

9 Referenser

Ahlenius, E., Collin, P. & Hedin, J., 1995. *Att konstruera med höghållfast stål*. 148 red. Stockholm: The Swedish Institute of Steel Construction.

Anon., 2016. [Online]

Available at: <http://www.jahn-us.com/projects/grand-spaces/sony-center/4>.

[Accessed 24 05 2016].

Baddoo, N. & Brown, D., 2015. High strength steel. *New steel construction*, September, pp. 24-26.

Cederfeldt, L. & Hansson, L., 2010. Swedbank Arena Takkonstruktionen. *Nyheter om Stålbyggnad*, pp. 20-26.

Cederfeldt, L. & Sperle, J.-O., 2012. *High strength steel in the roof of Swedbank arena savings in weight, cost and environmental impact*. Oslo, Norway, s.n.

Demeri, M. Y., 2013. *Advanced High-Strength Steels - Science, Technology, and Applications*. u.o.:ASM International.

Fundazioa, E., 2009. *EurekaAlert!*. [Online]

Available at: http://www.eurekaalert.org/pub_releases/2009-05/ef-car052009.php

[Använd 03 03 2016].

Hladnik, L., 1996. Slenderness Limit of Class 3 I Cross-sections Made of High Strength Steel. *Journal of Constructional Steel Research*, 38(3), pp. 201-217.

Huiyong, B., Gang, S., Yongjiu, S. & Yuanqing, W., 2012. Overall buckling behavior of 460 MPa high strength steel columns: Experimental investigation and design method. *Journal of Construction Steel Research*, Volym 74, pp. 140-150.

IIW - International Institute of Welding, 1968. Note on the carbon equivalent. *Welding in the world*, 6(2), pp. 78-81.

Jensen, L. & Matthew, B. L., 2009. *Application of high strength steel in super long span modern suspension bridge design*. Malmö, Nordic Steel Construction Conference.

Keeler, S. & Kimchi, M., 2014. *Advanced High-Strength Steels Application Guidelines Version 5.0*.

Kuoppa, J. o.a., 2010. *PLÅTHANDBOKEN - ATT KONSTRUERA OCH TILLVERKA I HÖGHÅLLFAST STÅL*. 1 red. Borlänge: Östbergs Sörmlandstryck AB.

Lancaster, J., 1997. *Handbook of Structural Welding: Processes, Materials and Methods Used in the Welding of Major Structures, Pipelines and Process Plant*. u.o.:Woodhead Publishing.

Lwin, M. M., 2002. *HIGH PERFORMANCE STEEL DESIGNERS' GUIDE*. 2 red. San Francisco.

Qiang, X., Frans, B. S. & Henk, K., 2012. Dependence of mechanical properties of high strength steel S690 on elevated temperatures. *Construction and Building Materials*, Volym 30, pp. 73-79.

Qiang, X., Frans, B. S. & Henk, K., 2012. Post-fire mechanical properties of high strength structural steels S460 and S690. *Engineering Structures*, Volume 35, pp. 1-10.

- Samuelsson, A. & Schröter, F., 2005. High-performance steels in Europe. In: *Use and Application of High-Performance Steels for Steel Structures*. Zürich: IABSE, pp. 99-122.
- Shi, G., Ban, H. & Bijlaard, F. S., 2012. Test and numerical study of ultra-high strength steel columns with end restraints. *Journal of Construction Steel Research*, Volym 70, pp. 236-247.
- Schröter, F., 2006. *Trends os using high-strength steel for heave steel structure*. Dillingen.
- SS-EN 1993-1-1, 2005. *Buildings, Eurocode 3: Design of steel structures - Part 1-1: General rules and rules for buildings*.
- SS-EN 1993-1-12, 2007. *Eurocode 3: Design of steel structures - Part 1-12: Additional rules for the extension of EN up to steel grades S700*.
- SS-EN 1993-1-5, 2006. *Eurocode 3: Design of steel structures - Part 1-5: Plated structural elements*.
- TIBNOR AB, 2011. *KONSTRUKTIONSTABELLER rör-balk-stång*. 9 red. u.o.:TIBNOR AB.
- Wang, Y.-B., Li, G.-Q., Chen, S.-W. & Sun, F.-F., 2012. Experimental and numerical study on the behaviour of axially compressed high strength steel columns with H-section. *Engineering Structures*, Volym 43, pp. 149-159.
- Willms, R., 2009. *High strength steel for steel constructions*. Malmö

Appendix A - IPE330 beam subjected to transversal loads

Calculation of the moment resistance as well as the design buckling resistance moment for a laterally unrestrained IPE300 beam.

It is shown that an increase in steel grade increases the moment resistance with and without regard to lateral torsional buckling. However the same increase is seen in deflection. A doubled load will double the deflection, regardless of the steel grade.

Input

$$E := 210 \text{ GPa}$$

$$G := 81000 \text{ MPa}$$

$$\gamma_M := 1$$

$$f_y := \begin{bmatrix} 355 \\ 420 \\ 460 \\ 500 \\ 620 \\ 690 \end{bmatrix} \text{ MPa}$$

$$\rho := 7850 \frac{\text{kg}}{\text{m}^3}$$

$$C_1 := 1.127$$

$$k := 1$$

$$k_w := 1$$

Width and thickness

$$h := 330 \text{ mm}$$

$$b := 160 \text{ mm}$$

$$t := 11.5 \text{ mm}$$

$$A := 6261 \text{ mm}^2$$

$$I_y := 11770 \cdot 10^4 \text{ mm}^4$$

$$I_z := 788 \cdot 10^4 \cdot \text{mm}^4$$

$$I_t := 0.283 \cdot 10^6 \text{ mm}^4$$

$$I_w := 199 \cdot 10^9 \text{ mm}^6$$

$$W_{el.y} := 713 \cdot 10^3 \text{ mm}^3$$

$$W_{pl.y} := 804 \cdot 10^3 \text{ mm}^3$$

Buckling curve

$$\frac{h}{b} = 2.063$$

$$\alpha_{LT} := 0.49$$

Length of beam

$$L := 4000 \text{ mm}$$

Cross section class

$$\varepsilon := \sqrt{\frac{235 \text{ MPa}}{f_y}} = \begin{bmatrix} 0.814 \\ 0.748 \\ 0.715 \\ 0.686 \\ 0.616 \\ 0.584 \end{bmatrix}$$

$$c := b - 2 t = 137 \text{ mm}$$

$$42 \varepsilon = \begin{bmatrix} 34.172 \\ 31.417 \\ 30.02 \\ 28.794 \\ 25.858 \\ 24.511 \end{bmatrix} \quad 38 \varepsilon = \begin{bmatrix} 30.917 \\ 28.425 \\ 27.161 \\ 26.051 \\ 23.395 \\ 22.176 \end{bmatrix} \quad 33 \varepsilon = \begin{bmatrix} 26.849 \\ 24.684 \\ 23.587 \\ 22.624 \\ 20.317 \\ 19.259 \end{bmatrix}$$

$$\frac{c}{t} = 11.913 \quad \text{Class 1}$$

Calculating elastic critical moment

$$M_{cr} := C_1 \cdot \frac{\pi^2 \cdot E \cdot I_z}{L^2} \cdot \sqrt{\frac{I_w}{I_z} + \frac{L^2 \cdot G \cdot I_t}{\pi^2 \cdot E \cdot I_z}} = 251.279 \text{ kN} \cdot \text{m}$$

Calculating Non-dimensional slenderness

$$\lambda_{LT} := \sqrt{\frac{W_{pl,y} \cdot f_y}{M_{cr}}} = \begin{bmatrix} 1.066 \\ 1.159 \\ 1.213 \\ 1.265 \\ 1.408 \\ 1.486 \end{bmatrix}$$

Calculating reduction factor

$$\lambda_{LT,0} := 0.4$$

$$\beta := 0.75$$

$$\Phi_{LT} := 0.5 \cdot \left(1 + \alpha_{LT} \cdot (\lambda_{LT} - \lambda_{LT,0}) + \beta \cdot \lambda_{LT}^2 \right) = \begin{bmatrix} 1.089 \\ 1.19 \\ 1.251 \\ 1.312 \\ 1.491 \\ 1.594 \end{bmatrix}$$

$$\chi_{LT} := \frac{1}{\Phi_{LT} + \sqrt{\Phi_{LT}^2 - \beta \cdot \lambda_{LT}^2}} = \begin{bmatrix} 0.6 \\ 0.547 \\ 0.518 \\ 0.492 \\ 0.426 \\ 0.395 \end{bmatrix}$$

$$\chi_{LT_0} < \begin{bmatrix} 1 \\ \lambda_{LT_0}^2 \\ 1 \end{bmatrix} = \begin{bmatrix} 1 \\ 1 \end{bmatrix} \quad \chi_{LT_2} < \begin{bmatrix} 1 \\ \lambda_{LT_2}^2 \\ 1 \end{bmatrix} = \begin{bmatrix} 1 \\ 1 \end{bmatrix} \quad \chi_{LT_4} < \begin{bmatrix} 1 \\ \lambda_{LT_4}^2 \\ 1 \end{bmatrix} = \begin{bmatrix} 1 \\ 1 \end{bmatrix}$$

$$\chi_{LT_1} < \begin{bmatrix} 1 \\ \lambda_{LT_1}^2 \\ 1 \end{bmatrix} = \begin{bmatrix} 1 \\ 1 \end{bmatrix} \quad \chi_{LT_3} < \begin{bmatrix} 1 \\ \lambda_{LT_3}^2 \\ 1 \end{bmatrix} = \begin{bmatrix} 1 \\ 1 \end{bmatrix} \quad \chi_{LT_5} < \begin{bmatrix} 1 \\ \lambda_{LT_5}^2 \\ 1 \end{bmatrix} = \begin{bmatrix} 1 \\ 1 \end{bmatrix}$$

OK

Moment resistance

$$M_{b,Rd} := W_{pl,y} \cdot \frac{f_y}{\gamma_M} = \begin{bmatrix} 285.42 \\ 337.68 \\ 369.84 \\ 402 \\ 498.48 \\ 554.76 \end{bmatrix} \text{ kN} \cdot \text{m}$$

Lateral torsional buckling moment resistance

$$M_{b,Rd,LT.355} := \chi_{LT_0} \cdot \frac{W_{pl,y} \cdot f_{y_0}}{\gamma_M} = 171.204 \text{ kN} \cdot \text{m} \quad \text{S355 steel}$$

$$M_{b,Rd,LT.420} := \chi_{LT_1} \cdot \frac{W_{pl,y} \cdot f_{y_1}}{\gamma_M} = 184.646 \text{ kN} \cdot \text{m} \quad \text{S420 steel}$$

$$M_{b,Rd,LT.460} := \chi_{LT_2} \cdot \frac{W_{pl,y} \cdot f_{y_2}}{\gamma_M} = 191.573 \text{ kN} \cdot \text{m} \quad \text{S460 steel}$$

$$M_{b,Rd,LT.500} := \chi_{LT_3} \cdot \frac{W_{pl,y} \cdot f_{y_3}}{\gamma_M} = 197.677 \text{ kN} \cdot \text{m} \quad \text{S500 steel}$$

$$M_{b.Rd.LT.620} := \chi_{LT_4} \cdot \frac{W_{pl.y} \cdot f_{y_4}}{\gamma_M} = 212.26 \text{ kN} \cdot \text{m} \quad \text{S620 steel}$$

$$M_{b.Rd.LT.690} := \chi_{LT_5} \cdot \frac{W_{pl.y} \cdot f_{y_5}}{\gamma_M} = 218.876 \text{ kN} \cdot \text{m} \quad \text{S690 steel}$$

Design load for the different steel grades

$$q := \frac{8 \cdot M_{b.Rd}}{L^2} = \begin{bmatrix} 142.71 \\ 168.84 \\ 184.92 \\ 201 \\ 249.24 \\ 277.38 \end{bmatrix} \frac{\text{kN}}{\text{m}}$$

Design load with regard to lateral torsional buckling

$$q_{LT.355} := \frac{8 \cdot M_{b.Rd.LT.355}}{L^2} = 85.602 \frac{\text{kN}}{\text{m}}$$

$$q_{LT.420} := \frac{8 \cdot M_{b.Rd.LT.420}}{L^2} = 92.323 \frac{\text{kN}}{\text{m}}$$

$$q_{LT.460} := \frac{8 \cdot M_{b.Rd.LT.460}}{L^2} = 95.787 \frac{\text{kN}}{\text{m}}$$

$$q_{LT.500} := \frac{8 \cdot M_{b.Rd.LT.500}}{L^2} = 98.839 \frac{\text{kN}}{\text{m}}$$

$$q_{LT.620} := \frac{8 \cdot M_{b.Rd.LT.620}}{L^2} = 106.13 \frac{\text{kN}}{\text{m}}$$

$$q_{LT.690} := \frac{8 \cdot M_{b.Rd.LT.690}}{L^2} = 109.438 \frac{\text{kN}}{\text{m}}$$

The same deflection will be seen for all steel grades subjected to the same load. Below is the deflection of the design load of the S355 beam.

$$p_1 := q_0 \cdot \frac{5 \cdot L^4}{384 \cdot E \cdot I_y} = 19.246 \text{ mm}$$

The magnitude of the deflection is directly linked to the steel grade. A higher steel grade can be subjected to a higher load but the deflection will be as many times greater as the load magnitude.

$$p_2 := q_5 \cdot \frac{5 \cdot L^4}{384 \cdot E \cdot I_y} = 0.037 \text{ m}$$

$$\frac{p_2}{p_1} = 1.944 \quad \frac{q_5}{q_0} = 1.944$$

The same result is seen for beams regarding lateral torsional buckling.

$$p_{1.LT} := q_{LT.355} \cdot \frac{5 L^4}{384 \cdot E \cdot I_y} = 11.544 \text{ mm}$$

$$p_{2.LT} := q_{LT.690} \cdot \frac{5 L^4}{384 \cdot E \cdot I_y} = 14.759 \text{ mm}$$

$$\frac{p_{2.LT}}{p_{1.LT}} = 1.278 \quad \frac{q_{LT.690}}{q_{LT.355}} = 1.278$$

Appendix B - Script verification

Script verification by comparing MATLAB script and TIBNOR values. This is a cross check to see that the MATLAB script is correct. This was done by calculating the design buckling resistance for a 120mm wide and 6.3mm thick column with four different lengths according to SS EN 1993-1-1 and 1993-1-5.

Input

$$E := 210 \text{ GPa}$$

$$\gamma_M := 1$$

$$\alpha := 0.21$$

$$f_y := 355 \text{ MPa}$$

$$\rho := 7850 \frac{\text{kg}}{\text{m}^3}$$

Width and thickness

$$b := 120 \text{ mm}$$

$$t := 6.3 \text{ mm}$$

Lengths of columns

$$L := \begin{bmatrix} 2.1 \\ 3.0 \\ 5.0 \\ 7.0 \end{bmatrix} \text{ m}$$

Cross section class

$$\varepsilon := \sqrt{\frac{235 \text{ MPa}}{f_y}} = 1$$

$$c := b - 2 t = 107 \text{ mm}$$

$$42 \varepsilon = 34$$

$$38 \varepsilon = 31$$

$$33 \varepsilon = 27$$

$$\frac{c}{t} = 17$$

Cross section class 1

Cross sectional area, moment of inertia and radius of gyration according to design table from TIBNOR.

$$A := 2820 \text{ mm}^2$$

$$I_y := 603 \cdot 10^4 \text{ mm}^4$$

$$i := 46.2 \text{ mm}$$

Calculating Non-dimensional slenderness

$$\lambda_1 := \pi \cdot \sqrt{\frac{E}{f_y}} = 76$$

$$\lambda_{bar} := \frac{L}{i} \cdot \frac{1}{\lambda_1} = \begin{bmatrix} 0.5949 \\ 0.8498 \\ 1.4164 \\ 1.9829 \end{bmatrix}$$

Calculating reduction factor

$$\Phi := 0.5 \cdot (1 + \alpha \cdot (\lambda_{bar} - 0.2) + \lambda_{bar}^2) = \begin{bmatrix} 0.7184 \\ 0.9293 \\ 1.6308 \\ 2.6532 \end{bmatrix}$$

$$\chi := \frac{1}{\Phi + \sqrt{\Phi^2 - \lambda_{bar}^2}} = \begin{bmatrix} 0.89192 \\ 0.76602 \\ 0.40999 \\ 0.22644 \end{bmatrix}$$

Elastic buckling resistance

$$N_{cr} := \frac{\pi^2 \cdot E \cdot I_y}{L^2} = \begin{bmatrix} 2833.99 \\ 1388.65 \\ 499.92 \\ 255.06 \end{bmatrix} \text{ kN}$$

Design buckling resistance

$$N_{b.Rd} := \chi \cdot \frac{A \cdot f_y}{\gamma_M} = \begin{bmatrix} 892.9046 \\ 766.8621 \\ 410.438 \\ 226.6935 \end{bmatrix} \text{ kN}$$

Design buckling resistance values from TIBNOR

$$N_{b.Rd.TIBNOR} := \begin{bmatrix} 894 \\ 768 \\ 411 \\ 227 \end{bmatrix} \text{ kN}$$

Design buckling resistance values from MATLAB

$$N_{b.Rd.MATLAB} := \begin{bmatrix} 892.904645844476 \\ 766.862086535369 \\ 410.437984960585 \\ 226.693514528984 \end{bmatrix} kN$$

Difference MATLAB / Mathcad

$$Diff_1 := 1 - \frac{N_{b.Rd}}{N_{b.Rd.MATLAB}} = \begin{bmatrix} 0 \\ 0 \\ 0 \\ 0 \end{bmatrix} \quad \text{No difference}$$

Difference MATLAB / true values

$$Diff_2 := 1 - \frac{N_{b.Rd.MATLAB}}{N_{b.Rd.TIBNOR}} = \begin{bmatrix} 0.0012252 \\ 0.0014817 \\ 0.0013674 \\ 0.0013502 \end{bmatrix} \quad \text{Very small difference}$$

The MATLAB script is considered to be accurate.

Appendix C - Corrugated cross section

This appendix calculates the area for two cross section, one in S355 steel and one in S690 steel. It is shown that it can be beneficial to modify cross sections so that they do not buckle instead of increasing the steel grade. Both columns are 6m long and have the same buckling resistance of 1000kN, but the S355 is able to have a smaller area.

The first calculation considers the corrugated S355 column.

Input

$$E := 210 \text{ GPa}$$

$$\gamma_M := 1$$

$$\alpha := 0.21$$

$$f_y := 355 \text{ MPa}$$

$$\rho := 7850 \frac{\text{kg}}{\text{m}^3}$$

Width and thickness of optimized cross section to resist 1000kN obtained from MATLAB script.

$$b := 280.00 \text{ mm}$$

$$t := 3 \text{ mm}$$

Lengths of column

$$L := 6 \text{ m}$$

Cross section class

$$\varepsilon := \sqrt{\frac{235 \text{ MPa}}{f_y}} = 0.814$$

$$c := b - 2 t = 274 \text{ mm}$$

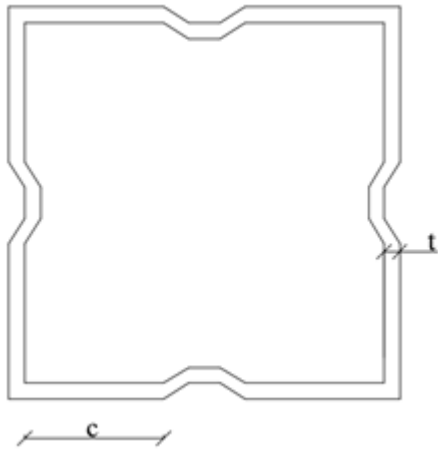
$$42 \varepsilon = 34.172$$

$$38 \varepsilon = 30.917$$

$$33 \varepsilon = 26.849$$

$$\frac{c}{t} = 91.333 \quad \text{Class 4}$$

The cross section is well above the limit of cross sections class 4. Analysis 3 however assumes that cross sections do not buckle due to modifications to the cross section. This can be achieved by for example corrugating the web, see figure:



The area of the cross section will not be reduced. It is considered to be fully utilized.

Cross sectional area, moment of inertia and radius of gyration

$$A_{S355} := 2 \cdot b \cdot t + 2 \cdot (b - 2t) \cdot t = 3324 \text{ mm}^2$$

$$I_y := \frac{b \cdot b^3}{12} - \frac{(b - 2t) \cdot (b - 2t)^3}{12} = 42512852 \text{ mm}^4$$

$$i := \sqrt{\frac{I_y}{A_{S355}}} = 113.091 \text{ mm}$$

Calculating Non-dimensional slenderness

$$\lambda_1 := \pi \cdot \sqrt{\frac{E}{f_y}} = 76.409$$

$$\lambda_{bar} := \frac{L}{i} \cdot \frac{1}{\lambda_1} = 0.694$$

Calculating reduction factor

$$\Phi := 0.5 \cdot (1 + \alpha \cdot (\lambda_{bar} - 0.2) + \lambda_{bar}^2) = 0.793$$

$$\chi := \frac{1}{\Phi + \sqrt{\Phi^2 - \lambda_{bar}^2}} = 0.85$$

Design buckling resistance

$$N_{b.Rd} := \chi \cdot \frac{A_{S355} \cdot f_y}{\gamma_M} = 1003.5 \text{ kN}$$

Weight

$$Weight := A_{S355} \cdot \rho = 26.093 \frac{\text{kg}}{\text{m}}$$

The second calculation considers the S690 cross sections, which is not corrugated.

Input

$$E := 210 \text{ GPa}$$

$$\gamma_M := 1$$

$$\alpha := 0.13$$

$$\rho := 7850 \frac{\text{kg}}{\text{m}^3}$$

$$f_y := 690 \text{ MPa}$$

Width and thickness of optimized cross section to resist 1000kN obtained from MATLAB script.

$$b := 210.53 \text{ mm}$$

$$t := 4.14 \text{ mm}$$

Length of column

$$L := 6 \text{ m}$$

Area

$$A_{S690} := 2 \cdot b \cdot t + 2 \cdot (b - 2 \cdot t) \cdot t = 3417.82 \text{ mm}^2$$

Cross section class

$$\varepsilon := \sqrt{\frac{235 \text{ MPa}}{f_y}} = 0.584$$

$$c := b - 2 t = 202.25 \text{ mm}$$

$$\frac{c}{t} = 48.853$$

$$42 \varepsilon = 24.511$$

$$38 \varepsilon = 22.176$$

$$33 \varepsilon = 19.259$$

Cross section class 4

Calculation of effective cross section area

$$b_{bar} := b - 2 t = 202.25 \text{ mm}$$

$$\psi := 1$$

$$k_{\sigma} := 4$$

$$\lambda_{bar.p} := \frac{\frac{b_{bar}}{t}}{28.4 \varepsilon \cdot \sqrt{k_{\sigma}}} = 1.474$$

$$\rho_1 := \frac{\lambda_{bar.p} - 0.055 \cdot (3 + \psi)}{\lambda_{bar.p}^2} = 0.577$$

Area reduction factor

$$A_{eff} := \rho_1 \cdot A_{S690} = 1972.908 \text{ mm}^2$$

Effective cross sectional area

$$\frac{A_{eff}}{A_{S690}} = 0.577$$

Moment of inertia and radius of gyration

$$I_y := \frac{b \cdot b^3}{12} - \frac{(b - 2t) \cdot (b - 2t)^3}{12} = 24274469.429 \text{ mm}^4$$

$$i := \sqrt{\frac{I_y}{A_{S690}}} = 84.275 \text{ mm}$$

Calculating Non-dimensional slenderness

$$\lambda_1 := \pi \cdot \sqrt{\frac{E}{f_y}} = 54.807$$

$$\lambda_{bar} := \frac{L}{i} \cdot \frac{\sqrt{\frac{A_{eff}}{A_{S690}}}}{\lambda_1} = 0.987$$

Calculating reduction factor

$$\Phi := 0.5 \cdot (1 + \alpha \cdot (\lambda_{bar} - 0.2) + \lambda_{bar}^2) = 1.038$$

$$\chi := \frac{1}{\Phi + \sqrt{\Phi^2 - \lambda_{bar}^2}} = 0.735$$

Design buckling resistance

$$N_{bRd} := \chi \cdot \frac{A_{eff} \cdot f_y}{\gamma_M} = 1000.74 \text{ kN}$$

The area of the corrugated cross section in S355 is smaller than the optimized cross section in S690 steel:

$$\frac{A_{S355}}{A_{S690}} = 0.973$$

Appendix D - Length break point of steel area optimization according to analysis 2

Calculation of an S355 column with a cross section of 120mm widths and 6.3mm thickness for the lengths 2500 and 2600mm. It is proven that a column made of S690 steel cannot be longer than 2500mm and remain 120mm wide and still keep the same design buckling resistance as the S355 column according to analysis 2. Calculations according to SS EN 1993-1-1 and 1993-1-5.

Input

$$E := 210 \text{ GPa}$$

$$\gamma_M := 1$$

$$\alpha := 0.21$$

$$f_y := 355 \text{ MPa}$$

$$\rho := 7850 \frac{\text{kg}}{\text{m}^3}$$

Width and thickness

$$b := 120 \text{ mm}$$

$$t := 6.3 \text{ mm}$$

Lengths of columns

$$L := \begin{bmatrix} 2500 \\ 2600 \end{bmatrix} \text{ mm}$$

Cross section class

$$\varepsilon := \sqrt{\frac{235 \text{ MPa}}{f_y}} = 0.814$$

$$c := b - 2 t = 107.4 \text{ mm}$$

$$42 \varepsilon = 34.172$$

$$38 \varepsilon = 30.917$$

$$33 \varepsilon = 26.849$$

$$\frac{c}{t} = 17.048$$

Class 1

Cross sectional area, moment of inertia and radius of gyration

$$A := 2 \cdot b \cdot t + 2 \cdot (b - 2 t) t = (2.865 \cdot 10^3) \text{ mm}^2$$

$$I_y := \frac{b \cdot b^3}{12} - \frac{(b-2t) \cdot (b-2t)^3}{12} = (6.192 \cdot 10^6) \text{ mm}^4$$

$$i := \sqrt{\frac{I_y}{A}} = 46.489 \text{ mm}$$

Calculating Non-dimensional slenderness

$$\lambda_1 := \pi \cdot \sqrt{\frac{E}{f_y}} = 76.409$$

$$\lambda_{bar} := \frac{L}{i} \cdot \frac{1}{\lambda_1} = \begin{bmatrix} 0.704 \\ 0.732 \end{bmatrix}$$

Calculating reduction factor

$$\Phi := 0.5 \cdot \left(1 + \alpha \cdot (\lambda_{bar} - 0.2) + \lambda_{bar}^2 \right) = \begin{bmatrix} 0.801 \\ 0.824 \end{bmatrix}$$

$$\chi := \frac{1}{\Phi + \sqrt{\Phi^2 - \lambda_{bar}^2}} = \begin{bmatrix} 0.846 \\ 0.832 \end{bmatrix}$$

Design buckling resistance

$$N_{b.Rd} := \chi \cdot \frac{A \cdot f_y}{\gamma_M} = \begin{bmatrix} 860.46917 \\ 846.5129 \end{bmatrix} \text{ kN}$$

Calculation of the design buckling resistance for an optimized column in S690 steel. The column regards the steel optimization approach according to analysis 2. It is shown that according to this analysis, in order to get the best weight saving of an S690 column compared to a 120mm wide and 6.3mm thick S355 column the length cannot exceed 2500mm. Calculations according to SS EN 1993-1-1 and 1993-1-5.

Input

$$E := 210 \text{ GPa}$$

$$\gamma_M := 1$$

$$\alpha := 0.13$$

$$\rho := 7850 \frac{\text{kg}}{\text{m}^3}$$

$$f_y := 690 \text{ MPa}$$

Column from MATLAB

$$b := 120 \text{ mm}$$

$$t := 3.9 \text{ mm}$$

$$L := \begin{bmatrix} 2500 \\ 2600 \end{bmatrix} \text{ mm}$$

$$A := 2 \cdot b \cdot t + 2 \cdot (b - 2 \cdot t) \cdot t = 0.00181 \text{ m}^2$$

Cross section class

$$\varepsilon := \sqrt{\frac{235 \text{ MPa}}{f_y}} = 0.584$$

$$c := b - 2 t = 112.2 \text{ mm}$$

$$\frac{c}{t} = 28.769$$

$$42 \varepsilon = 24.511$$

$$38 \varepsilon = 22.176$$

$$33 \varepsilon = 19.259$$

Cross section class 4

Calculation of effective cross section area

$$b_{bar} := b - 2 t = 112.2 \text{ mm}$$

$$\psi := 1$$

$$k_\sigma := 4$$

$$\lambda_{bar.p} := \frac{\frac{b_{bar}}{t}}{28.4 \varepsilon \cdot \sqrt{k_\sigma}} = 0.868$$

$$\rho_1 := \frac{\lambda_{bar.p} - 0.055 \cdot (3 + \psi)}{\lambda_{bar.p}^2} = 0.86$$

Area reduction factor

$$A_{eff} := \rho_1 \cdot A = (1.558 \cdot 10^3) \text{ mm}^2$$

Effective cross sectional area

$$\frac{A_{eff}}{A} = 0.86$$

Moment of inertia and radius of gyration

$$I_y := \frac{b \cdot b^3}{12} - \frac{(b - 2t) \cdot (b - 2t)^3}{12} = (4.073 \cdot 10^6) \text{ mm}^4$$

$$i := \sqrt{\frac{I_y}{A}} = 47.424 \text{ mm}$$

Calculating Non-dimensional slenderness

$$\lambda_1 := \pi \cdot \sqrt{\frac{E}{f_y}} = 54.807$$

$$\lambda_{bar} := \frac{L}{i} \cdot \frac{\sqrt{\frac{A_{eff}}{A}}}{\lambda_1} = \begin{bmatrix} 0.892 \\ 0.928 \end{bmatrix}$$

Non-dimensional slenderness

Calculating reduction factor

$$\Phi := 0.5 \cdot (1 + \alpha \cdot (\lambda_{bar} - 0.2) + \lambda_{bar}^2) = \begin{bmatrix} 0.943 \\ 0.978 \end{bmatrix}$$

$$\chi := \frac{1}{\Phi + \sqrt{\Phi^2 - \lambda_{bar}^2}} = \begin{bmatrix} 0.801 \\ 0.778 \end{bmatrix}$$

Reduction factor

Design buckling resistance

$$N_{bRd} := \chi \cdot \frac{A_{eff} \cdot f_y}{\gamma_M} = \begin{bmatrix} 861.175295 \\ 835.83764824 \end{bmatrix} \text{ kN}$$

Weight

$$Weight := A \cdot \rho = 14.218 \frac{\text{kg}}{\text{m}}$$

Longer lengths than 2500mm would need another cross section to keep the design buckling resistance. The best weight saving is seen by increasing the widths and not the thickness. Breakpoint in length of S690 columns according to this analysis is 2500mm.

```

%%                                APPENDIX E                                %%

%-----%
%
%   HOT ROLLED QUADRATIC COLUMNS
%
%   This script loops trough pre-selected cross-sectional dimensions,
%   yield strengths and columns lengths to find the smallest
%   possible steel area for a pre-defined load effect.
%
%   All calculations is referred to:
%   SS EN 1993-1-1:2005 denoted as [1]
%   SS EN 1993-1-5:2006 denoted as [2]
%   SS EN 1993-1-12:2007 (additional rules for steel grades
%                           up to S700)
%
%-----%

clc
clf
clear all
close all

%% Indata

% Selection of including Cross Section Class (CSC) 4, or not.
% Analysis = 1 ==> CSC 4 is not included
% Analysis = 2 ==> CSC 4 is included and NRd is calculated with A_eff
% Analysis = 3 ==> CSC 4 is included without A_eff
Analysis=1;

% Elastic modulus
E=210e9;      % [Pa]

% Partial factor
gamma_M1=1.0; % Resistance of members to instability assessed
              % by member checks [1] 6.1 (1) NOTE 2B

% Column geometry
b_start=40;   % [mm] Width, start value
b_end=400;    % [mm] Width, end value
t_start=3;    % [mm] Thickness, start value
t_end=16;     % [mm] Thickness, end value
L_start=0;    % [m] Column length, start value
L_end=12;     % [m] Column length, end value

% Define vectors consisting of the column geometry
lin_dim=400;  % Number of steps in the geometry vectors
lin_length=13; % Number of steps in the length vectors

b=linspace(b_start,b_end,lin_dim)*10^-3; % [m] Width
h=b; % [m] Height
t=linspace(t_start,t_end,lin_dim)*10^-3; % [m] Plate thickness
L=linspace(L_start,L_end,lin_length); % [m] Column length

% Yield strengths
fy=[355 420 460 500 620 690]*10^6; % [Pa]

```

```

% Pre-defined load effect
NEd=1000; % [kN]

%% Calculating cross-sectional constants

% Pre-allocate space
A=zeros(lin_dim);
Iy=zeros(lin_dim);
i=zeros(lin_dim);

for j=1:lin_dim;
for k=1:lin_dim;

    % Cross sectional area [m^2]
    A(j,k)=2*b(j)*t(k)+2*(b(j)-2*t(k))*t(k);

    % Remove unrealistic cross sectional areas
    A_replace_HSS=find((A(j,k))<=0);
    A(j,k(A_replace_HSS))=NaN;

    % Moment of inertia for each cross section [m^4]
    Iy(j,k)=(b(j)*h(j)^3-(b(j)-2*t(k))*(h(j)-2*t(k))^3)/12;

    % Remove unrealistic moments of inertias
    Iy_replace_HSS=find((Iy(j,k))<=0);
    Iy(j,k(Iy_replace_HSS))=NaN;

    % Radius of gyration for each cross section [m]
    i(j,k)=sqrt(Iy(j,k)/A(j,k));

end
end

%% Calculating cross-section classes [1] Table 5.2

% Pre-allocate space
hw=zeros(lin_dim);
epsilon=zeros(1,length(fy));
CSC=zeros(lin_dim,lin_dim,length(fy));

%Internal compression parts
for j=1:lin_dim;      % j=width, b
for k=1:lin_dim;      % k=thickness, t
for s=1:length(fy);  % s=yield strength

    % Height web [m]
    hw(j,k)=h(j)-2*t(k);
    hw_replace=find((hw(j,k))<=0);
    hw(j,k(hw_replace))=NaN;

    % Calculating epsilon
    epsilon(s)=sqrt(235/(fy(s)*10^-6));

    % Calculating cross-sectional class (CSC) for each column
if hw(j,k)/t(k) <= 33*epsilon(s);
    CSC(j,k,s)=1;
elseif hw(j,k)/t(k) > 33*epsilon(s) && hw(j,k)/t(k)<= 38*epsilon(s);
    CSC(j,k,s)=2;
elseif hw(j,k)/t(k) > 38*epsilon(s) && hw(j,k)/t(k)<= 42*epsilon(s);
    CSC(j,k,s)=3;

```



```

else
    CSC(j,k,s)=4;
end
end
end
end

% Remove and replace all cross sections in cross-section class 4
% with NaN

if Analysis==1;
    replace=find((CSC)==4);
    CSC(replace)=NaN;
end

% Calculating number of cross sections in class 4
if Analysis==1
    Class_4_355=isnan(CSC(:,:,1));
    Class_4_420=isnan(CSC(:,:,2));
    Class_4_460=isnan(CSC(:,:,3));
    Class_4_500=isnan(CSC(:,:,4));
    Class_4_620=isnan(CSC(:,:,5));
    Class_4_690=isnan(CSC(:,:,6));

    number_of_Class_4_355=sum(sum(Class_4_355));
    number_of_Class_4_420=sum(sum(Class_4_420));
    number_of_Class_4_460=sum(sum(Class_4_460));
    number_of_Class_4_500=sum(sum(Class_4_500));
    number_of_Class_4_620=sum(sum(Class_4_620));
    number_of_Class_4_690=sum(sum(Class_4_690));
end

%% Calculating buckling resistance for cross-section classes 1,2 & 3
if Analysis==1 || Analysis==3;

% Pre-allocate space
lambda_1=zeros(1,length(fy));
lambda_non=zeros(lin_dim,lin_dim,length(fy),length(L));
alpha=zeros(1,length(fy));
phi=zeros(lin_dim,lin_dim,length(fy),length(L));
xsi=zeros(lin_dim,lin_dim,length(fy),length(L));
NRd=zeros(lin_dim,lin_dim,length(fy),length(L));

for j=1:lin_dim;      % j=width, b
for k=1:lin_dim;      % k=thickness, t
for s=1:length(fy);  % s=yield strength
for m=1:lin_length;  % m=column length

    % Calculate slenderness values [1] 6.3.1.3
    lambda_1(s)=pi*sqrt(E/fy(s));

    % Calculate only for cross-sections in class 1,2 and 3
if Analysis==1
if CSC(j,k,s)<4

    % Non-dimensional slenderness [1] 6.3.1.3 (6.50)

```

```

        lambda_non(j,k,s,m)=L(m)/(i(j,k)*lambda_1(s));
else
    lambda_non(j,k,s,m)=NaN;
end
end

% Calculate only for cross-sections in class 4
if Analysis==3
% Non-dimensional slenderness [1] 6.3.1.3 (6.50)
    lambda_non(j,k,s,m)=L(m)/(i(j,k)*lambda_1(s));
end

% Determine imperfection factor alpha [1] Table 6.1 & 6.2
% Yield strength < 460MPa
if fy(s)<460*10^6;
    alpha(s)=0.21;

% Yield strength >= 460MPa
else
    alpha(s)=0.13;
end

% Calculating buckling curves [1] 6.3.1.2

% phi
phi(j,k,s,m)=0.5*(1+alpha(s)*(lambda_non(j,k,s,m)-0.2)+...
    lambda_non(j,k,s,m)^2);

% Calculating reduction factor, xsi [1] 6.3.1.2 (6.49)
xsi(j,k,s,m)=1/(phi(j,k,s,m)+sqrt(phi(j,k,s,m)^2-...
    lambda_non(j,k,s,m)^2));

% Calculating design buckling resistance [1] 6.3.1.1 (6.47)
% For columns with xsi >1
if xsi(j,k,s,m)>1
    xsi(j,k,s,m)=1;
    NRd(j,k,s,m)=xsi(j,k,s,m)*A(j,k)*fy(s)/(gamma_M1*1000);

% For columns with xsi <=1
else
    NRd(j,k,s,m)=xsi(j,k,s,m)*A(j,k)*fy(s)/(gamma_M1*1000);
end
end
end
end
end

%% Calculating buckling resistance for cross-section class 1,2,3 & 4

elseif Analysis==2;

% Pre-allocate space
lambda_1=zeros(1,length(fy));
lambda_non=zeros(lin_dim,lin_dim,length(fy),length(L));
b_bar=zeros(lin_dim,lin_dim,length(fy));
lambda_bar_p=zeros(lin_dim,lin_dim,length(fy));

```

```

rho=zeros(lin_dim,lin_dim,length(fy));
A_eff=zeros(lin_dim,lin_dim,length(fy));
alpha=zeros(1,length(fy));
phi=zeros(lin_dim,lin_dim,length(fy),length(L));
xsi=zeros(lin_dim,lin_dim,length(fy),length(L));
NRd=zeros(lin_dim,lin_dim,length(fy),length(L));

for j=1:lin_dim;      % j=width, b
for k=1:lin_dim;      % k=thickness, t
for s=1:length(fy);  % s=yield strength
for m=1:lin_length;  % m=column length

    % Calculate slenderness
    lambda_1(s)=pi*sqrt(E/fy(s)); % [1] 6.3.1.3

    % Calculate only for cross-sections in class 1,2 and 3
if CSC(j,k,s)<4
    % Non-dimensional slenderness [1] 6.3.1.3 (6.50)
    lambda_non(j,k,s,m)=L(m)/(i(j,k)*lambda_1(s));

    % Calculate only for cross-sections in class 4
else
    % Stress distribution factor [2] table 4.1
    psi=1;
    % Buckling factor [2] table 4.1
    k_kappa=4;

    % Possible applied width [2] 4.4
    b_bar(j,k,s)=b(j)-2*t(k);

if b_bar(j,k,s)<0
    b_bar(j,k,s)=0;
end

    % Non-dimensional slenderness for effective cross section [2] 4.4
    lambda_bar_p(j,k,s)=b_bar(j,k,s)/(t(k)*28.4*epsilon(s)*...
        k_kappa^0.5);

if lambda_bar_p(j,k,s)>0.673
    % Reduction factor with respect to buckling [2] 4.4 (4.2)
    rho(j,k,s)=(lambda_bar_p(j,k,s)-0.055*(3+psi))/...
        (lambda_bar_p(j,k,s))^2;
elseif lambda_bar_p(j,k,s)<=0.673 && lambda_bar_p(j,k,s)>0
    rho(j,k,s)=1;
else
    rho(j,k,s)=NaN;
end

    % Effective cross section area [2] 4.4 (4.1)
    A_eff(j,k,s)=rho(j,k,s)*A(j,k);

    % Non-dimensional slenderness [1] 6.3.1.3 (6.51)
    lambda_non(j,k,s,m)=(L(m)*(A_eff(j,k,s)/A(j,k))^0.5)/(i(j,k)*...
        *lambda_1(s));
end

    % Determine imperfection factor [1] Table 6.1 & 6.2

    % Yield strength < 460MPa
if fy(s)<460*10^6;

```

```

        alpha(s)=0.21;
    % Yield strength >= 460MPa
else
    alpha(s)=0.13;
end

    % Calculating buckling curves [1] 6.3.1.2
    % phi
    phi(j,k,s,m)=0.5*(1+alpha(s)*(lambda_non(j,k,s,m)-0.2)+...
        lambda_non(j,k,s,m)^2);

    % Calculating reduction factor, xsi [1] 6.3.1.2 (6.49)
    xsi(j,k,s,m)=1/(phi(j,k,s,m)+sqrt(phi(j,k,s,m)^2-...
        lambda_non(j,k,s,m)^2));

    % Calculating design buckling resistance [1] 6.3.1.1 (6.47) &
    % (6.48)

    % For columns with xsi >1
if xsi(j,k,s,m)>1
    xsi(j,k,s,m)=1;
    % For columns in cross section class 1,2 & 3
if CSC(j,k,s)<4
    NRd(j,k,s,m)=xsi(j,k,s,m)*A(j,k)*fy(s)/(gamma_M1*1000);
else
    % For columns in cross section class 4
    NRd(j,k,s,m)=xsi(j,k,s,m)*A_eff(j,k,s)*fy(s)/(gamma_M1*1000);
end
else

    % For columns with xsi <=1
    % For columns in cross section class 1,2 & 3
if CSC(j,k,s)<4
    NRd(j,k,s,m)=xsi(j,k,s,m)*A(j,k)*fy(s)/(gamma_M1*1000);
else
    % For columns in cross section class 4
    NRd(j,k,s,m)=xsi(j,k,s,m)*A_eff(j,k,s)*fy(s)/(gamma_M1*1000);
end

end
end
end
end
end

end

%% The iterative process - find the smallest steel area

% This part searches trough all columns for the different yield
% strengths and find the column with the smallest possible steel area
% which can resist the pre-defined load effect. This part also
% generates corresponding results for the optimized column, such as
% cross section dimensions, reduction factors, and
% non-dimensional slenderness values.

```

```

% Pre-allocate space

% Define min area for the optimized column
min_area_355=zeros(lin_length,1);
min_area_420=zeros(lin_length,1);
min_area_460=zeros(lin_length,1);
min_area_500=zeros(lin_length,1);
min_area_620=zeros(lin_length,1);
min_area_690=zeros(lin_length,1);

% Position of the optimized column in the cross sectional area matrix
for each column length
pos_355=zeros(lin_length,1);
pos_420=zeros(lin_length,1);
pos_460=zeros(lin_length,1);
pos_500=zeros(lin_length,1);
pos_620=zeros(lin_length,1);
pos_690=zeros(lin_length,1);

% Position of optimized width in the width vector for each column
length
pos_b_355=zeros(lin_length,1);
pos_b_420=zeros(lin_length,1);
pos_b_460=zeros(lin_length,1);
pos_b_500=zeros(lin_length,1);
pos_b_620=zeros(lin_length,1);
pos_b_690=zeros(lin_length,1);

% Position of optimized thickness in the thickness vector for each
column length
pos_t_355=zeros(lin_length,1);
pos_t_420=zeros(lin_length,1);
pos_t_460=zeros(lin_length,1);
pos_t_500=zeros(lin_length,1);
pos_t_620=zeros(lin_length,1);
pos_t_690=zeros(lin_length,1);

% Optimized width for each column length
b_355=zeros(lin_length,1);
b_420=zeros(lin_length,1);
b_460=zeros(lin_length,1);
b_500=zeros(lin_length,1);
b_620=zeros(lin_length,1);
b_690=zeros(lin_length,1);

% Optimized thickness for each column length
t_355=zeros(lin_length,1);
t_420=zeros(lin_length,1);
t_460=zeros(lin_length,1);
t_500=zeros(lin_length,1);
t_620=zeros(lin_length,1);
t_690=zeros(lin_length,1);

% Buckling resistance the optimized column for each column length
NRd_min_area_355=zeros(lin_length,1);
NRd_min_area_420=zeros(lin_length,1);
NRd_min_area_460=zeros(lin_length,1);
NRd_min_area_500=zeros(lin_length,1);
NRd_min_area_620=zeros(lin_length,1);
NRd_min_area_690=zeros(lin_length,1);

```

```

% Non dimensional slenderness value for the optimized column for each
% column length
lambda_non_355=zeros(lin_length,1);
lambda_non_420=zeros(lin_length,1);
lambda_non_460=zeros(lin_length,1);
lambda_non_500=zeros(lin_length,1);
lambda_non_620=zeros(lin_length,1);
lambda_non_690=zeros(lin_length,1);

% Reduction factor for the optimized column for each column length
xsi_355=zeros(lin_length,1);
xsi_420=zeros(lin_length,1);
xsi_460=zeros(lin_length,1);
xsi_500=zeros(lin_length,1);
xsi_620=zeros(lin_length,1);
xsi_690=zeros(lin_length,1);

% Loop that find the column with the smallest steel area for the
% pre-defined load effect, NEd
for m=1:lin_length;

    % Steel grade: S355

    % Iteration to find the optimized column with the smallest
    % steel area
    NRd_find_355=find(NRd(:, :, 1, m)>NEd);
    [min_area_355(m), pos_355(m)]=min(A(NRd_find_355));
    [pos_b_355(m) ,pos_t_355(m)]=find(A==(min_area_355(m)),1);

    % Optimized column dimensions
    b_355(m)=b(pos_b_355(m));
    t_355(m)=t(pos_t_355(m));

    % Non-dimensional slenderness and reduction factor
    lambda_non_355(m)=lambda_non(pos_b_355(m),pos_t_355(m),1,m);
    xsi_355(m)=xsi(pos_b_355(m),pos_t_355(m),1,m);

    % Actual buckling resistance value corresponds to NEd
    NRd_min_area_355(m)=NRd(pos_b_355(m),pos_t_355(m),1,m);

    % Steel grade: S420

    % Iteration to find the optimized column with the smallest
    % steel area
    NRd_find_420=find(NRd(:, :, 2, m)>NEd);
    [min_area_420(m), pos_420(m)]=min(A(NRd_find_420));
    [pos_b_420(m) ,pos_t_420(m)]=find(A==(min_area_420(m)),1);

    % Optimized column dimensions
    b_420(m)=b(pos_b_420(m));
    t_420(m)=t(pos_t_420(m));

    % Non-dimensional slenderness and reduction factor
    lambda_non_420(m)=lambda_non(pos_b_420(m),pos_t_420(m),2,m);
    xsi_420(m)=xsi(pos_b_420(m),pos_t_420(m),2,m);

```

```

% Actual buckling resistance value corresponds to NEd
NRd_min_area_420(m)=NRd(pos_b_420(m),pos_t_420(m),2,m);

% Steel grade: S460

% Iteration to find the optimized column with the smallest
% steel area
NRd_find_460=find(NRd(:, :, 3,m)>NEd);
[min_area_460(m), pos_460(m)]=min(A(NRd_find_460));
[pos_b_460(m) ,pos_t_460(m)]=find(A==(min_area_460(m)),1);

% Optimized column dimensions
b_460(m)=b(pos_b_460(m));
t_460(m)=t(pos_t_460(m));

% Non-dimensional slenderness and reduction factor
lambda_non_460(m)=lambda_non(pos_b_460(m),pos_t_460(m),3,m);
xsi_460(m)=xsi(pos_b_460(m),pos_t_460(m),3,m);

% Actual buckling resistance value corresponds to NEd
NRd_min_area_460(m)=NRd(pos_b_460(m),pos_t_460(m),3,m);

% Steel grade: S500

% Iteration to find the optimized column with the smallest
% steel area
NRd_find_500=find(NRd(:, :, 4,m)>NEd);
[min_area_500(m), pos_500(m)]=min(A(NRd_find_500));
[pos_b_500(m) ,pos_t_500(m)]=find(A==min(min_area_500(m)),1);

% Optimized column dimensions
b_500(m)=b(pos_b_500(m));
t_500(m)=t(pos_t_500(m));

% Non-dimensional slenderness and reduction factor
lambda_non_500(m)=lambda_non(pos_b_500(m),pos_t_500(m),4,m);
xsi_500(m)=xsi(pos_b_500(m),pos_t_500(m),4,m);

% Actual buckling resistance value corresponds to NEd
NRd_min_area_500(m)=NRd(pos_b_500(m),pos_t_500(m),4,m);

% Steel grade: S620

% Iteration to find the optimized column with the smallest
% steel area
NRd_find_620=find(NRd(:, :, 5,m)>NEd);
[min_area_620(m), pos_620(m)]=min(A(NRd_find_620));
[pos_b_620(m) ,pos_t_620(m)]=find(A==(min_area_620(m)),1);

```

```

% Optimized column dimensions
b_620(m)=b(pos_b_620(m));
t_620(m)=t(pos_t_620(m));

% Non-dimensional slenderness and reduction factor
lambda_non_620(m)=lambda_non(pos_b_620(m),pos_t_620(m),5,m);
xsi_620(m)=xsi(pos_b_620(m),pos_t_620(m),5,m);

% Actual buckling resistance value corresponds to NEd
NRd_min_area_620(m)=NRd(pos_b_620(m),pos_t_620(m),5,m);

% Steel grade: S690

% Iteration to find the optimized column with the smallest
% steel area
NRd_find_690=find(NRd(:, :, 6, m) > NEd);
[min_area_690(m), pos_690(m)] = min(A(NRd_find_690));
[pos_b_690(m), pos_t_690(m)] = find(A == (min_area_690(m)), 1);

% Optimized column dimensions
b_690(m)=b(pos_b_690(m));
t_690(m)=t(pos_t_690(m));

% Non-dimensional slenderness and reduction factor
lambda_non_690(m)=lambda_non(pos_b_690(m),pos_t_690(m),6,m);
xsi_690(m)=xsi(pos_b_690(m),pos_t_690(m),6,m);

% Actual buckling resistance value corresponds to NEd
NRd_min_area_690(m)=NRd(pos_b_690(m),pos_t_690(m),6,m);

end

%% Saving data for Analysis 1, Analysis 2 and Analysis 3
if Analysis==1
    save('Analysis_1_355.txt', 'min_area_355', '-ascii');
    save('Analysis_1_420.txt', 'min_area_420', '-ascii');
    save('Analysis_1_460.txt', 'min_area_460', '-ascii');
    save('Analysis_1_500.txt', 'min_area_500', '-ascii');
    save('Analysis_1_620.txt', 'min_area_620', '-ascii');
    save('Analysis_1_690.txt', 'min_area_690', '-ascii');
end

if Analysis==2
    save('Analysis_2_355.txt', 'min_area_355', '-ascii');
    save('Analysis_2_420.txt', 'min_area_420', '-ascii');
    save('Analysis_2_460.txt', 'min_area_460', '-ascii');
    save('Analysis_2_500.txt', 'min_area_500', '-ascii');
    save('Analysis_2_620.txt', 'min_area_620', '-ascii');
    save('Analysis_2_690.txt', 'min_area_690', '-ascii');
end

if Analysis==3
    save('Analysis_3_355.txt', 'min_area_355', '-ascii');
    save('Analysis_3_420.txt', 'min_area_420', '-ascii');
    save('Analysis_3_460.txt', 'min_area_460', '-ascii');
    save('Analysis_3_500.txt', 'min_area_500', '-ascii');
end

```



```

    save('Analysis_3_620.txt','min_area_620','-ascii');
    save('Analysis_3_690.txt','min_area_690','-ascii');
end

%% Plot of the results

% Calculating the ratio between the HSS grades and the S355 steel
A_ratio_analysis_355=min_area_355./min_area_355;
A_ratio_analysis_420=min_area_420./min_area_355;
A_ratio_analysis_460=min_area_460./min_area_355;
A_ratio_analysis_500=min_area_500./min_area_355;
A_ratio_analysis_620=min_area_620./min_area_355;
A_ratio_analysis_690=min_area_690./min_area_355;

% Find the intersection points to define when HSS is beneficial
[xout_420,yout_420]=intersections(L,A_ratio_analysis_355,L,...
    A_ratio_analysis_420,1);
[xout_460,yout_460]=intersections(L,A_ratio_analysis_355,L,...
    A_ratio_analysis_460,1);
[xout_500,yout_500]=intersections(L,A_ratio_analysis_355,L,...
    A_ratio_analysis_500,1);
[xout_620,yout_620]=intersections(L,A_ratio_analysis_355,L,...
    A_ratio_analysis_620,1);
[xout_690,yout_690]=intersections(L,A_ratio_analysis_355,L,...
    A_ratio_analysis_690,1);

figure(1)
plot(L,A_ratio_analysis_355)
hold on
plot(L,A_ratio_analysis_420,'--')
plot(L,A_ratio_analysis_460,'-.' )
plot(L,A_ratio_analysis_500,':','LineWidth',2)
plot(L,A_ratio_analysis_620,'-x')
plot(L,A_ratio_analysis_690,'.-')

plot(xout_420,yout_420,'r.','markersize',22)
plot(xout_460,yout_460,'r.','markersize',22)
plot(xout_500,yout_500,'r.','markersize',22)
plot(xout_620,yout_620,'r.','markersize',22)
plot(xout_690,yout_690,'r.','markersize',22)

xlabel('L [m]','FontSize',20,'FontWeight','Bold')
ylabel('A_H_S_S/A_N_S_S','FontSize',20,'FontWeight','Bold')
set(legend('S355 / S355','S420 / S355','S460 / S355',...
    'S500 / S355','S620 / S355','S690 / S355',...
    'Location','SouthEast'),'FontSize',18)
grid on
axis([0 12 0.4 1.2])
set(gca,'fontsize',18)

```